



Inglewood Oil Field Hydraulic Fracturing Report

Prepared for:



Plains Exploration & Production Company

5640 S. Fairfax Ave.

Los Angeles, CA 90056

Version 5

Submitted by:

Denver Tech Team

Halliburton

July 13th, 2012

Inglewood Oil Field Hydraulic Fracturing Report

Table of Contents

1.	Los Angeles Basin	9
1.1.	Introduction.....	9
1.2.	Geological Development of the Los Angeles Basin	11
1.3.	History of Oil Production in Los Angeles Basin	14
1.4.	Assessment of Remaining Oil Potential in Los Angeles Basin	15
2.	Inglewood Oil Field	17
2.1.	Introduction.....	17
2.2.	Location	17
2.3.	Inglewood Oil Field Stratigraphy	18
2.4.	History of Inglewood Oil Field.....	22
2.5.	Structure of Inglewood Field	23
3.	3D Earth Modeling	27
4.	Well Construction and Hydraulic Fracturing.....	35
4.1.	Drilling Process.....	35
4.2.	What Is Hydraulic Fracturing?.....	39
5.	Hydraulic Fracturing and HRGP Analysis	53
5.1.	Methodology to Perform Pressure History Matching	53
5.2.	Well List for Hydraulic Fracturing Report	56
5.3.	High-Rate Gravel Pack Analysis (HRGP)	58
5.3.1.	<i>Vickers and Rindge Formation</i>	<i>58</i>
5.4.	Hydraulic Fracturing Analysis Results	64
5.4.1.	<i>Sentous Formation</i>	<i>64</i>
5.4.2.	<i>Nodular Shale Zone</i>	<i>69</i>
5.4.3.	<i>Moynier Formation</i>	<i>74</i>
6.	Microseismic Monitoring	79
6.1.	What is Microseismic Monitoring?.....	79
6.2.	Microseismic Fracture Mapping Analysis and Results.....	86
6.2.1.	<i>Well VIC1-330 Analysis and Results.....</i>	<i>87</i>
6.2.2.	<i>Well VIC1-635 Analysis and Results.....</i>	<i>91</i>
7.	Hydraulic Fracturing Fluids Disclosure	95
7.1.	Frac Focus Report for VIC1-330 in the Nodular Formation.....	96
7.2.	Frac Focus Report for VIC1-635 in the Nodular Formation.....	99
8.	Fracture Height Growth and Containment of Hydraulic Fractures	102
8.1.	Factors Contributing to Fracture Height Containment.....	106
8.2.	Hydraulic Fracturing and Water Contamination.....	107
9.	High-Rate Gravel Packs.....	109
10.	Summary and Conclusions	111

List of Figures

1. *Fig. 1.1 Map of Southern California showing the location of the Los Angeles Basin.*
2. *Fig. 1.2. Map showing the locations of oil fields in the Los Angeles Basin (Source: Gautier, et al. USGS report presented at AAPG 2012 Annual Convention & Exhibition, Long Beach, California)*
3. *Fig. 1.3. Major structural features in the Los Angeles Basin (Elliott et al., 2009, after Wright, 1991)*
4. *Fig. 1.4. Chronology of major Cenozoic events in the Los Angeles region. Note that geologic time is presented on a logarithmic scale (Wright, 1991).*
5. *Fig. 2.1. Location map showing the productive boundaries of the Inglewood Oil Field (Elliott et al., 2009).*
6. *Fig. 2.2. Stratigraphic column for the Inglewood Oil Field (Elliott et al., 2009).*
7. *Fig. 2.3a. Investment Zone Type Log of Inglewood Field*
8. *Fig. 2.3b. Vickers-Rindge Zone Type Log of Inglewood Field*
9. *Fig. 2.3c. Ruble Zone Type Log of Inglewood Field*
10. *Fig. 2.3d. Moynier Zone Type Log of Inglewood Field*
11. *Fig. 2.3e. City of Inglewood Zone Type Log of Inglewood Field*
12. *Fig. 2.3f. Bradna-Sentous Zone Type Log of Inglewood Field*
13. *Fig. 2.4. Inglewood Exploration / Production History (Dalton).*
14. *Fig.2.5a. Schematic cross section of the Inglewood Oil Field (Elliot, 2009).*
15. *Fig. 2.5b. Schematic cross section of Inglewood Field, southern portion (Elliot, 2009).*
16. *Fig. 2.5c. Schematic cross section of Inglewood Field, central portion (Elliott 2009).*
17. *Fig. 2.5d. Schematic cross section of Inglewood Field, northern portion (Elliot, 2009).*
18. *Fig. 3.1. Cross section of the Inglewood Oil Field Earth Model showing different formation, geologic structure and perched water bodies near surface.*
19. *Fig. 3.2.Snapshots”a” through v“ depicting structural evolution of the Inglewood Oil Field*
20. *Fig. 4.1 Casing Strings in a Well (Graphic courtesy, Texas Oil and Gas Association; Source: Fracfocus.org).*
21. *Fig. 4.2. A tight, permanent cement sheath between the casing and the formation stabilizes the wellbore and protects fluid movement.*

22. *Fig. 4.3. Drawing illustrating the well perforating process. Left, the shaped charge is detonated and a jet of very hot, high-pressure gas vaporizes the steel pipe, cement, and formation in its path. Right, the result is an isolated tunnel that connects the inside of the production casing to the formation. These tunnels are isolated by the cement. Additionally, the producing zone itself is isolated outside the production casing by the cement above and below the zone (API, 2009)*
23. *Fig. 4.4 Illustration of the flow into a non-fractured well, i.e., a natural completion (top) and a fractured well (bottom) (API, 2009).*
24. *Fig. 4.5. Comparison of the production rate and cumulative production for untreated well and a well treated with hydraulic fracturing.*
25. *Fig. 4.6a. Illustration of common hydraulic fracturing equipment on surface (www.hydraulicfracturing.com)*
26. *Fig. 4.6b. Illustration of common hydraulic fracturing equipment on surface (Source: Encana)*
27. *Fig. 4.7. In 1947, Stanolind Oil conducted the first experimental hydraulic fracturing job in the Hugoton field, located in southwestern Kansas (Montgomery and Smith, 2010).*
28. *Fig. 4.8. Illustration of flow of hydrocarbon molecules from the reservoir to the wellbore.*
29. *Fig. 4.9a. Well is drilled through a number of individual reservoirs.*
30. *Fig. 4.9b. The target zones to be produced are perforated, typically using a perforating gun equipped with shaped charges.*
31. *Fig. 4.9c. After perforating, fluid is pumped under pressure sufficient to crack (fracture) the reservoir rock.*
32. *Fig. 4.9d. After the fracture is initiated, fluid carrying proppant is pumped into the fracture. The proppant will remain in the fracture to hold it open.*
33. *Fig. 4.9e. The Fracturing treatment of the two zones is complete and proppant is being removed from the wellbore.*
34. *Fig. 4.9f. Wellbore and formation are clean and hydrocarbon production begins.*
35. *Fig. 4.10. Composition of a typical fracturing fluid (GWPC, 2009a).*
36. *Fig. 4.11. Casing and cementing requirements by percentage of the 27 states reviewed (GWPC, 2009b)*
37. *Fig. 5.1. Aerial Photo of the Inglewood Oil Field showing the locations of the wells used in the fracturing study*
38. *Fig. 5.2. Side view of the Inglewood Oil Field showing the locations of the fracture study wells and reservoir zone surfaces.*
39. *Fig. 5.3. Inglewood Oil Field stratigraphic column showing the position of the Vickers and Rindge zones (Lockman, 2005) and well log from that zone.*
40. *Fig. 5.4a. Side view showing modeled HRGP geometries in the Vickers zone.*

41. *Fig. 5.4b. Zoomed in side view showing modeled HRGP geometries in the Vickers zone.*
42. *Fig. 5.4c. Side view showing modeled HRGP geometries in the Vickers zone and structure (faults).*
43. *Fig. 5.4d. Side viewing showing modeled HRGP geometries in the Vickers zone and major faults*
44. *Fig. 5.4e. Side view showing modeled HRGP geometries in the Vickers zone and major faults.*
45. *Fig. 5.4f. Side view showing modeled HRGP geometries in the Vickers zone and major faults.*
46. *Fig. 5.5. Stratigraphic column for the Inglewood Oil Field showing the various reservoir zones (Lockman, 2005).*
47. *Fig. 5.6a. Side view of the Sentous zone modeled fracture geometries.*
48. *Fig. 5.6b. Detailed side view of Sentous zone modeled fracture geometries with structural features (faults).*
49. *Fig. 5.6c. Side view showing modeled fracture geometries for study well in the Sentous zone together with structural features (faults).*
50. *Fig. 5.6d. Side view showing the study wells with modeled fracture geometries in the Sentous zone and the Newport-Inglewood fault..*
51. *Fig. 5.6e. Detailed side view of the modeled fracture geometries in the study wells in the Sentous zone and structure.*
52. *Fig. 5.7. Stratigraphic column for the Inglewood oil field showing the various reservoir zones and highlighting the Nodular zone (Lockman, 2005).*
53. *Fig. 5.8a. Side view of the Nodular shale zone modeled fracture geometries and the Newport-Inglewood fault.*
54. *Fig. 5.8b. Zoomed in view of the Nodular shale zone modeled fracture geometries and structure (faults).*
55. *Fig. 5.8c. Zoomed in and Detailed side view of the Nodular shale zone modeled fracture geometries.*
56. *Fig. 5.8d. Zoomed in side view of Well VIC1-635 showing modeled fracture geometry in the Nodular shale zone.*
57. *Fig. 5.8e. Zoomed in side view of Well VIC1-330 with modeled fracture geometry in the Nodular shale zone.*
58. *Fig. 5.9. Inglewood oil field stratigraphic column (Lockman, 2005) and a well log showing the position of the Moynier zone.*
59. *Fig. 5.10a. Side view showing the modeled fracture geometries in the Moynier zone and the Newport-Inglewood fault.*
60. *Fig. 5.10b. Zoomed in side view of modeled fracture geometries in the Moynier zone.*
61. *Fig. 5.10c. Detailed side view of modeled fracture geometries in the Moynier zone with structure (faults).*
62. *Fig. 5.10d. Detailed side view of modeled fracture geometries in the Moynier zone with structure.*

63. *Fig. 6.1. Plot of microseismic events recorded during a fracture treatment. The colors indicate different treatment stages.*
64. *Fig. 6.2. Microseismic events imported in the structure model being analyzed to identify the extent of hydraulic fracturing treatment.*
65. *Fig 6.3. Typical layout of Treatment and Observation Wells used in a microseismic monitoring*
66. *Fig 6.4. Typical layout used in a microseismic monitoring test*
67. *Fig. 6.5 Summary of the magnitude of microseismic events in different gas-shale basins [data in figure taken from SPE 151597].*
68. *Fig. 6.6. Zoomed in and Detailed side view of the microseismic events detected during the hydraulic treatments in the Sentous zone in Wells VIC1-330 and VIC1-635.*
69. *Fig 6.7. Earth model visualization showing the microseismic events recorded during hydraulic fracture treatment in the Nodular Shale zone in wells VIC1-330 and VIC1-635.*
70. *Fig 6.8. Earth model visualization showing the location of the treated well perforations and geophones in the monitor well. Distances measured from the midpoint of the geophone array to the mid-perforation location of the stages shown*
71. *Fig 6.10. Map view showing the microseismic event locations color coded by time.*
72. *Fig 6.11. Depth view visualization towards north of showing microseismic events color coded by time.*
73. *Fig 6.12: Map view showing the surface location of the treated well, VIC1-635, and the two monitor wells, VIC1-735 and VIC1-935*
74. *Fig 6.13. Top (map) (left) and side (cross section) (right) views of the perforation string shot and their alignment with the wellbore.*
75. *Fig 6.14 Detailed side view visualization showing the microseismic events recorded in Well VIC1-635*
76. *Fig. 6.15. Map view of the microseismic events recorded during the VIC1-635 stage I fracture treatment.*
77. *Fig.6.16 Microseismic events mapped for the VIC1-635 mainstage fracture treatment are shown in plan (map) view (left) and in cross section (right).*
78. *Fig. 8.1. Side view visualization showing the modeled HRGP geometries in the Vickers zone.*
79. *Fig. 8.2a. Barnett shale measured fracture heights sorted by depth and compared to aquifers (Fisher and Warpinski, 2011)*
80. *Fig. 8.2b. Woodford shale measured fracture heights sorted by depth and compared to aquifer depths (Fisher and Warpinski, 2011).*
81. *Fig. 8.2c. Marcellus shale measured fracture heights sorted by depth and compared to aquifer depths (Fisher and Warpinski, 2011).*
82. *Fig. 8.3. Side View of the Inglewood Oil Field structure with the microseismic events recorded in the two wells completed in the Nodular Shale zone*

83. *Fig. 9.1. Illustration of the high-rate gravel pack process.*

List of Tables

1. *Table 1.1. Principal Oil Fields in the Los Angeles Basin (CDOGGR, 2010)*
2. *Table 1.2 Assessment of Ten Oil Fields in the LA Basin (Source: Gautier, et al., USGS presented at AAPG 2012 Annual Convention & Exhibition, April 22-25, held at Long Beach, California)*
3. *Table 2 Inglewood Oil Field Horizons, Formations and Faults in 3D Earth Model*
4. *Table 3. Wells used in the Inglewood Oil Field fracturing Study*
5. *Table 6.1. Comparison of the seismic energy released and rock volume affected different magnitude events generated by a hydraulic fracture treatment (Warpinski)*
6. *Table 7.1. List of typical fracturing fluid additives at VICI-330 well in the Inglewood Nodular formation*
7. *Table 7.2. Composition of fracturing fluid additives in VICI-330 well in the Inglewood Nodular formation*
8. *Table 7.3. Composition of fracturing fluid in VICI-330 well in the Inglewood Nodular formation*
9. *Table 7.4. List of typical fracturing fluid additives at VICI-635 well in the Inglewood Nodular formation*
10. *Table 7.6. Composition of fracturing fluid in VICI-635 well in the Inglewood Nodular formation*

1. Los Angeles Basin

1.1. Introduction

The Los Angeles Basin is a stratigraphic and structural basin in Southern California, USA, located between the Peninsular and Transverse ranges and the continental borderland, extending from Point Dume south to Dana Point. The onshore portion of the basin extends approximately 50 mi in a northwest-southeast direction and 20 mi in a northeast-southwest direction (Lindblom and Dupler, 2003) and is bounded on the north by the Santa Monica Mountains and Puente Hills, and on the east and south by the Santa Ana Mountains and San Joaquin Hills (Fig. 1.1). The Palos Verdes Peninsula marks the outer edge of the basin along the coast.



Fig. 1.1 Map of Southern California showing the location of the Los Angeles Basin.

The Los Angeles Basin is a major oil and gas province. Due to its relatively small size, large discovered reserves, and great sedimentary thickness it is considered the world's most productive basin in terms of hydrocarbon volume per volume of sedimentary rock fill (Biddle, 1991). Since oil production began in California in 1880, more than 65 fields have been discovered (Biddle, 1991), many of which are still producing today (Fig. 1.2, Table 1).

Plains Exploration & Production Company
 Inglewood Oil Field Hydraulic Fracturing Report

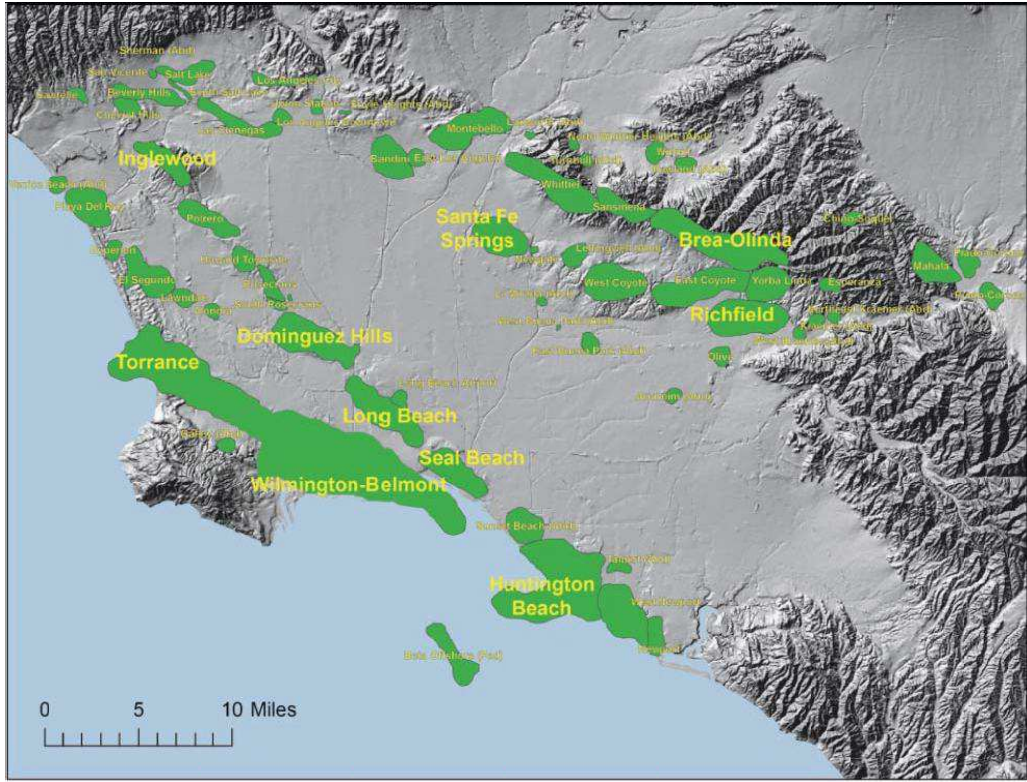


Fig. 1.2. Map showing the locations of oil fields in the Los Angeles Basin (Source: Gautier, et al. USGS presented at AAPG 2012 Annual Convention & Exhibition, Long Beach, California) .

TABLE 1. PRINCIPAL OIL FIELDS IN THE LOS ANGELES BASIN (CDOGGR, 2010)					
Field	Discovery Year	Cumulative Oil Production MMBO	Estimated Remaining Oil Reserves MMBO	Cumulative Gas Production Bcf	Estimated Remaining Gas Reserves Bcf
Wilmington-Belmont	1932	2,701	283	1,207	59
Huntington Beach	1920	1,133	32	857	13
Long Beach	1921	944	2	1,090	2.2
Santa Fe Springs	1919	629	5	838	<1
Brea-Olinda	1880	413	18	474	13
Inglewood	1924	399	30	286	6
Dominguez	1923	274	<1	387	<1
Coyote West	1909	253	0	271	0
Torrance	1922	226	5	148	2
Seal Beach	1924	215	6	222	7
Montebello	1917	205	6	226	3
Richfield	1919	203	3	173	<1
Beverly Hills East	1966	119	9	186	6
Coyote East	1911	116	4	61	2
Yorba Linda	1930	93	0	2	0
Rosecrans (including Rosecrans South & East)	1924	92	2	190	1
TOTAL		8,015		6,618	
EUR (BOE)		8,015		1,943	9,958

Table. 1.1. Principal Oil Fields in the Los Angeles Basin (CDOGGR, 2010)

1.2. Geological Development of the Los Angeles Basin

The Los Angeles Basin, is located at the juncture of the northwest-southeast trending Peninsula Ranges and continental borderland, and the east-west trending Transverse Ranges and shares the geologic histories and characteristics of all three (Wright, 1991). Consequently, the basin is located at the intersection of two major active fault systems, the northwest-trending, right-lateral strike-slip San Andreas-type faults and the east-west faults, mostly left-lateral or thrust faults that bound the Transverse Ranges (Fig. 1.3). The formation of the Los Angeles basin and its evolution as a major hydrocarbon-producing basin are tied to the evolution of the Pacific-North American tectonic plate boundary. The interplay of strike-slip deformation and rapid subsidence has largely controlled the development of the Los Angeles basin as a major hydrocarbon-producing basin (Biddle and Phelps, 1987).



Fig. 1.3. Major structural features in the Los Angeles Basin (Elliott et al., 2009, after Wright, 1991)

The Los Angeles Basin has undergone a multi-phase tectonic evolution that has included (1) Cretaceous and early Cenozoic subduction that ended in the Oligocene, approximately 30 million years ago (Ma), (2) Middle Miocene (20 to 10 Ma) shift from subduction to transform margin (strike slip) tectonics that resulted in rifting and clockwise rotation of the Transverse Ranges, (3) Late Miocene to Early Pliocene (7 to 4 Ma) extension and

strike-slip movement that accompanying the opening of the Gulf of California, and (4) Pliocene to Recent shortening (compression) associated with uplift of the Transverse Ranges and limited strike slip tectonics (Fig. 1.4) (Wright, 1987; Biddle, 1991; Bilodeau et al., 2007). Major northwest-trending strike-slip faults, such as the Whittier, Newport–Inglewood, and Palos Verdes faults, dominate the present-day basin (Fig. 1.3). The structural extension resulted in basin subsidence, deposition of most of the sediment fill in the basin, and maturation of the source rocks resulting from sedimentary and structural loading. The topographic highs that punctuate the surface of the present-day alluvial plain are surface expressions of these major tectonic trends that serve as trapping mechanisms for many of the basin’s oil and gas accumulations. Prior to 1925, most discoveries were based on oil seeps or topographic highs along the Whittier and Newport–Inglewood fault zones and in the Coyote Hills. Later discoveries have been in geologic structures with little or no surface expression (Wright, 1991).

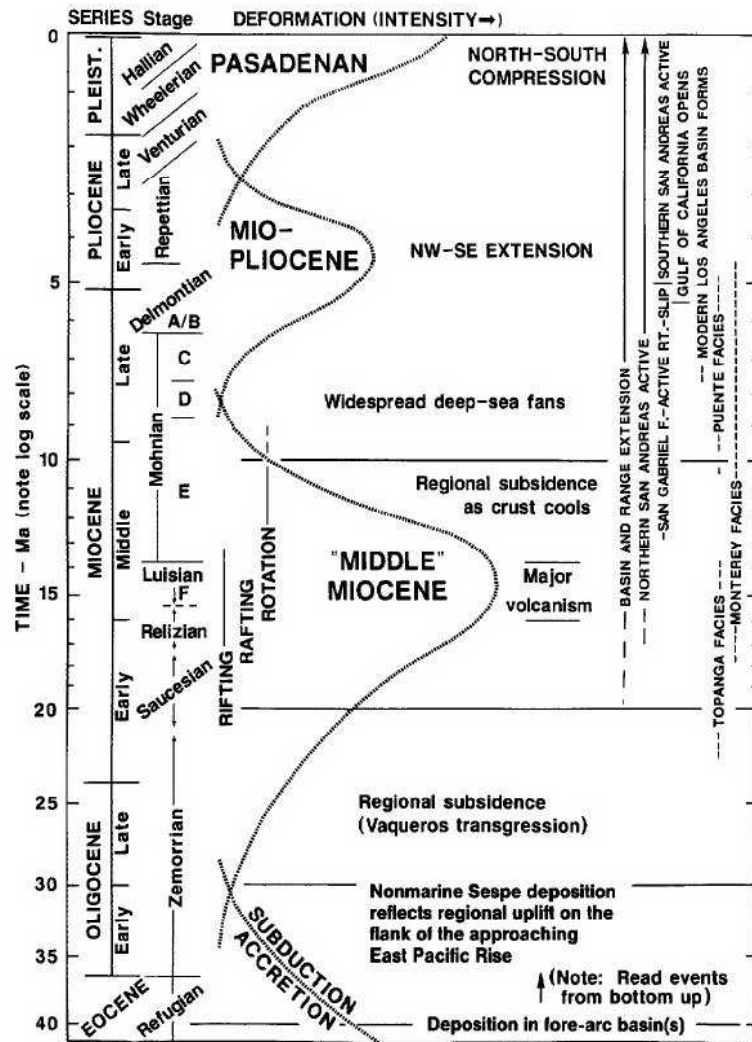


Fig. 1.4. Chronology of major Cenozoic events in the Los Angeles region. Note that geologic time is presented on a logarithmic scale (Wright, 1991).

During the Middle Miocene rifting phase deepwater organic-rich shales and diatomaceous rocks that provide the basin's prolific source rocks were deposited. The basin geometry led to restricted ocean circulation and contributed oxygen depletion in the bottom waters, which enhanced preservation of the organic matter in these rocks (Biddle, 1991). Towards the end of Middle Miocene time, approximately 13 ma, the rifted basins to the north and northeast of the present Los Angeles Basin became filled with sands and muds deposited by coastal rivers. Rivers in the area of the present Mojave Desert and southern Sierra Nevada fed sands onto the continental shelf that eventually flowed down submarine canyons via turbidity currents to build large deepsea fans that extended into the Los Angeles area (Wright, 1987). These submarine fan deposits provide the reservoir rocks for the majority of the oil accumulations in the basin. The extensive and continuous nature of these sands allowed excellent communication (migration pathways) between the mature oil-generating source rocks and the traps. This process ultimately produced a very thick interval of alternating sandstones, siltstones and shales. The sedimentary fill in the central trough of the Los Angeles basin, a structural low between the Whittier and Newport–Inglewood faults, consists of Mesozoic/Cenozoic basement rocks. This sedimentary fill as it rose above sea level began forming what we now call the “Los Angeles Basin”. In effect, Los Angeles has not been “falling in to the sea”, as popularly believed, but rather “rising from the ocean”.

The geologic development of the Los Angeles Basin provided a nearly optimum combination of conditions favorable for petroleum generation and accumulation (Wright, 1987). These include:

1. Rich and abundant organic source rocks - Middle Miocene deepwater organic-rich shales and diatomaceous rocks.
2. Adequate hydrocarbon maturation temperatures - Generated by rapid subsidence and burial under the thick sedimentary sequence.
3. Widespread porous reservoir sands - Most oil occurs in laterally continuous deepwater fan turbidite sandstones of late Miocene to early Pliocene age.
4. Early development of structural traps around most of the basin's margins - Most of the oil (73%) in the Los Angeles Basin is trapped in faulted anticlines (Wright, 1991).

References

- Biddle, K.T., 1991, The Los Angeles Basin--An Overview, Chapter 1, in Biddle, K.T., editor, *Active Margin Basins: AAPG Memoir 52*, p. 5-24.
- Biddle, K.T., and Phelps, D.W., 1987, Evolution of the Los Angeles Basin: Formation of major hydrocarbon basin, presented at the 1987 AAPG Annual Convention: AAPG Search and Discovery Article No. 91038
- Bilodeau, W.L., Bilodeau, S.W., Gath, E.M., Osborne, M., and Proctor, R.J., 2007, Geology of Los Angeles, California, USA: Environmental & Engineering Geoscience, v. 13, no. 3, May, p. 99-160.

California Division of Oil, Gas, and Geothermal Resources, 2010, 2009 Annual Report of the State Oil and Gas Supervisor PR06, Production and Reserves, p. 83-111.

Elliott, J.P., Lockman, D., and Canady, W., 2009, Multiple uses for image logs within the Los Angeles Basin, Paper G, in 50th Annual Logging Symposium Transactions: Society of Petrophysicists and Log Analysts, p. 1-15.

Lindblom, R.G., and Dupler, P.C., 2003, Urban oil field development in the Los Angeles Basin--An historical and current perspective on the East Beverly Hills and San Vicente fields, presented at the 2003 AAPG Pacific Section/SPE Western Regional Joint Meeting: AAPG Search and Discovery Article No. 90014.

Wright, T., 1987, Geologic summary of the Los Angeles Basin, in Wright, T., and Heck, R., editors, *Petroleum Geology of Coastal California*: AAPG Pacific Section Guidebook 60, p. 21-31.

Wright, T.L., 1991, Structural geology and tectonic evolution of the Los Angeles Basin, California, Chapter 3, in Biddle, K.T., editor, *Active Margin Basins*: AAPG Memoir 52, p. 35-134.

Yerkes, R.F., McCulloh, T.H., Schoellhamer, J.E., and Vedder, J.G., 1965, Geology of the Los Angeles basin, California--An introduction: U.S. Geological Survey Professional Paper No. 420-A, p. 1-57.

1.3. History of Oil Production in Los Angeles Basin

The Los Angeles Basin is labeled as the most dense producing oil region in the world. Oil was first discovered in the Los Angeles Basin around 130 years ago.

Oil production in the Los Angeles Basin started with the discovery of the Brea-Olinda Oil Field in 1880, and continued with the development of the Los Angeles City Oil Field in 1893, the Beverly Hills Oil Field in 1900, the Salt Lake Oil Field in 1902, and many others. The discovery of the Long Beach Oil Field in 1921, which proved to be the world's richest in production per-acre of the time, increased the importance of the Los Angeles Basin as a worldwide oil producer. This increased again with the discovery of the Wilmington Oil Field in 1932, and the development of the Port of Los Angeles as a means of shipping crude oil overseas.

1.4. Assessment of Remaining Oil Potential in Los Angeles Basin

(from 2012 USGS Report by Donald Gautier)

How much recoverable oil remains in the Los Angeles basin?

The U.S. Geological Survey recently assessed remaining recoverable oil in major fields of the Los Angeles Basin using a probabilistic methodology. The methodology considers estimated original oil in place (OOIP), recovery efficiency, and extent of application of available production technologies. The recovery efficiency in the major fields remains low and basin-wide production continues to fall in spite of one of the world's greatest concentrations of oil per unit area. For example, along the Wilmington Anticline and Newport-Inglewood Fault Zone, where at least six fields have estimated OOIP volumes in excess of 1 billion barrels. These fields have been on production for about 90 years and now most fields are widely viewed as nearly depleted. However, with average recovery of less than 28 % of OOIP, recovery in such major fields could reasonably be expected to reach at least 40 to 50%. The USGS assessment suggests the most likely case is that volumes well in excess of one billion barrels of oil could be recovered from existing fields through widespread application of current best practice industry technology (AAPG Search and Discovery Article #90142 © 2012 AAPG Annual Convention and Exhibition, April 22-25, 2012, Long Beach, California)

More than three (between 1.4 - 5.6 billion barrels) billion barrels of recoverable oil remains in the ten fields of the Los Angeles Basin (Gautier, et al., USGS).

Los Angeles Basin Petroleum System

The key features of the LA Basin petroleum system are given below (Gautier, et al., USGS):

- Prolific Miocene source rock
- Active petroleum system; ideal timing
- Submarine fan and slope channel reservoirs
- Largest traps are faulted anticlines
- World's highest known oil/sediment ratio

Assessment of Ten Oil Fields

	OOIP BB	EUR BB	% RE	% RE _{max}	Remaining BB
Brea-Olinda	1.2 – 2.4	0.431	18 - 36	35 - 45	.081 - .407
Dominguez Hills	1.0 – 1.45	0.274	19 - 27	35 - 50	.146 - .321
Huntington Beach	3.25 – 6.0	1.164	19 - 36	35 - 55	.117 - .866
Inglewood	1.0 – 2.5	0.430	17 - 43	40 - 55	.067 - .520
Long Beach	3.0 – 3.6	0.946	26 - 32	35 - 55	.208 - .664
Richfield	0.8 – 2.4	0.206	09 - 26	26 - 45	.048 - .357
Santa Fe Springs	2.1 – 2.7	0.634	23 - 30	30 - 40	.097 - .308
Seal Beach	0.85 – 1.0	0.221	22 - 26	35 - 50	.110 - .210
Torrance	0.9 – 2.0	0.232	12 - 26	35 - 55	.128 - .394
Wilmington-Belmont	7.6 – 12.0	2.984	25 - 39	35 - 55	.200 - 1.948

Table 1.2 Assessment of Ten Oil Fields in the LA Basin (Source: Gautier, et al., USGS presented at AAPG 2012 Annual Convention & Exhibition, April 22-25, held at Long Beach, California)

Note: Please refer to Attachment 1A titled, “Forgone Oil in the L.A. Basin by USGS”, by Gautier, Donald L.; Tennyson, M. E.; Charpentier, R. R.; Cook, Troy A.; Klett, Timothy R.

2. Inglewood Oil Field

2.1. Introduction

The Inglewood Oil Field is one of the largest urban oil fields in the United States. The Inglewood Field was discovered in 1924 and over the past 86 years, more than 399 million barrels of oil has been produced from the field has an estimated ultimate recovery of 430 million barrels of oil (Table 1.1). USGS EUR for Inglewood Field is 67 - 520 million barrels based on technology and ultimate recovery efficiency. The oil and natural gas produced from the Inglewood Oil Field is consumed entirely in California.

2.2. Location

Covering approximately 1,000 acres, the Inglewood Oil Field is one of the largest urban oil fields in the United States. It is located in the northwestern portion of Los Angeles Basin, ten miles southwest of downtown Los Angeles. The Inglewood Field is not actually in the city of Inglewood, but is primarily located in Baldwin Hills and is surrounded by Culver City and several Los Angeles communities including View Park, Windsor Hills, Blair Hills and Ladera Heights.

The field is bisected by La Cienega Boulevard, north of Slauson Avenue (Fig. 2.1). Its natural boundaries encompass the cities of Los Angeles and Culver City, as well as the West Los Angeles Community College campus and the Kenneth Hahn State Recreation Area.

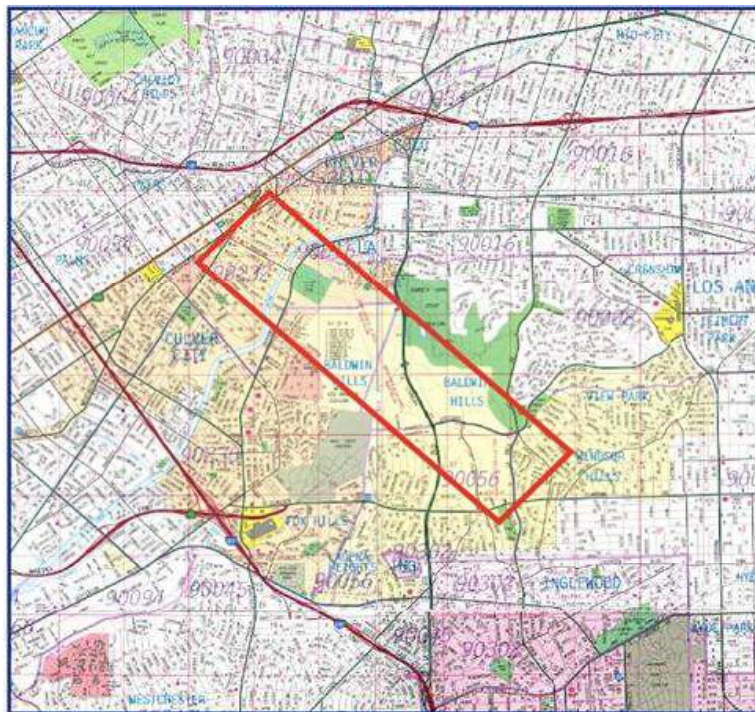


Fig. 2.1. Location map showing the productive boundaries of the Inglewood Oil Field (Elliott et al., 2009).

2.3. Inglewood Oil Field Stratigraphy

The ages of the producing zones in the Inglewood Oil Field range from early Middle Miocene to earliest Pleistocene)—approximately about 15 to 2 Ma (Fig. 2) (Wright,1987) and include both the oldest and the youngest productive zones found along the Newport-Inglewood Fault trend. Early production was primarily from the Pliocene zones where the geologic structure was more fully understood. More than half of the produced oil occurs in the E middle Pliocene Vickers zone (Wright, 1987). Most recently, older (deeper), middle Miocene zones have been the targets of new development.

Figure 2.2 shows the stratigraphy of the Inglewood Oil Field.

EPOCH	FORMATION	RESERVOIR	LITHOLOGY	THICKNESS	DESCRIPTION
PLEISTOCENE	SAN PEDRO			0' - 200'	Recent Sediments
	INGLEWOOD			150' - 300'	Unconsolidated sands and silts
UPPER PLIOCENE	PICO	Upper		150' - 300'	Unconsolidated sands and silts
		Middle	Investment	200' - 300'	Unconsolidated discontinuous sand lenses
		Lower	Vickers	1500' - 1700'	Thin Bedded unconsolidated sands, silts, and shales
LOWER PLIOCENE	REPETTO	Upper	Rindge	900' - 1000'	Thin Bedded sandstone, silt and shale
		Middle	U Rubel	250' - 300'	Thick bedded poorly cemented sandstone with thin silt and shale
			L Rubel	600' - 700'	Thick bedded poorly cemented sandstone with thin silt and shale
		Lower	U Moynier	300' - 400'	Cemented interbeds of sandstone, silt and shale
			L Moynier	600' - 700'	Cemented interbeds of sandstone, silt and shale
		UPPER MIOCENE	PUENTE	Bradna	700' - 1800'
MIDDLE MIOCENE	PUENTE	City of Iwood	0' - 250'	Crst sand and siltstone	
		Nodular Sh	150' - 175'	Siliceous Shale and siltstone	
	TOPANGA	Sentous	200' - 1000'	Cemented interbeds of sandstone, silt and shale	
		Topanga	1500'	Fine grained sandstone, conglomerate, silts and shales, intrusive and extrusive volcanics	

Fig. 2.2. Stratigraphic column for the Inglewood Oil Field (Elliott et al., 2009).

The late Miocene and Pliocene producing zones at the Inglewood Oil Field were all deposited in a similar marine environment at water depths of 3,000 to 6,000 ft. The sandstones and siltstones represent the outer fringes of deepwater fans, deposited by turbidity currents (or similar mechanisms) sweeping across the abyssal plain from their sources to the northeast. The shales were deposited more gradually from the clouds of suspended clay particles that accompanied these submarine flows and landslides, or were carried into the sea by flooded rivers (Wright, 1987). The stratigraphic section at the Inglewood Oil Field suggests that during late Miocene time, the northwest Los Angeles Basin was largely beyond the reach of deepwater fan deposition. The Bradna zone (Fig. 2.3) contains only a few thin sands, and the interval above it is entirely shale (Wright, 1987).

Type Log Displays of Inglewood Stratigraphy

Figures 2.3a - d illustrate the type log displays that help tell the story of what the geologic stratigraphic section looks like between the 3D layers. The section is a sand shale sequence. Oil reservoirs show SP & GR sand excursion associated with high resistivity, highlighted green. The e-log markers correlate the reservoirs across the field and bio stratigraphic zones have been established across the basin based on fossil fauna to correlate the oil field producing measures.

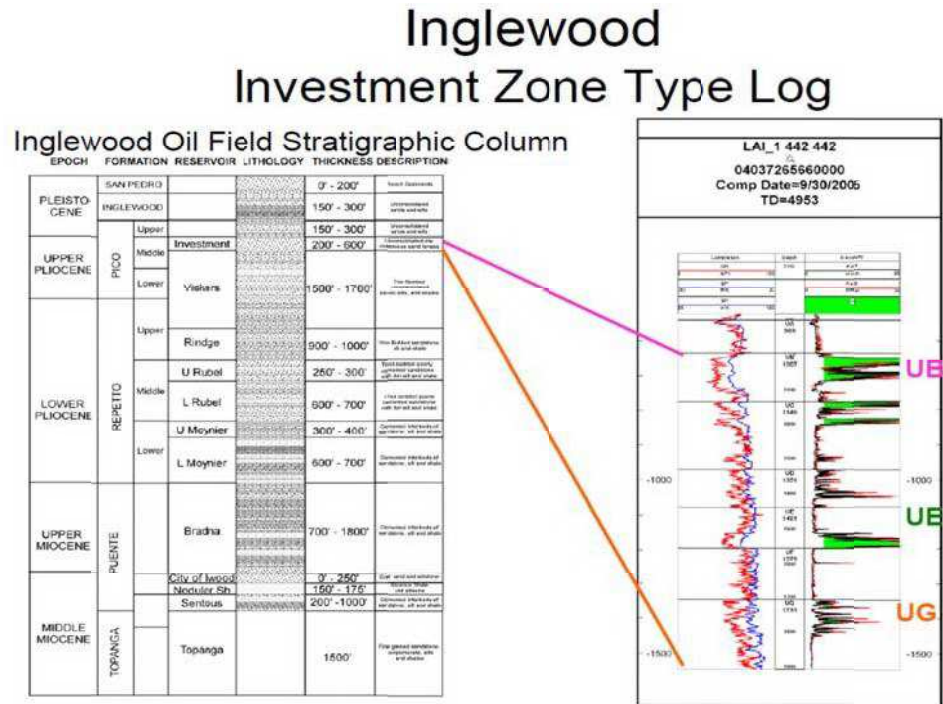


Fig. 2.3a. Investment Zone Type Log of Inglewood Field

Inglewood Vickers-Rindge Type Log

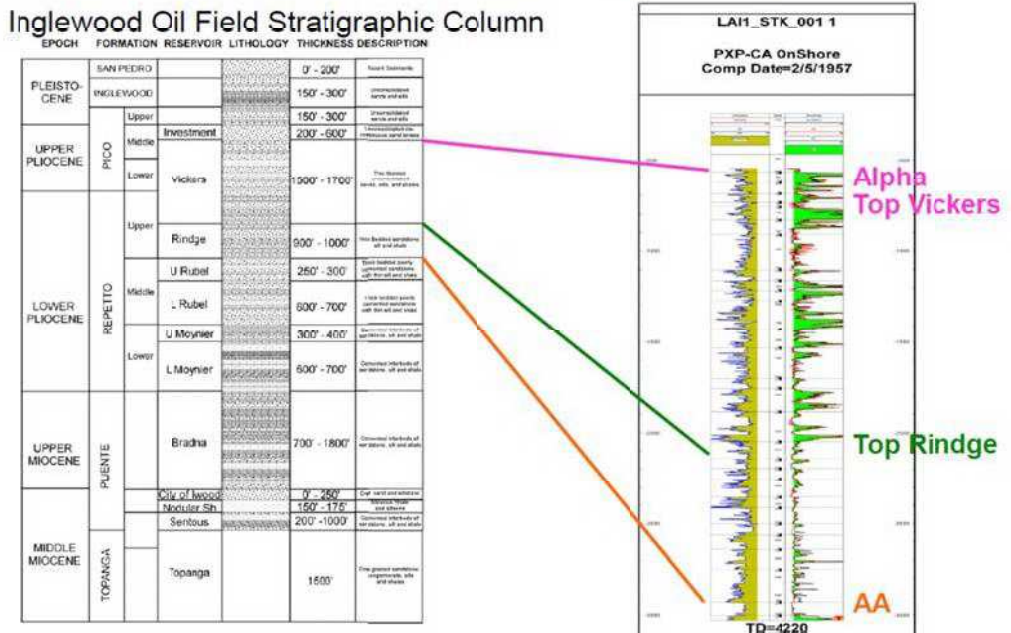


Fig. 2.3b. Vickers-Rindge Zone Type Log of Inglewood Field

Inglewood Rubel Type Log

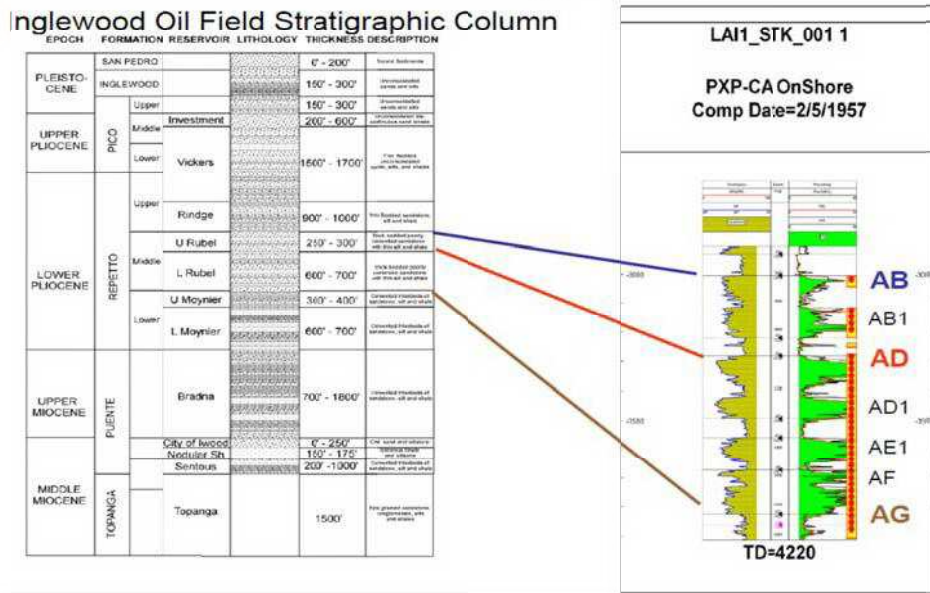


Fig. 2.3c Rubel Zone Type Log of Inglewood Field

Inglewood Moynier Type Log

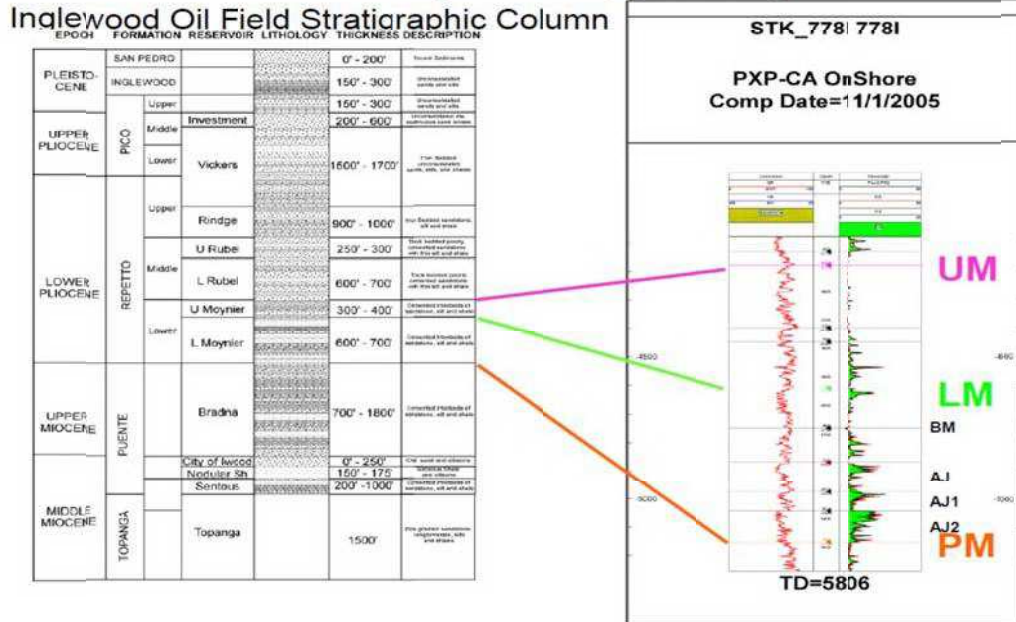


Fig. 2.3d Moynier Zone Type Log of Inglewood Field

Inglewood City of Inglewood Type Log

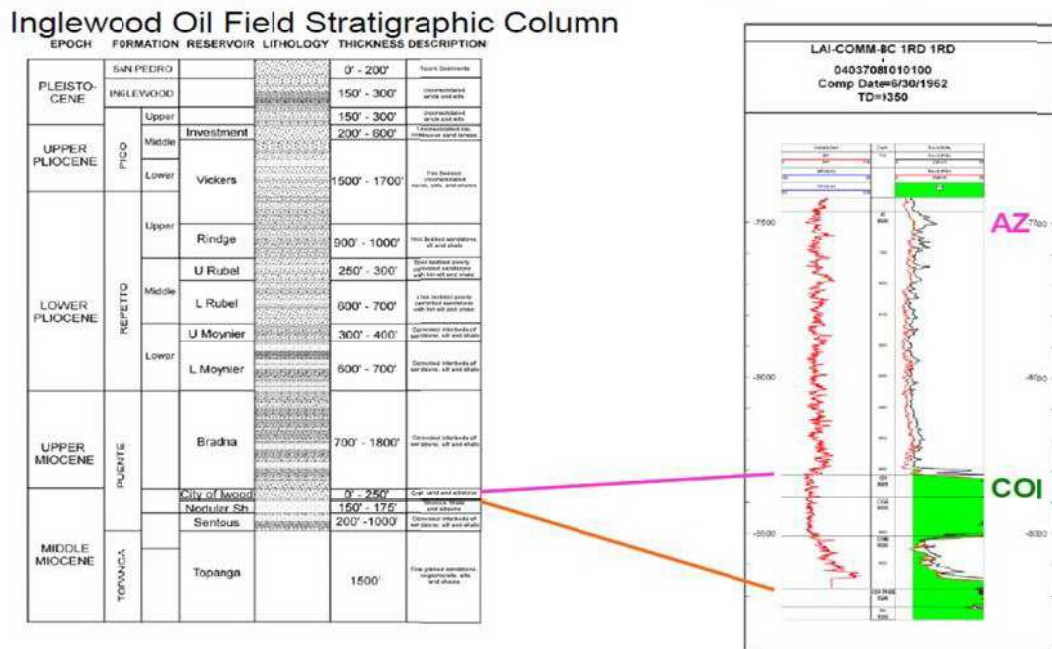


Fig. 2.3e City of Inglewood Zone Type Log of Inglewood Field

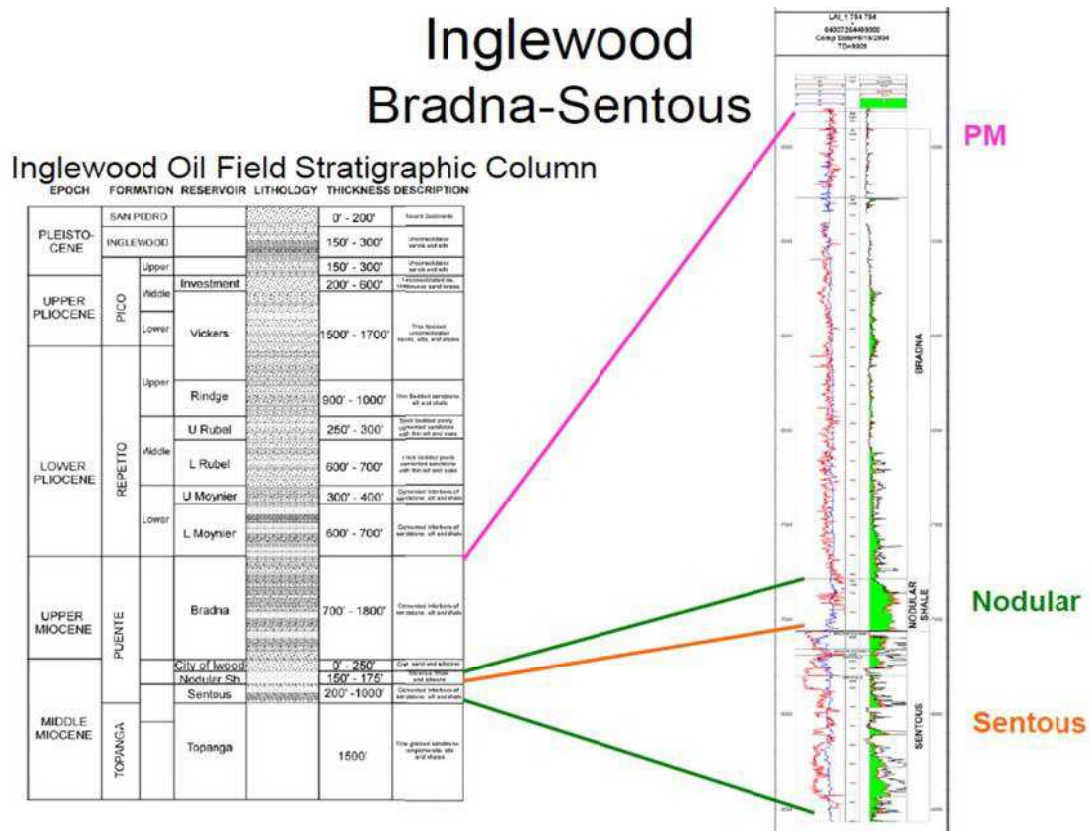


Fig. 2.3f Bradna-Sentous Zone Type Log of Inglewood Field

2.4. History of Inglewood Oil Field

The Inglewood Oil Field has played a major role in the history of Los Angeles. Over the field's history and lifespan more than 1,829 wells have been drilled within the historical boundaries of the field.

The field is located at the northern end of the prolific Newport-Inglewood Fault trend. Figures 1.2 and 1.3 show the location of the Inglewood Oil Field in relation to major structural features and other oil fields in the Los Angeles Basin.

The field, which was discovered in 1924 and first commercially produced by Standard Oil of California (Chevron), has undergone several phases of development since the initial discovery. Initial development was based solely on drilling topographic highs. At the time of the initial discovery, the area consisted primarily of farming and grazing lands. Oil drilling and production predated the residential communities that were subsequently built around its perimeter.

Fig. 2.4 gives a brief description of the Inglewood Exploration and Production history.

Inglewood Exploration / Production History

- **Initial Exploration: 1916 - 1924**
 - Dry holes in the topographic highs and southern slope
 - Discovery in deep ravine that cuts center of hills
- **Reservoir Development: 1994 - Present**
 - Vickers zones**
 - Discovered 1924
 - Peak Production 1925 – 50,278 bbls/day
 - Water Flood Secondary Recovery 1954 - present
 - Normal Fault Compartments / NP- Inglewood Fault
 - Rindge zones**
 - Discovered 1925
 - Peak Production 1937 – 5,336 bbls/day
 - Water Flood Secondary Recovery 1954 - present
 - Normal Fault Compartments / NP Inglewood Fault
 - Rubel zones**
 - Discovered 1934
 - Peak Production 1938 – 4,668 bbls/day
 - Water Flood Secondary Recovery 1960 - present
 - Normal Fault / Thrusted anticline / NP- Inglewood Fault
 - Moynier Zones**
 - Discovered 1932
 - Peak Production 1962 – 4,780 bbls/day
 - Water Flood Secondary Recovery 1968 - present
 - Thrusted anticline
 - Bradna zones**
 - Discovered 1943
 - Peak Production 1959 – 765 bbl/day
 - Thrusted anticline / Channel sand stratigraphic traps
 - Sentous zones**
 - Discovered 1948
 - Peak Production 2005 – 3,290 bbl/day
 - Thrusted anticline
- **Near Field Exploration: 1960**
 - Bradna zone / City of Inglewood sand**
 - Discovered 1960
 - Peak Production 2005 – 933 bbls/day
 - Thrusted anticline / Channel sand stratigraphic traps

EPOCH	FORMATION	RESERVOIR	LITHOLOGY	THICKNESS	DESCRIPTION		
PLEISTOCENE	SAN PEDRO	Base Fresh water		0' - 200'	Recent sediments		
	INGLEWOOD	200-350		150' - 300'	Unconsolidated sands and silts		
UPPER PLEIOCENE	PICO	Upper		150' - 300'	Unconsolidated sands and silts		
		Middle	Investment	2000'	200' - 600'	Unconsolidated fine-grained sandstones	
		Lower	Vickers		1500' - 1700'	The best bedded sandstone, silts, shales and shales	
		Upper	Rindge	4000'	900' - 1000'	The best bedded sandstone, silts and shales	
LOWER PLEIOCENE	REPETTO	Middle	U Rubel		250' - 300'	This bedded poorly cemented sandstone with thin silt and shale	
		Middle	L Rubel		600' - 700'	This bedded poorly cemented sandstone with thin silt and shale	
		Lower	U Moynier		300' - 400'	Cemented beds of sandstone, silt and shale	
		Lower	L Moynier		000' - 700'	Cemented beds of sandstone, silt and shale	
UPPER MIOCENE	PUENTE	Bradna		700' - 1800'	Cemented beds of sandstone, silt and shale		
MIDDLE MIOCENE	TOPANGA		City of Inwood Nodular Sh	8000'	0' - 250'	Thin bedded sandstone and shales	
			Sentous		150' - 175'	200' - 1000'	Cemented beds of sandstone, silt and shale
			Topanga		1500'	Fire baked sandstone, shales, silts, shales and shales. Intrusive and volcanic rocks	

Fig. 2.4. Inglewood Exploration / Production History (Dalton).

2.5. Structure of Inglewood Field

The Inglewood Field is a faulted northwest-trending anticline. The Sentous thrust fault is present on the southwest flank and both this fault and the anticlinal crest are offset in a right-lateral direction by the Newport-Inglewood fault (Fig. 2.5a) (Wright, 1991). This offset took place in latest Pliocene and Pleistocene time.

Figures 2.5 “a through d” represent the structural interpretation of the Inglewood Oil Field based on image logs from 36 wells.

Note: Please refer to Attachment 2A title, “Multiple Uses for Image Logs Within the Los Angeles Basin”, by Elliott, J.P; Lockman, Dalton and Canady, Wyatt, presented at the SPWLA 50th Annual Logging Symposium held in The Woodlands, Texas, June 21-24, 2009.

The figures illustrate the faults, dips, igneous rocks and map of the lower portion of the Inglewood Oil Field Structure from different views.

The Inglewood field is a faulted asymmetrical northwest-trending anticline with west flank dipping about 20 degrees and steeper east flank about 50 degrees. Note the index map shows 3 cross sections from south to north. The Newport-Inglewood fault is a right lateral near vertical fault in the southern portion of the field with the east side up and west side down. Volcanic intrusions appear in the east block. There are a few isolated transtensional faults associated with the shallow Rindge, Vickers and Investment section. The cross section across the central portion of the field

show the Newport-Inglewood fault to cut only the shallower Rubel thru Pleistocene Inglewood and is associated with a large number of transtensional faults and appears to be transtensional up on east dipping westward. This fault system forms what is called the central graben. The deeper section (Nodular, Bradna, Ruble and Rindge) in this portion of the field is cut by 3 Sentous reverse faults that have been interpreted as a thrust system soling out in the Nodular Shale on the steeper east flank of the structure. The core of the anticline is more intensely intruded by volcanic dikes and sills. The northern cross section has been interpreted as an extension of the central area containing 2 Sentous fault traces with volcanic intrusion in the Sentous formation with the Newport-Inglewood not clearly recognizable but probably related to several near vertical faults that cut the steeper east flank. The central graben is also not clearly recognizable.

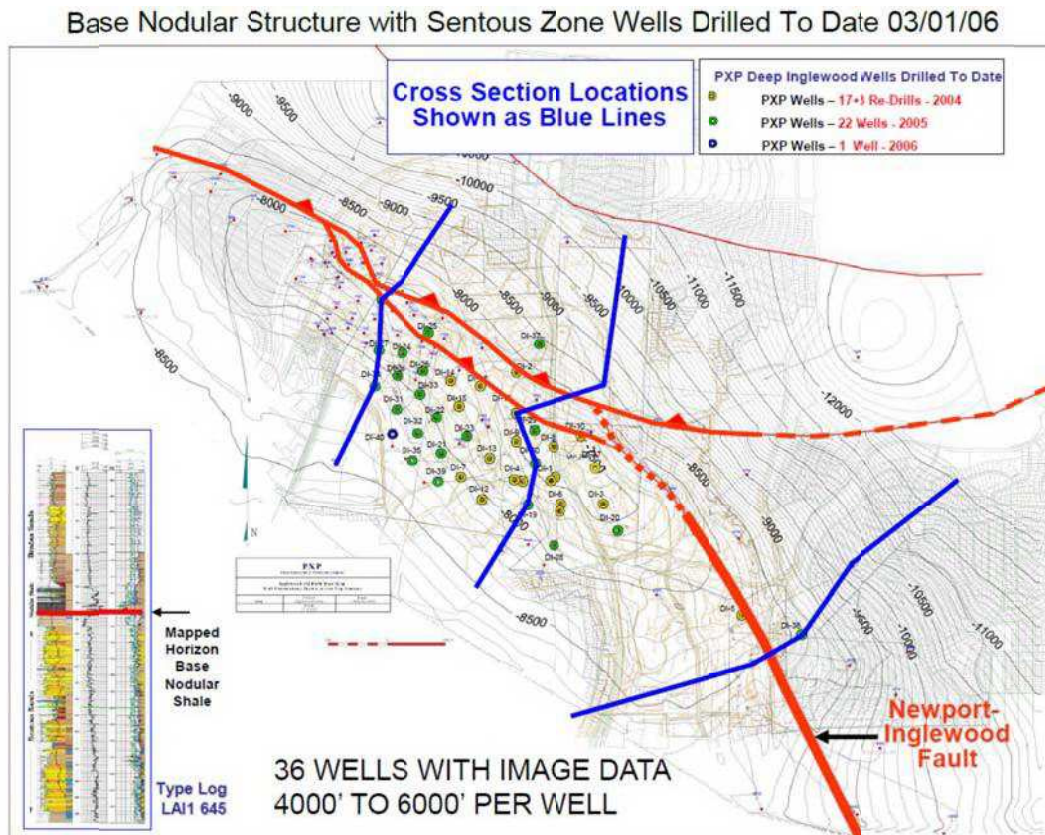


Fig. 2.5a. Schematic cross section of the Inglewood Oil Field (Elliot, 2009)

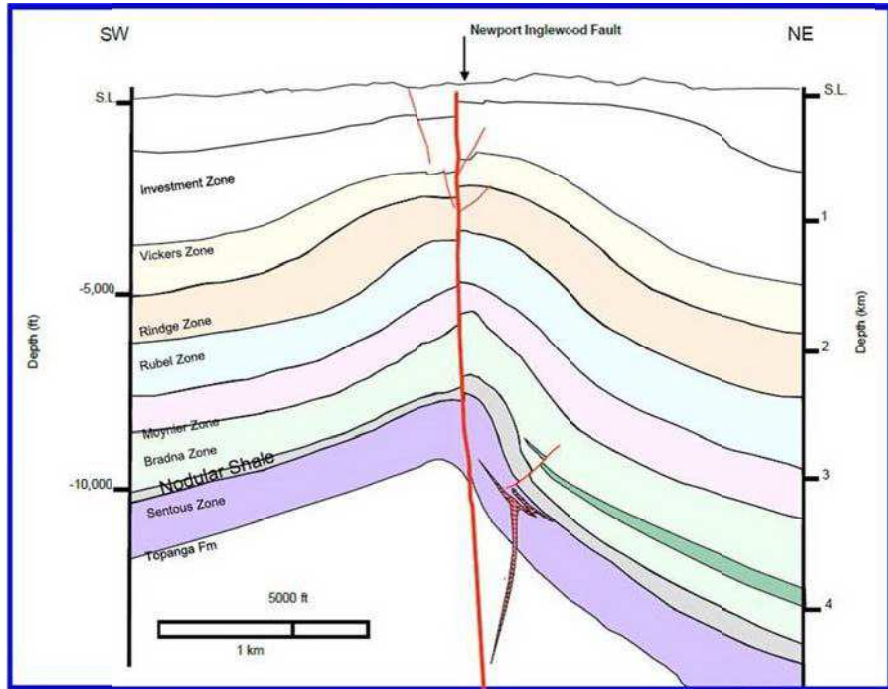


Fig. 2.5b. Schematic cross section of Inglewood Field, southern portion (Elliot, 2009).

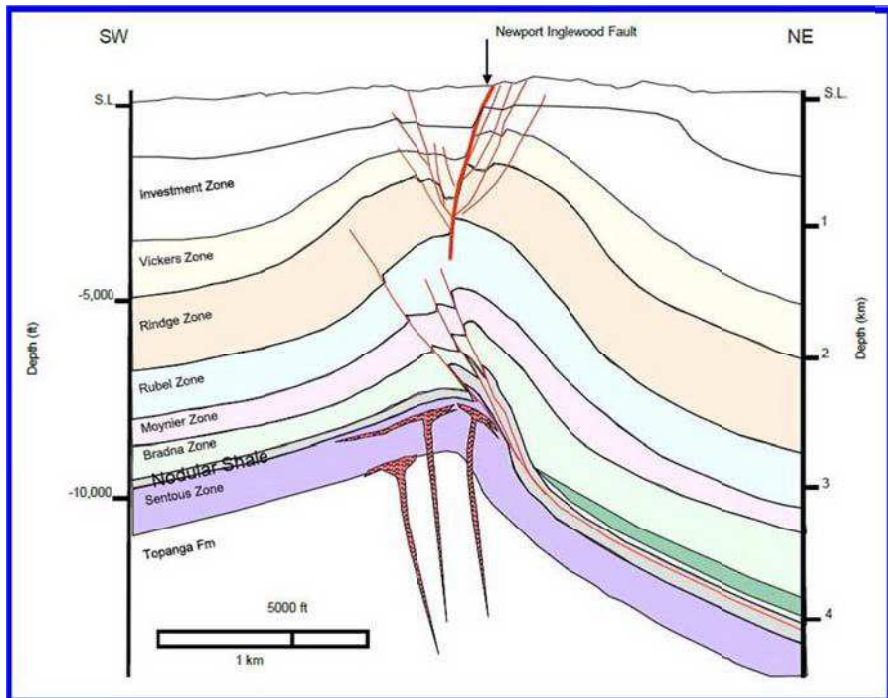


Fig. 2.5c. Schematic cross section of Inglewood Field, central portion (Elliot, 2009).

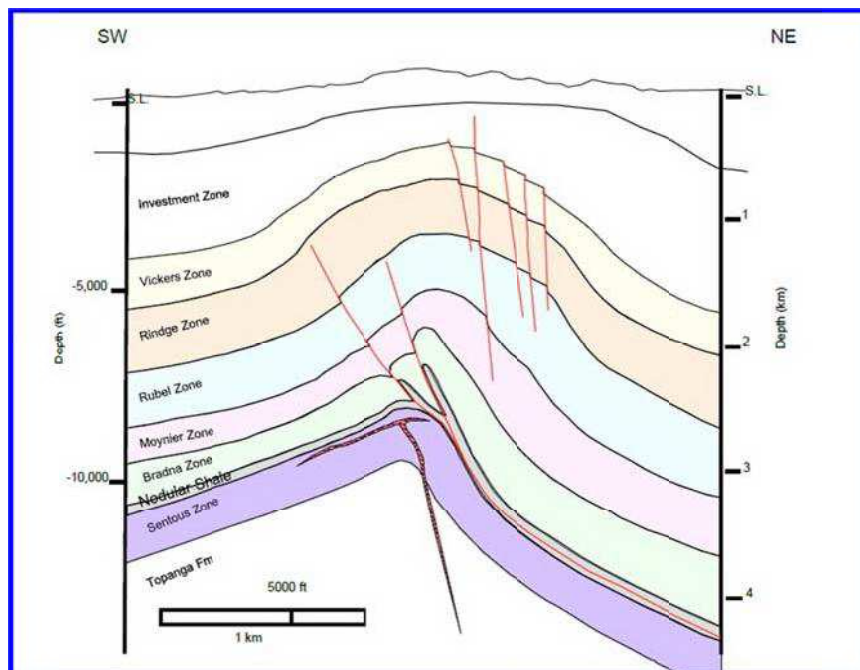


Fig. 2.5d. Schematic cross section of Inglewood Field, northern portion (Elliot, 2009).

References

- Lockman, D., 2005, Los Angeles 3D survey leads to deep drilling: The Leading Edge, v. 24, no. 10, p. 1008-1014.
- Wright, T., 1987, The Inglewood oil field, in Wright, T., and Heck, R., editors, *Petroleum Geology of Coastal California: AAPG Pacific Section Guidebook 60*, p. 41-49.
- Wright, T.L., 1991, Structural geology and tectonic evolution of the Los Angeles Basin, California, Chapter 3, in Biddle, K.T., editor, *Active Margin Basins: AAPG Memoir 52*, p. 35-134.
- Elliot, J.P., 2009, Multiple uses for Image Logs within the Los Angeles Basin, presented at the SPWLA 50th Annual Logging Symposium held in The Woodlands, Texas, June 21-24, 2009

3. 3D Earth Modeling

As described in the last section, the geologic structure of the Inglewood Oil Field is very complex. Building 3D structured earth model helps in understanding the structural complexity. The 3D model also acts as an excellent visualization tool to understand how the different horizons and faults are interlinked with each other.

A 3D structural earth model constructed for the Inglewood Oil Field is used to improve our knowledge of earth structure and assist in the monitoring of subsurface hydraulic fracturing treatments performed at the field. Additionally, this 3D model is used to achieve measurable increases in our abilities to characterize the effect of hydraulic fracturing on near-surface discontinuous ground water bodies and seismic ground motions. A 3D model can capture the full physics of hydraulic fracture propagation, thus leading to a more complete understanding of hydraulic fracturing's impact at the surface.

The general procedure and guidelines used to build this 3D structural earth model, which is built on data from well logs identifying faults and horizons (formation tops and fault picks), is described in this section. The number of geologic formation tops, available from well control, used to construct the individual horizons in the 3D Earth Model were higher in the shallower zones of the model such as Pico, Vickers, Vickers "H" Sand and Rindge (~550 well tops) and lower in the deeper zones of the model such as the Bradna, Nodular and Sentous zones (~120 well tops). This is primarily due to the fact that there are more well penetrations in the shallower zones of Inglewood Field as compared to the deeper zones.

A 3D structural model is a mathematical representation of structural information obtained from a variety of subsurface sources, including 3D seismic data and well log formation tops. Understanding the spatial organization of subsurface structures is essential for quantitative modeling of geological processes and is vital to a wide spectrum of human activities including hydrocarbon exploration and production and environmental engineering. These models also provide the framework that supports numerical simulations of complex phenomena in which structure plays an important role.

The input data used to create the Inglewood 3D structural model consisted exclusively of irregularly-spaced well log formation tops and well log fault picks provided by PXP as Excel spreadsheets. Seismic data were not included in this study. Because a number of different PXP geoscientists had picked the various formation tops it was necessary to apply data management procedures and quality control measures (contribution weights, uncertainty analysis, spatial filtering) to ensure consistency between the geologic horizons and fault networks in the model. Additionally, 3D visualization techniques for simultaneously inspecting the entire datasets provided an effective means for checking for irregularities in the data. 3D visualization was used extensively in this process and was an important step in validating the final input data into the 3D model.

Table 2 lists the horizons and fault surfaces used to construct the Inglewood 3D structural model. These horizons and faults surfaces honor the available well log data described above.

Table 2. Inglewood Field Horizons, Formations and Faults in 3D Earth Model		
Horizons	Geologic Formation	Intersecting Faults
Horizon 1	Sentous	Newport-Inglewood Fault Sentous IIIB Thrust Fault
Horizon 2	Nodular Shale	Newport-Inglewood Fault Sentous IIIB Thrust Fault
Horizon 3	Bradna	Newport-Inglewood Fault Sentous IIIB Thrust Fault Sentous II Thrust Fault
Horizon 4	Moynier	Newport-Inglewood Fault Sentous IIIB Thrust Fault Sentous II Thrust Fault
Horizon 5	Rubel	Newport-Inglewood Fault Sentous IIIB Thrust Fault Sentous II Thrust Fault VRU 278 Normal Fault
Horizon 6	Rindge	Newport-Inglewood Fault Sentous IIIB Thrust Fault Sentous II Thrust Fault VRU 278 Normal Fault LAI 361 Normal Fault VRU 303 Normal Fault VRU 901 Normal Fault VIC 242 Reverse fault
Horizon 7	H-Sand	Newport-Inglewood Fault Sentous IIIB Thrust Fault LAI 361 Normal Fault LAI 394 Normal Fault VRU 278 Normal Fault VRU 303 Normal Fault VRU 901 Normal Fault NI North Normal Fault VIC 242 Reverse fault
Horizon 8	Vickers	Newport-Inglewood Fault LAI 361 Normal Fault LAI 394 Normal Fault VRU 278 Normal Fault VRU 303 Normal Fault VRU 901 Normal Fault NI North Normal Fault
Horizon 9	B-UIHZ	Newport-Inglewood Fault VRU 278 Normal Fault
Horizon 10	Pico	Newport-Inglewood Fault
Horizon 11	Surface	Newport-Inglewood Fault

The Inglewood 3D structural model is consistent with both fitting the observation data (i.e. well log formation tops, fault picks) and the correct relationships between the geological interfaces such as thickness and self-intersecting constraints. Special emphasis and effort was placed on determining how the complex fault network within the field and the geologic horizons are interrelated. The structural history of this field is extremely complicated due to the complex interactions between the compressional faults, strike-slip faults and normal faulting over geologic time. Accordingly, the sealed fault network was initially created and quality controlled before any geologic horizon were put into the model.

All faults and geologic horizons comprising the Inglewood Oil Field 3D model were constructed using triangulated meshes. These triangulated meshes allow for varying resolution depending on the level of detail needed on a particular surface (i.e. fault-horizon intersection, curvature anomaly, etc.) and the input data density. In this 3D model, the resolution of the model and mesh quality were such that the misfit between each horizon and the input data describing the horizon was within the range of data uncertainty. For complex 3D structural models, this need for adaptive resolution is the motivation for using triangulated surfaces (triangulated irregular networks) rather than rigid 2D gridded surfaces. This approach produces superior topological results and was critical to the success in building the Inglewood 3D structural model.

The Inglewood structural model was achieved in two steps. First, the sealed fault network was built to partition the study area into fault blocks, and second, the geologic horizons were created.

The generated fault network was first determined by examining how the individual faults terminated into each other. Defining the connectivity between the fault surfaces is the most important step in structural modeling, even before considering the geological surfaces. The input fault point data were visually inspected for spatial relationships and, in most cases, the input data needed to be both extended and truncated into main and branching fault relationships. In the Vickers/Rindge sections of the model, a series of antithetic normal faults were modeled to truncate into the main Newport-Inglewood fault creating the central graben in this part of the section. This central graben terminated at depth and was not present in the deeper sections of the model, dominated instead by the Sentous thrust faults. Of particular consequence was the relationship of the Newport-Inglewood fault to the deeper Sentous thrust faults and the older geologic horizons. The attitude of the Newport-Inglewood fault was determined through the use of fault juxtaposition diagrams made from the model and microresistivity-based borehole images and published cross sections provided by PXP. Geologic horizon construction was initiated after the sealed fault network was validated and completed for the final model,

For the horizon-modeling step, all of the 11 horizons were created at once, without the faults, and then cut by the fault network and re-interpolated using the fault constraints. This approach automatically computes the topology of the horizon (fault blocks, logical borders) and the boundary conditions necessary for model validity. This procedure is very sensitive to the quality of the fault-network representation and the triangulated mesh along the fault-cut intersection line; however, this model produced results that are consistent with the fault network and stratigraphic layering rules. Careful quality control on all interpolated horizons in the 3D model centered on mesh refinement, thickness variations between the geologic horizons, surface curvature analysis, horizon/fault intersections, hanging wall/foot wall relationships, abrupt fault displacements, strike variations and other geometric constraints.

The Inglewood Oil Field 3D structural earth model was developed to more fully understand the structural complexity present in the subsurface and its relationship to hydrocarbon production & surface ground motion. Additionally, this recently advanced 3D model presents a new prospect for accurately monitoring hydraulic fracturing activities at Inglewood field. This structural model (Fig. 3.1) now provides the framework to characterize the geomechanical and petrophysical properties needed for stress/strain studies.

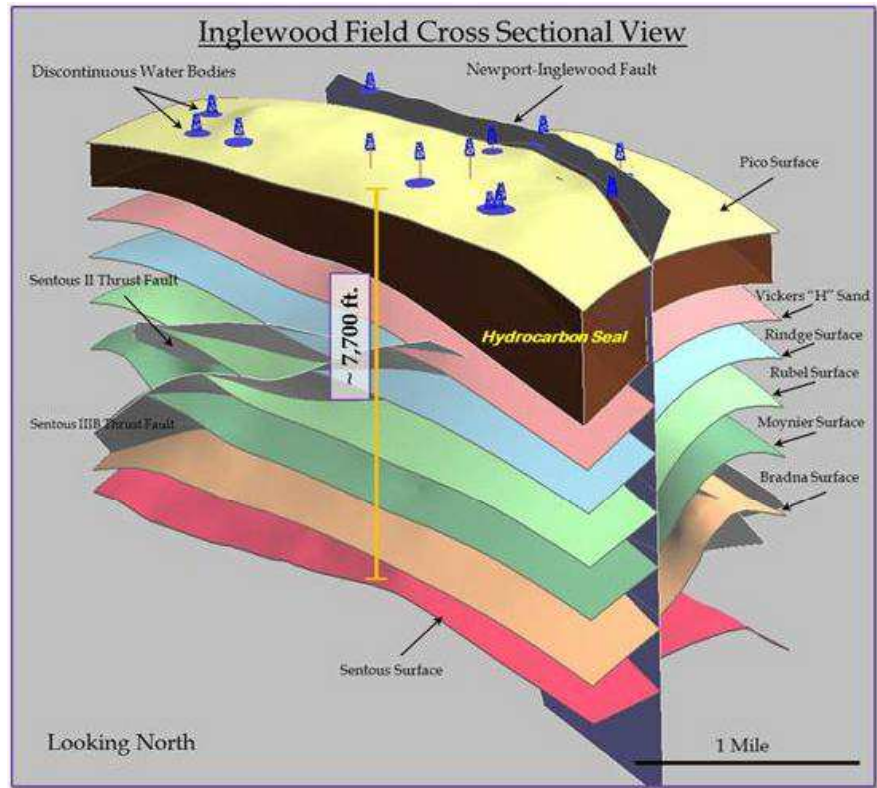
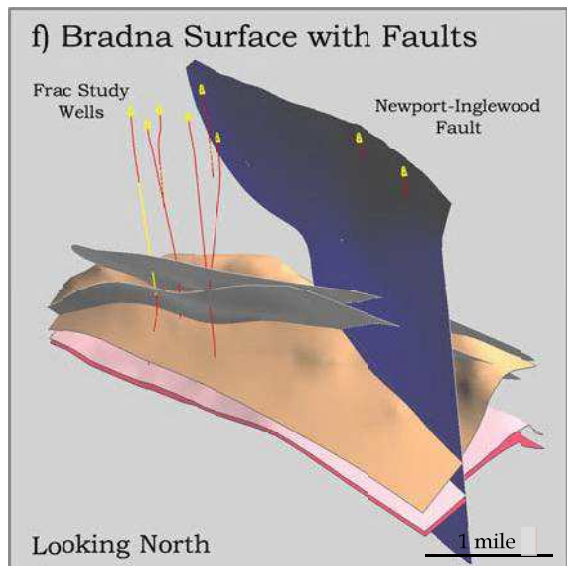
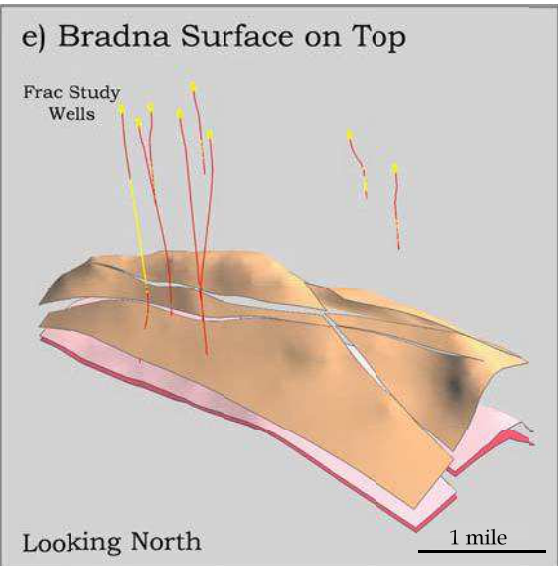
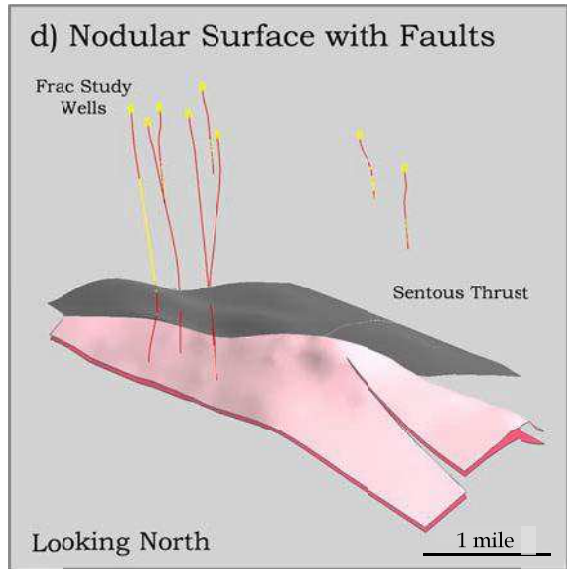
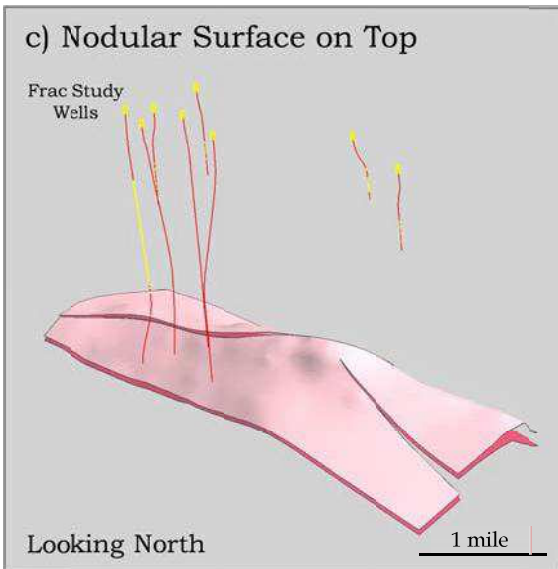
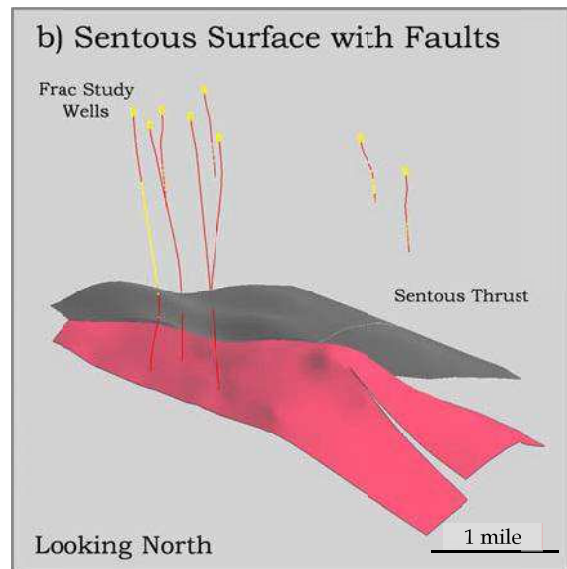
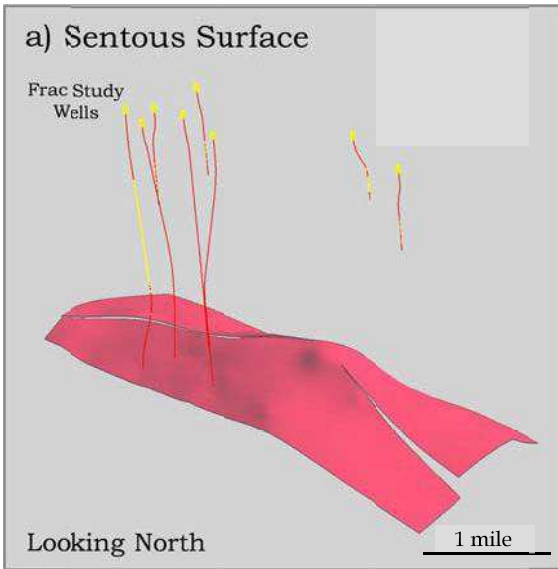
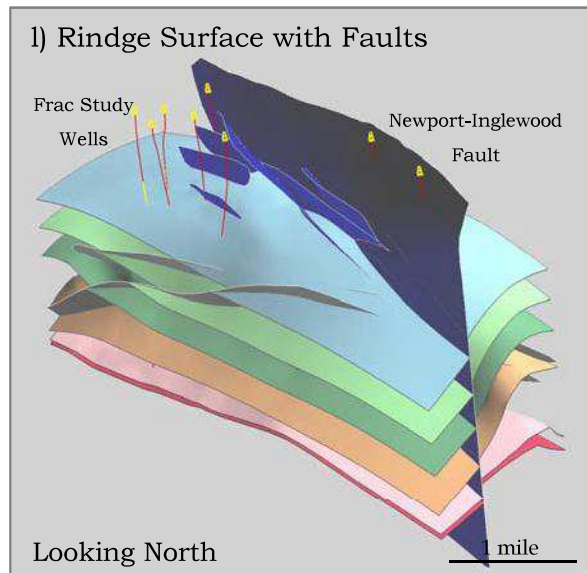
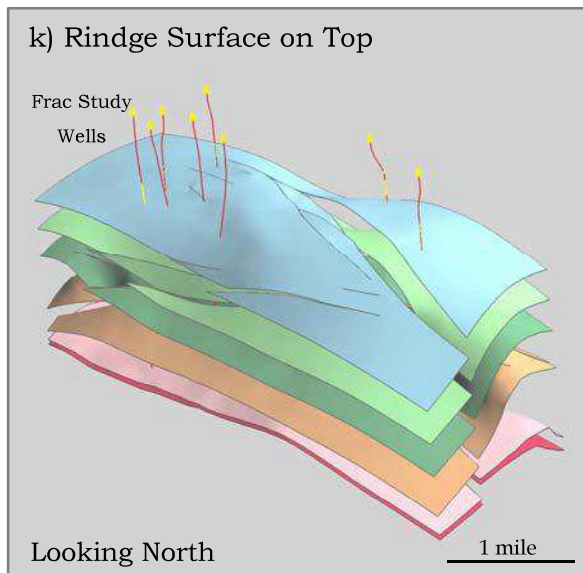
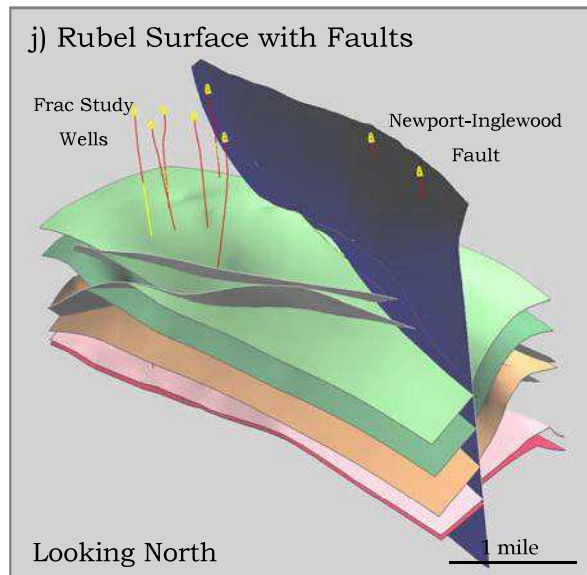
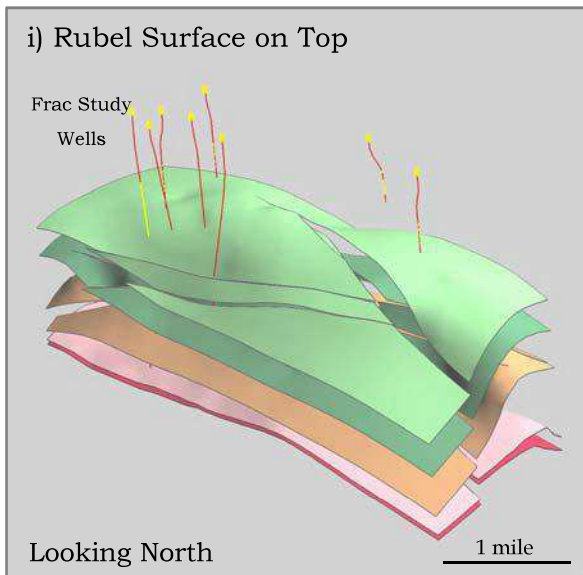
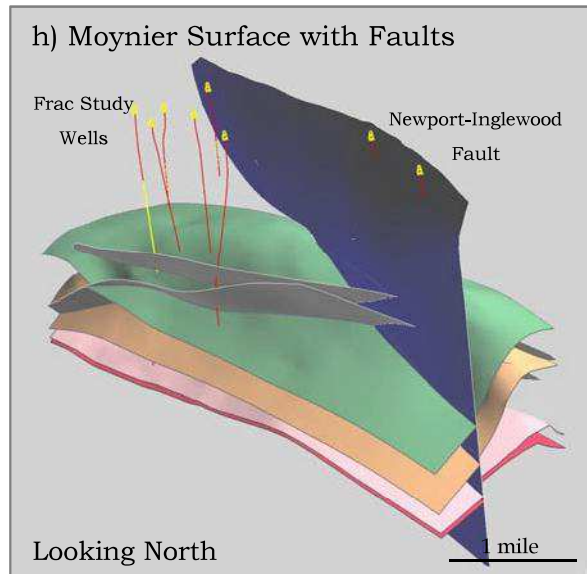
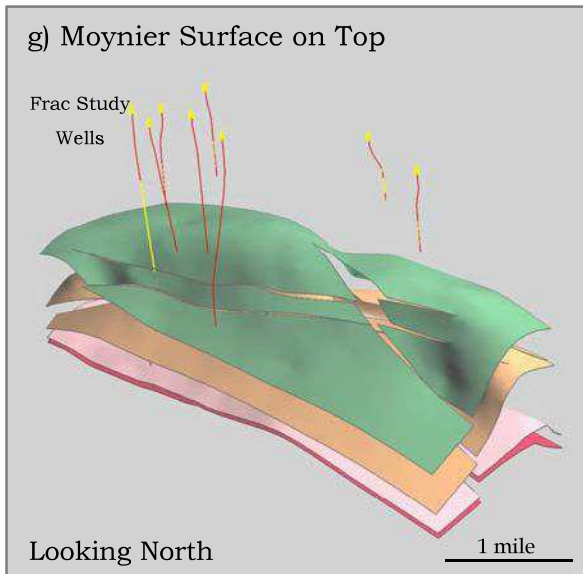
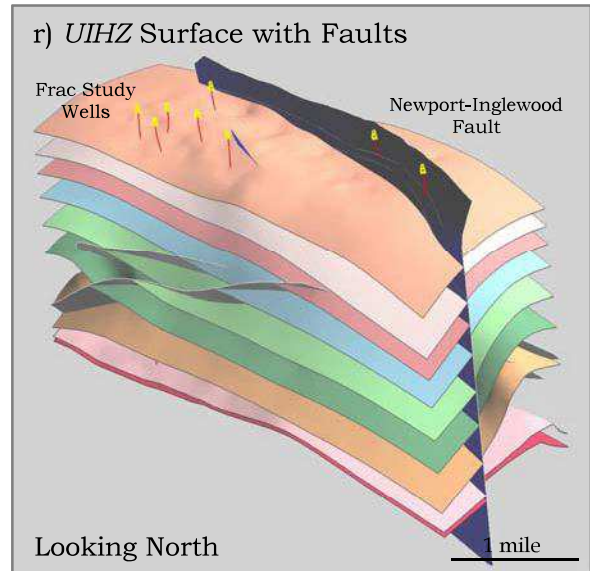
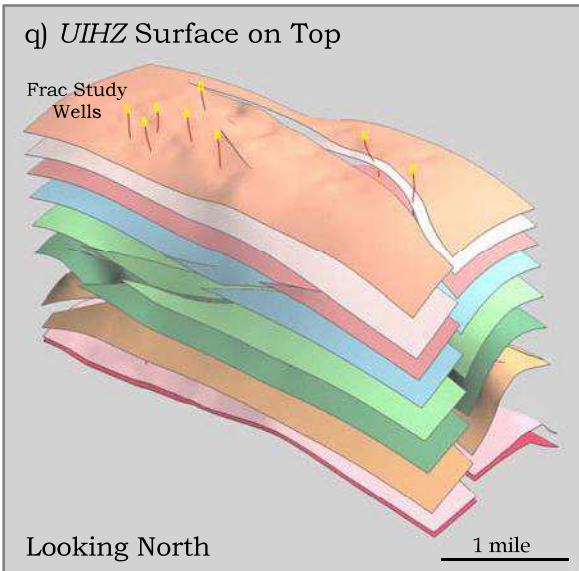
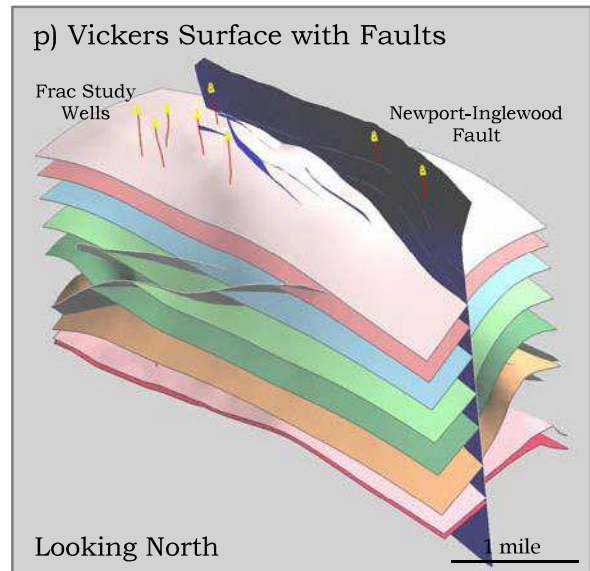
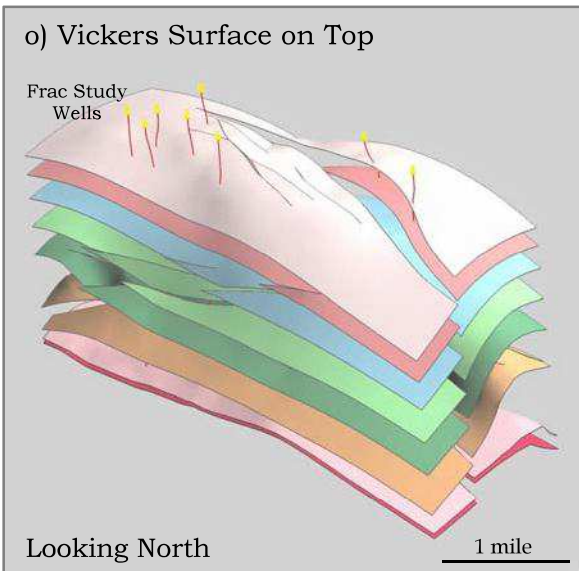
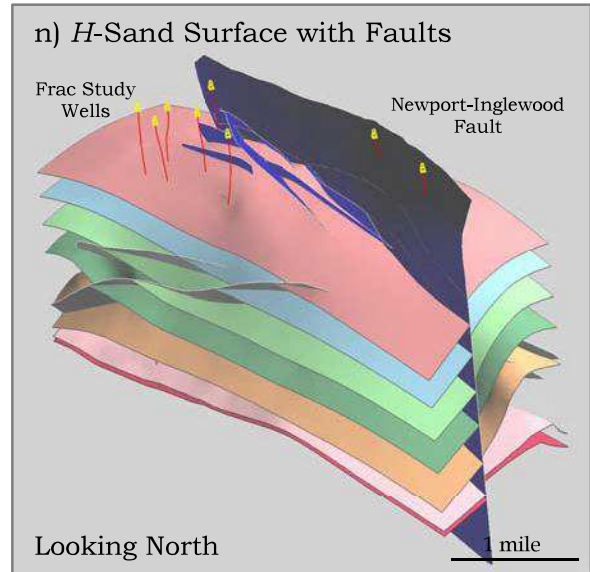
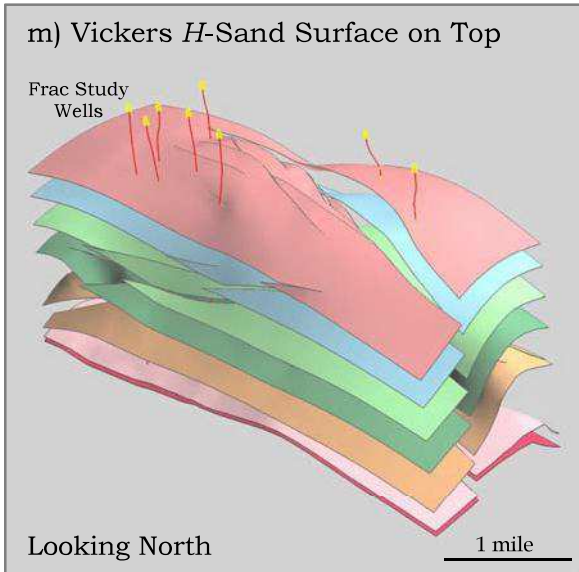


Fig. 3.1. Cross section of the Inglewood Oil Field Earth Model showing different formation, geologic structure and perched water bodies near surface.

The final model constructed is presented as a series of snapshots (Fig. 3.2 "a" through "v") depicting the structural evolution of the Inglewood Oil Field. The snapshots show the different formation layers as they were deposited over time starting from the oldest to the newest. The wells selected for the fracturing study are also shown. Fig. 3.1 "u" shows the hydrocarbon seal in the Inglewood Oil Field Structure.







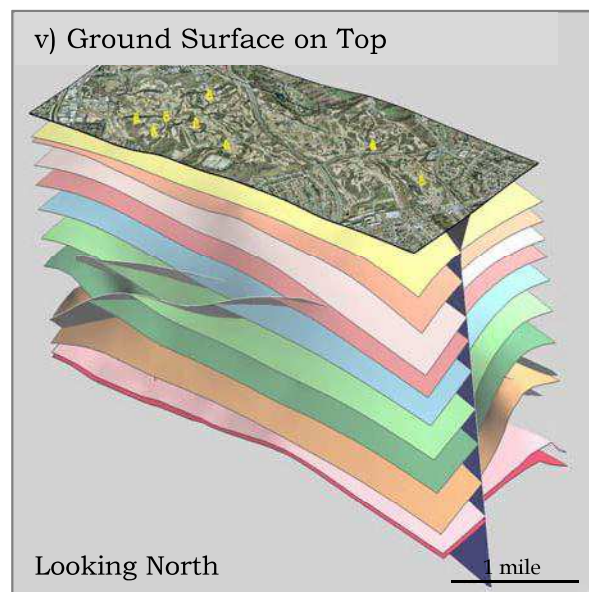
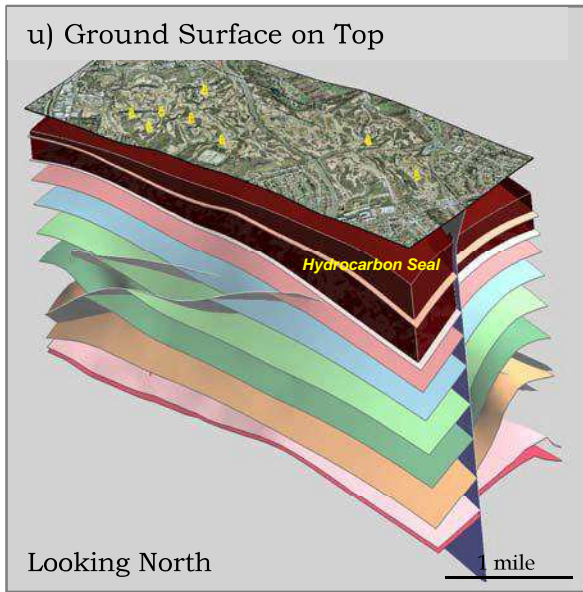
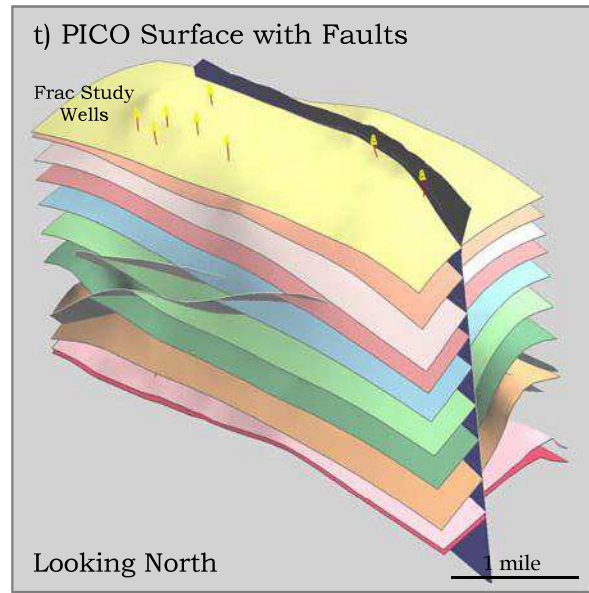
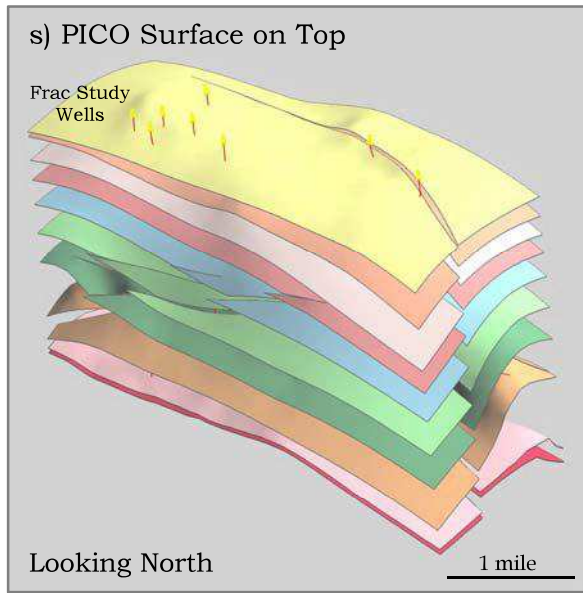


Fig. 3.2.Snapshots "a" through "v" depicting structural evolution of the Inglewood Oil Field.

4. Well Construction and Hydraulic Fracturing

4.1. Drilling Process

Oil and natural gas reserves are buried deep inside the earth trapped in rock formations as described in Section 1.2. Wells are drilled to access these reserves and produce them. These wellbores are designed to last for the life of the well and are often remediated to maintain integrity beyond the designated lifespan. The drilling process starts once the operator has identified the reserves, selected the area and obtained the rights to drill. During the drilling of an oil or gas well, all the formations through which the wellbore passes are protected by steel casing that is held in place by a sheath of cement that surrounds the pipe and is bonded to the formation. The well then goes through a cycle of drilling, casing and cementing until the target depth is reached.

Groundwater and water-bearing zones are protected from the contents of the well during drilling and production operations by a combination of steel casing, cement sheaths, and other mechanical isolation devices installed as a part of the well construction process.

It is important to understand that the impermeable rock formations that lie between the hydrocarbon-producing formations and the shallower groundwater zones have already isolated the groundwater over millions of years. The construction of the well is done in a way to prevent communication (migration and/or transport of fluids) between these subsurface layers.

Casing

The first step in completing a well after a specific section of hole is drilled is to case and cement the hole. Casing ensures that after the well is drilled and drilling fluid is removed, the well will not close in upon itself. At the same time, casing also protects the fluid moving through the well from outside contaminants, like water or sand. (www.rigzone.com)

Casing is typically a hollow steel pipe used to line the inside of the drilled hole or wellbore. Each full length of casing is often referred to as a casing string. Wells are typically constructed of multiple casing strings including a surface string and a production string. These strings are set in the well and cemented in place under specific state and local requirements.

Casing strings are an important element of well completion in regards to protecting groundwater resources, where present, because they isolate freshwater bearing zones and groundwater from the contents of the wellbore, including drilling fluids, completion fluids and flowback, or produced oil and natural gas. In this regard, surface casing provides the first line of defense and production casing provides a second layer of protection.

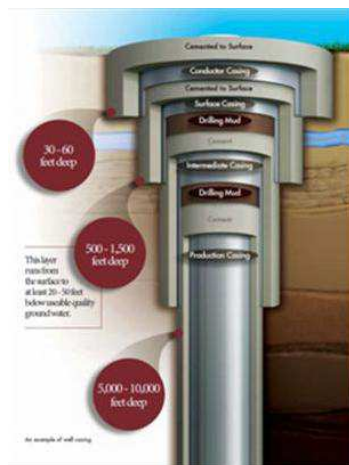


Fig. 4.1 Casing Strings in a Well. Graphic Courtesy of Texas Oil and Gas Association; Source: Fractofocus.org

Steel surface casing is inserted, i.e., run, into the wellbore from surface to depths between 60 and 1,500 ft. to protect local water bearing zones (Fig. 4.1). Steel intermediate casing is inserted into the well from surface to depths near the half-way point of the well to protect formations that might contain higher or lower pressure than the target formation located at the bottom of the well. Steel production casing is inserted into the well from surface to the total well depth to create a controlled flow path to allow safe production of oil or natural gas to surface.

Cementing

After the casing has been run into the drilled hole, it must be cemented in place. Cementing is the process of placing a cement sheath around casing strings (Fig. 4.2). The annulus, the space between these concentric casing “strings” and the drilled hole (wellbore), is filled with cement. Extensive research and development have gone into developing cement blends and procedures that will form a tight, permanent seal both to the casing and to the formation.

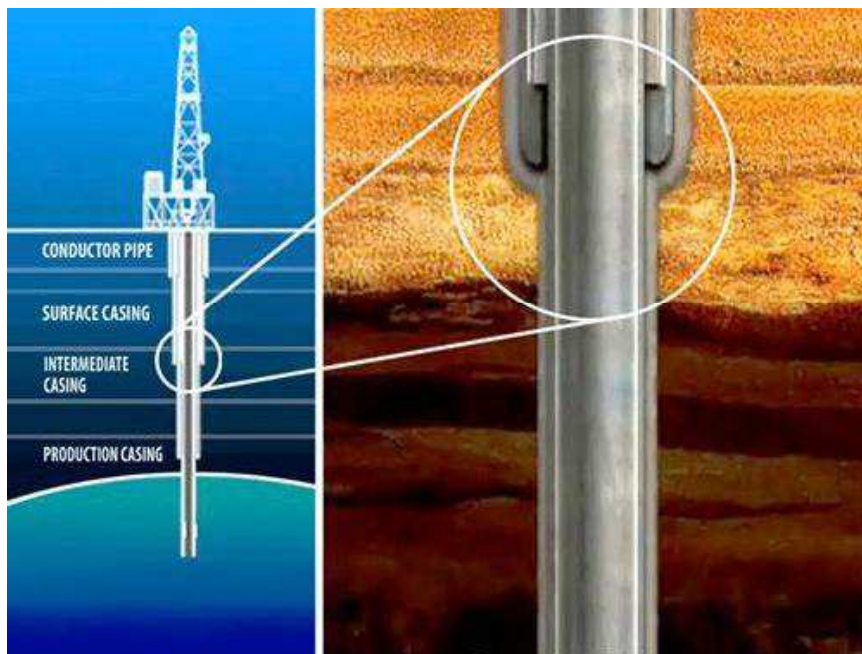


Fig. 4.2. A tight, permanent cement sheath between the casing and the formation stabilizes the wellbore and protects fluid movement.

The purpose of cementing the casing is to provide zonal isolation between different formations, including complete isolation of any groundwater and to provide structural support for the well. Cement is fundamental in maintaining integrity throughout the life of the well and also provides corrosion protection for casing.

Cementing is accomplished by pumping the cement (commonly known as slurry) down the inside of the casing into the well to displace the existing drilling fluids and fill in the space between the casing and the actual sides of the drilled borehole. The slurry, which consists of a special mixture of

additives and cement, is left to harden, thereby sealing the well from non-hydrocarbons that might try to enter the well stream, as well as permanently positioning the casing into place.

After the cement has set, the drilling continues from the bottom of the surface or intermediate cemented steel casing to the next casing depth. This process is repeated, using smaller diameter steel casing each time, until the targeted oil and natural gas-bearing reservoir is reached.

California State Regulations:

All oil and gas wells drilled and constructed in California must adhere to strict requirements, particularly from the California Department of Conservation Division of Oil, Gas and Geothermal Resources (DOGGR). These requirements include general laws and regulations regarding the protection of underground and surface water, and specific regulations regarding the integrity of the well casing, the cement used to secure the well casing inside the bore hole, and the cement and equipment used to seal off the well from underground zones bearing fresh water and other hydrocarbon resources. (See California Public Resources Code sections 3106, 3203, 3211, 3220, 3222, 3224, 3255; Title 14 of the California Code of Regulations, sections 1722.2, 1722.3, 1722.4, etc.)

http://www.conservation.ca.gov/dog/general_information/Pages/HydraulicFracturing.aspx

A brief summary of California's cementing regulations is given below.

1722.4. Cementing Casing.

Surface casing shall be cemented with sufficient cement to fill the annular space from the shoe to the surface. Intermediate and production casings, if not cemented to the surface, shall be cemented with sufficient cement to fill the annular space to at least 500 feet above oil and gas zones, and anomalous pressure intervals. Sufficient cement shall also be used to fill the annular space to at least 100 feet above the base of the freshwater zone, either by lifting cement around the casing shoe or cementing through perforations or a cementing device placed at or below the base of the freshwater zone. All casing shall be cemented in a manner that ensures proper distribution and bonding of cement in the annular spaces. The appropriate Division district deputy may require a cement bond log, temperature survey, or other survey to determine cement fill behind casing. If it is determined that the casing is not cemented adequately by the primary cementing operation, the operator shall re-cement in such a manner as to comply with the above requirements. If supported by known geologic conditions, an exception to the cement placement requirements of this section may be allowed by the appropriate Division district deputy.

NOTE: Authority cited: Section 3013, Public Resources Code. Reference: Sections 3106, 3220 and 3222-3224, Public Resources Code.

Link to website:

http://www.conservation.ca.gov/dog/pubs_stats/Pages/law_regulations.aspx

Perforating

Once the well is drilled to the target zone, cased and cemented in place, the pay zone is then sealed off by the casing and cement. Perforation is the process of creating holes, i.e., perforations, in the casing and cement and into the rock formation to allow oil and natural to flow into the well from the target zone and be produced to surface.

Figure 4.3 illustrates the perforation process. A shaped charge is used to create the pinpoint holes or isolated tunnels through the casing and cement sheath that connect the inside of the production casing to the formation. Since the perforation only creates a pinpoint hole, the producing zone itself is isolated outside the production casing by the cement above and below the zone, as well as by the cement in between the perforations (API, 2009). The cement on the outside of the casing isolates these perforation tunnels from other zones above or below and allows communication from the wellbore to the formation and vice versa.

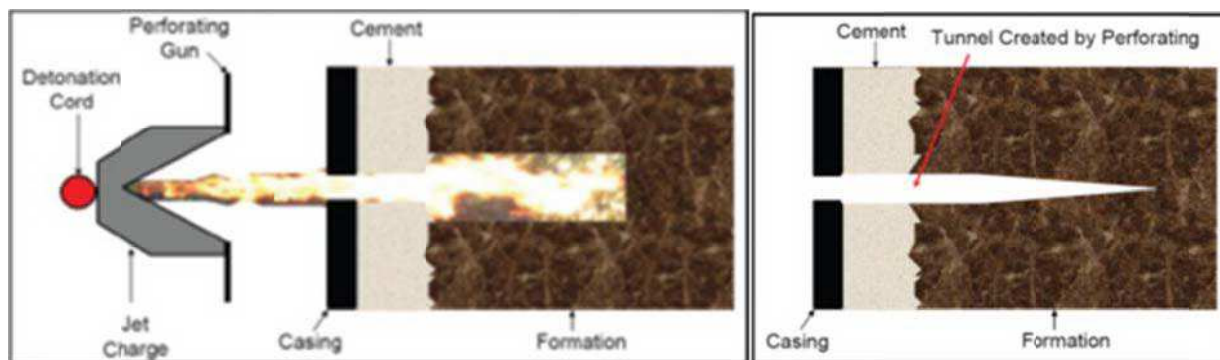


Fig. 4.3. Drawing illustrating the well perforating process. Left, the shaped charge creates a hole through the steel pipe, cement, and formation in its path. Right, the result is an isolated tunnel that connects the inside of the production casing to the formation. These tunnels are isolated by the cement. Additionally, the producing zone itself is isolated outside the production casing by the cement above and below the zone (API, 2009)

The casing and cement stabilize and protect the wellbore and prevent fluids from moving between the formation layers. Casing and cementing helps protect the groundwater, where present, from contamination. Proper sealing of annular spaces with cement creates a hydraulic barrier to both vertical and horizontal fluid migration.

4.2. What Is Hydraulic Fracturing?

Hydraulic fracturing is *NOT* a “drilling process.” Hydraulic fracturing is a well completion method that is done after the well has been drilled and the drilling rig has moved off.

Hydraulic fracturing is the practice of injecting a well with fracturing fluids (typically 99.5% water and sand) and proppants (small, granular solids) at pressures sufficient to break the rocks and to create or restore older fractures that extend from a wellbore into targeted rock formations. Proppants are pumped in a viscous fluid and placed in the created fractures to help ensure the crack remains open after the hydraulic pressure is no longer being applied. This creates a highly conductive path between the reservoir and the wellbore and helps to increase the rate at which fluids can be produced from reservoir formations, in some cases by many hundreds of percent (Fig. 4.4).

In existing and mature wells, hydraulic fracturing is done to increase the output of a well or enhance oil and natural gas recovery.

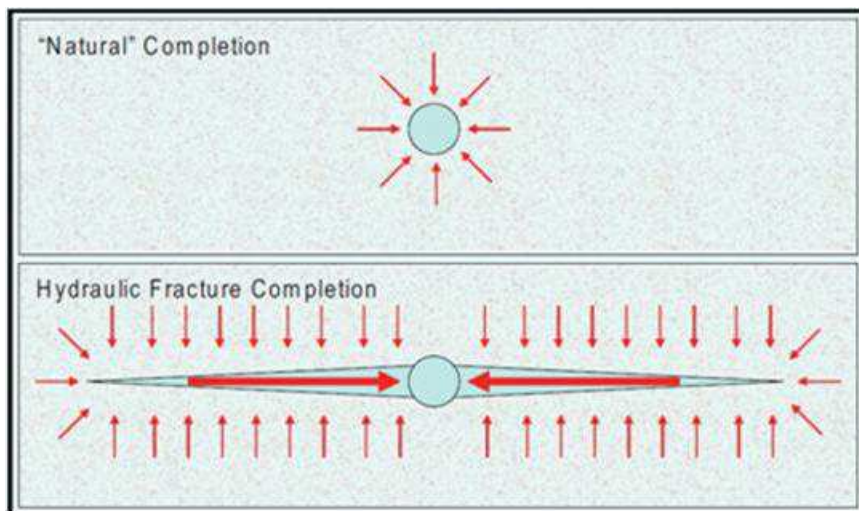


Fig. 4.4 Illustration of the flow into a non-fractured well, i.e., a natural completion (top) and a fractured well (bottom) (API, 2009).

Figure 4.5 compares the production rate and cumulative production for an untreated well and a well that has had a hydraulic fracture treatment, i.e., has been stimulated. It can be clearly seen that hydraulic fracture treatments significantly increase the production of oil and natural gas from the formations. In both the graphs, the red curve represents the untreated well and green curve is for the well that is treated with hydraulic fracturing.

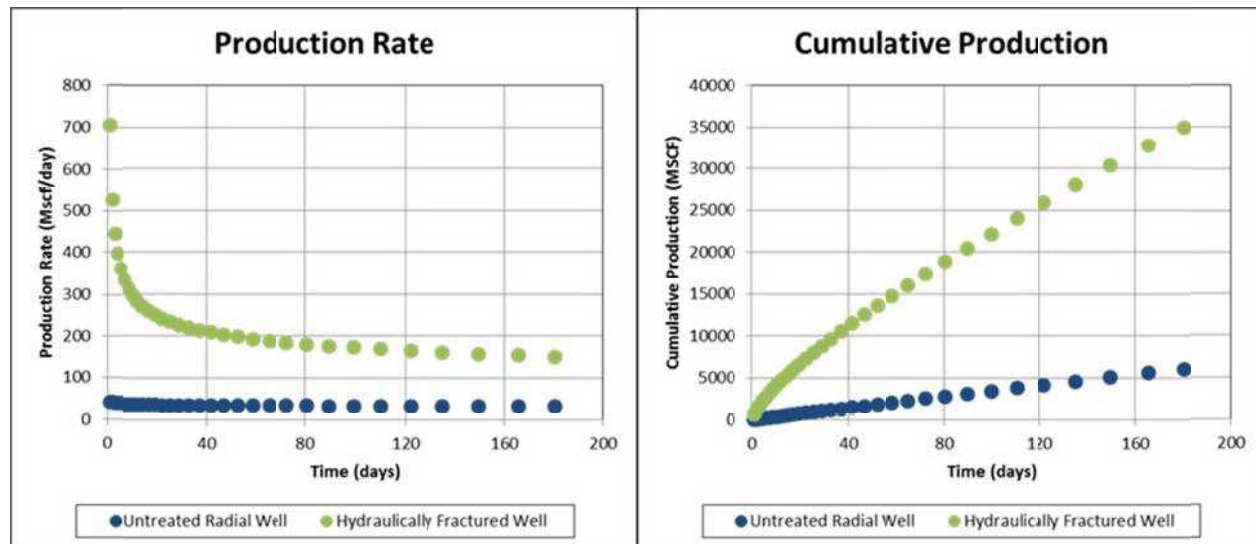


Fig. 4.5. Comparison of the production rate and cumulative production for untreated well and a well treated with hydraulic fracturing.

The figure given below illustrates a typical hydraulic fracturing operation along with surface equipment layout and a downhole view of the process.

Figure. 4.6a shows common hydraulic equipment used on surface in a typical fracturing operation. Fig. 4.6b illustrates a typical hydraulic fracturing operation and a downhole view of the process.

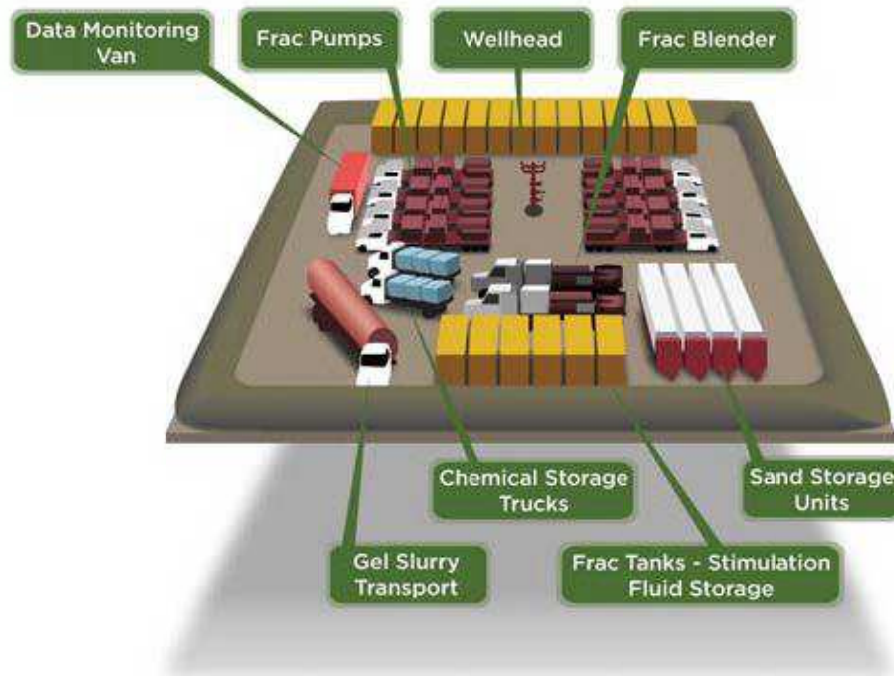


Fig. 4.6a. Illustration of common hydraulic fracturing equipment on surface (www.hydraulicfracturing.com)

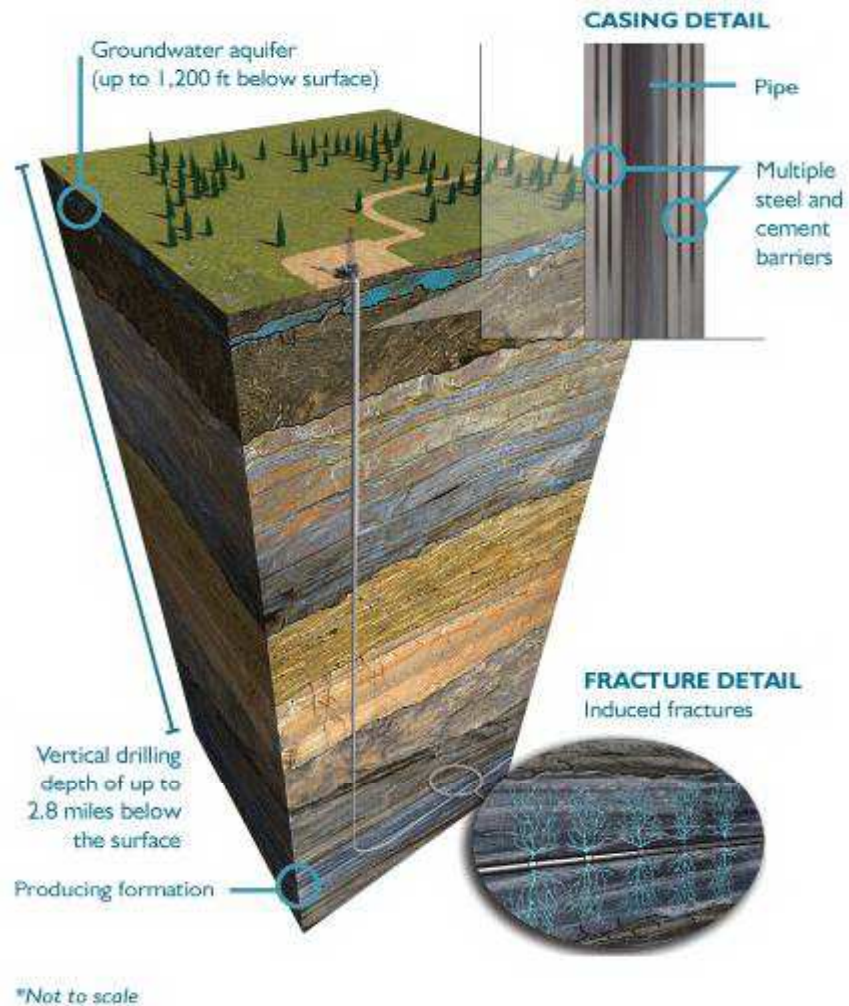


Fig. 4.6b. Illustration of common hydraulic fracturing equipment on surface (Source: Encana)

Hydraulic Fracturing - A Historic Perspective

The origin of hydraulic fracturing can be traced to the 1860s, when liquid nitroglycerin (NG) was first used to successfully stimulate oil wells in Pennsylvania, New York, Kentucky, and West Virginia. This principle was soon applied to natural gas and water wells. The first hydraulic fracturing treatment was performed by Stanolind Oil in 1947 in Grant County, Kansas, to stimulate a limestone formation in the Hugoton field at a depth of 2,400 ft. (Fig. 4.7). It's first commercial application was in 1949, and the success of this technique in increasing production from oil wells resulted in rapid adoption by the oil and natural gas industry.



Fig. 4.7. In 1947, Stanolind Oil conducted the first experimental hydraulic fracturing job in the Hugoton field, located in southwestern Kansas (Montgomery and Smith, 2010).

In 1948, the “Hydrafrac” process was introduced more widely to the industry in a technical paper presented by Stanolind Oil (Clark, 1949). A patent was issued in 1949, with an exclusive license granted to the Halliburton Oil Well Cementing Company (Howco) to pump the new Hydrafrac process. That year 332 wells in the United States were treated with an average production increase of 75%. By the mid-1950s, up to 3,000 wells were hydraulically fractured per month. Today, there are tens of thousands of hydraulic fracturing treatments pumped annually worldwide.

Fracturing fluid technology has evolved since the first treatments. Through the early-1950s, treatments used gelled crude oil or kerosene. Water became a viable fracturing fluid in 1953 as a number of gelling agents were developed. The early 1960s saw the introduction of crosslinked gels. In the early 1970s, the industry began using metal crosslinking agents. This allowed fracturing fluids to achieve the desired viscosity while using less gel. A majority of the fracturing treatments performed these days contain aqueous fluids, water or brines as the base fluid with a small amount of additives like surfactant, biocides, crosslinker, clay content and gel.

Note: Please refer to sections titled “Fracturing Fluid” and “What’s in Fracturing Fluid” on Page 47 for additional details.

Since Stanolind Oil introduced hydraulic fracturing in 1949, close to 2.5 million fracture treatments have been performed worldwide. Fracture stimulation not only increases the production rate, but is also credited with adding to reserves—9 billion bbl. of oil and more than 700 trillion ft³ of natural gas have been added since 1949 to US reserves alone—which otherwise would have been uneconomical to develop (Hydraulic Fracturing, JPT, December 2010).

Hydraulic fracturing has had an enormous impact on America's energy history, particularly in recent times. The ability to produce more oil and natural gas from older wells and to develop new production once thought impossible has made the process valuable for US domestic energy production. Without hydraulic fracturing, as much as 80% of production from formations such as gas shales would be, on a practical basis, impossible to recover.

Many fields would not exist today without hydraulic fracturing. In the US, these include the Sprayberry trend in west Texas; Pine Island field, Louisiana; Anadarko basin; Morrow wells, northwestern Oklahoma; the entire San Juan basin, New Mexico; the Denver Julesburg basin, Colorado; the east Texas and north Louisiana trend, Cotton Valley; the tight gas sands of south Texas and western Colorado; the overthrust belt of western Wyoming; and many producing areas in the northeastern US.

Why is Hydraulic Fracturing Needed?

Hydrocarbons are located in the pore space between grains of reservoir rock and are generally found in rock formations deep below the earth's surface (generally 5,000ft. to 20,000 ft., or more). At these depths, there may not be sufficient permeability to allow these hydrocarbon molecules to naturally flow from the rock into the wellbore at economic rates. In many reservoirs such as gas shales, the rocks have such low permeability (which is measured in the microdarcy to nanodarcy range) that the flow capacity of the rock is so low that hydrocarbons cannot naturally flow out of the rock into the wellbore. This is the case with the Nodular shale formation found in the Inglewood Oil Field.

Hydraulic fracturing is a requirement in low-permeability reservoirs to make it economical. In medium permeability reservoirs, it is done to accelerate recovery. In high permeability reservoirs, it is done to bypass near wellbore restriction to the formation (when present) and enhance production. Hydraulic fracturing increases the contact area between the well and the reservoir and allows for greatly increased hydrocarbon recovery.

Production can be achieved in such wells with the help of a reservoir stimulation method, i.e., hydraulic fracturing treatment. Fig. 4.8 illustrates how the hydrocarbon molecules flow from the reservoir to the wellbore.

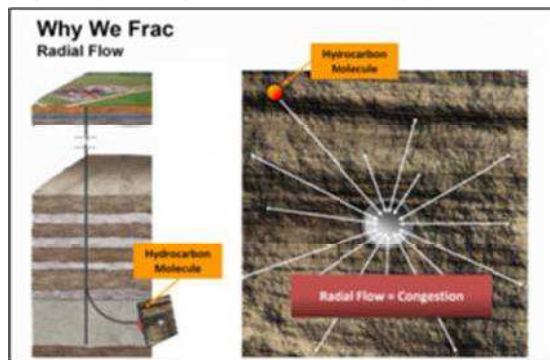


Fig. 4.8. Illustration of flow of hydrocarbon molecules from the reservoir to the wellbore.

Hydraulic Fracturing: The Process

The wellbore is constructed and stabilized as mentioned in Section 4.1 before the fracturing process begins. The hydraulic fracturing process involves the placement of proppant carried using a viscous fluid in the reservoir at the targeted depths.

The frac fluids used in the fracturing process (about 99.5% water and sand) pass down the well inside of the steel casing until they reach the zone to be fractured. The sand and proppant, carried by the fluid, occupies the newly created cracks in the rocks and holds them open. The propped hydraulic fracture then becomes a high conductivity conduit and creates passageways through which the formation fluids can be produced back to the well. A small percentage of additives (like surfactant, biocides, crosslinker, clay control, gel, etc.) are typically included to aid in the delivery of the fracturing treatment to the intended formation.

Note: Please refer to Section titled, "What's in Hydraulic Fracturing Fluid" on Page 41 for additional details.

At this point, the fracturing process is considered complete. On average, the fracturing process may require anywhere from 1 to 10 days to complete, depending on the number of zones to be treated.

Once the rock has been fractured, fracturing fluids are flowed back out of the well and in many cases recycled and reused or properly treated at permitted disposal facilities. Once the flowback water is removed, the newly stimulated well will produce oil or natural gas.

The equipment for the hydraulic fracturing treatment, e.g., pumps and trucks, and the associated traffic needed to do the job are removed. In most cases, the only equipment remaining typically consists of production valve and collection equipment.

The reservoir zones that are fractured are several thousand feet below the surface, far below the water-bearing bodies that supply drinking water. The hydrocarbon reservoirs are sealed by the surrounding rock formations and contain a finite amount of producible material. Hydrocarbon production is not related to water-bearing bodies near the surface except by the sealed wellbore that passes through the water zone on the way to the much deeper hydrocarbon zones.

Figures 4.9 a-f illustrate the hydraulic fracturing process in sequence.

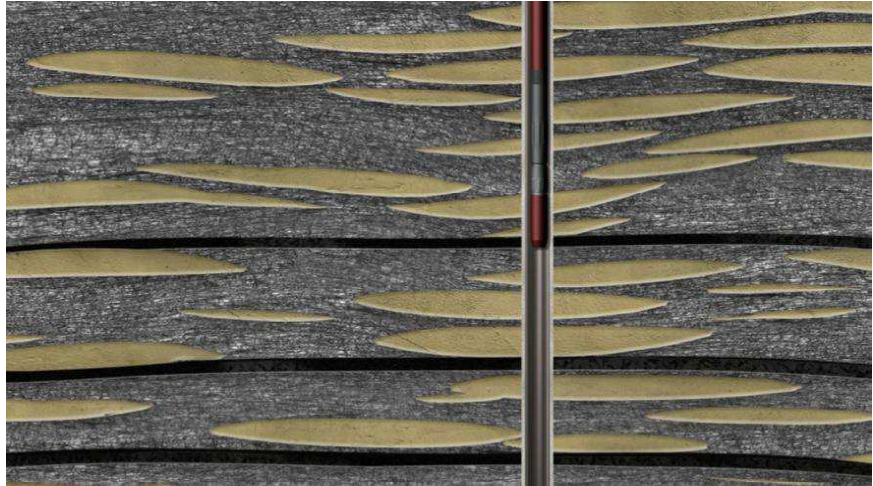


Fig. 4.9a. Well is drilled through a number of individual reservoirs.

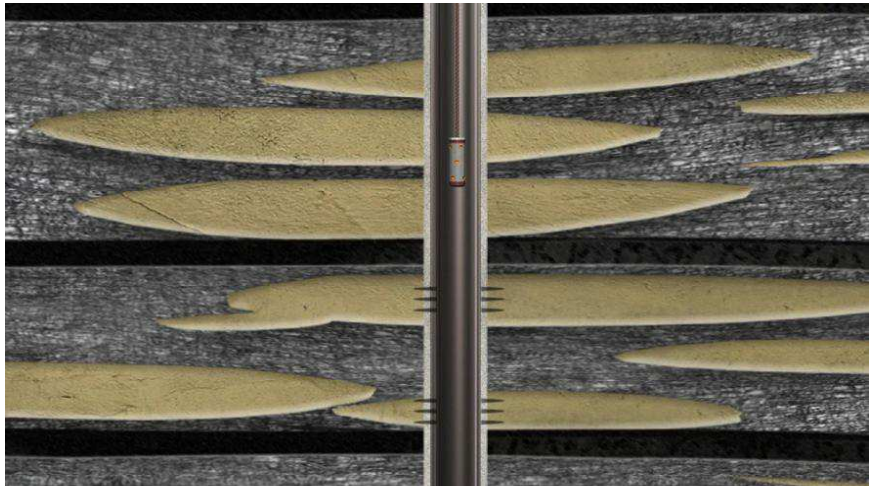


Fig. 4.9b. The target zones to be produced are perforated, typically using a perforating gun equipped with shaped charges.

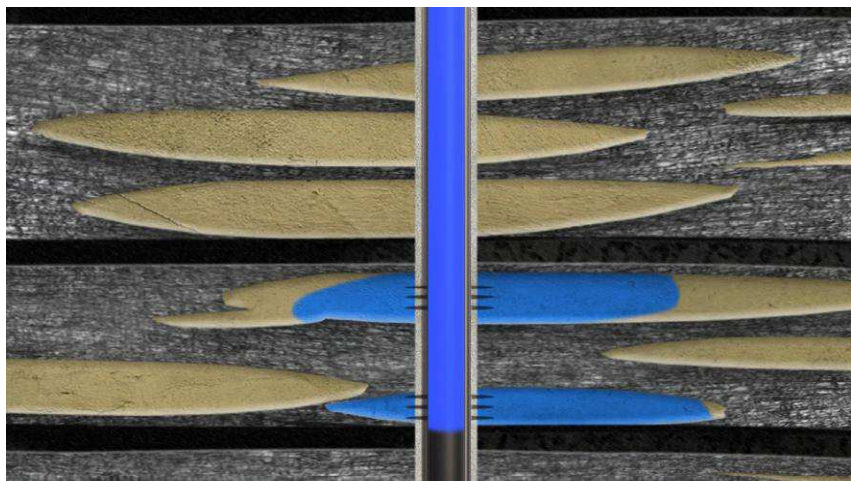


Fig. 4.9c. After perforating, fluid is pumped under pressure sufficient to crack (fracture) the reservoir rock.

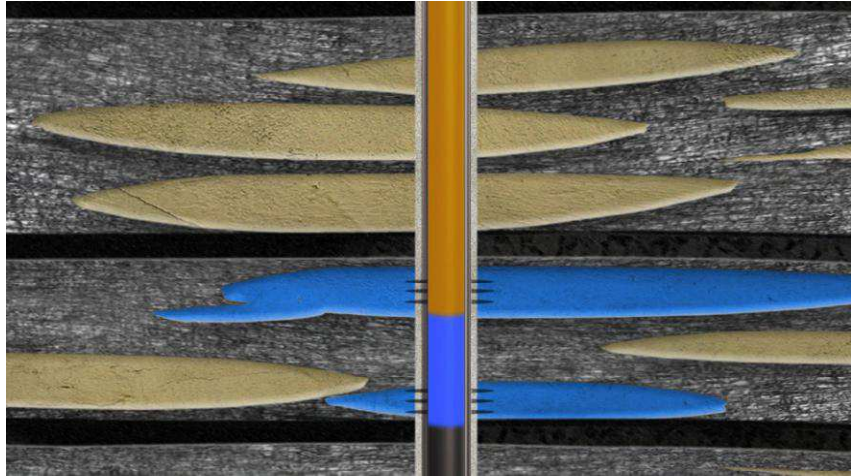


Fig. 4.9d. After the fracture is initiated, fluid carrying proppant is pumped into the fracture. The proppant will remain in the fracture to hold it open.

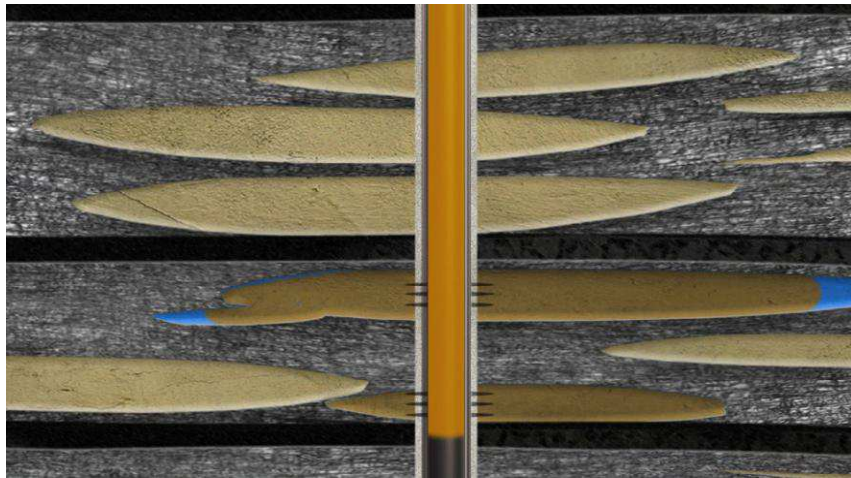


Fig. 4.9e. The Fracturing treatment of the two zones is complete and proppant is being removed from the wellbore.

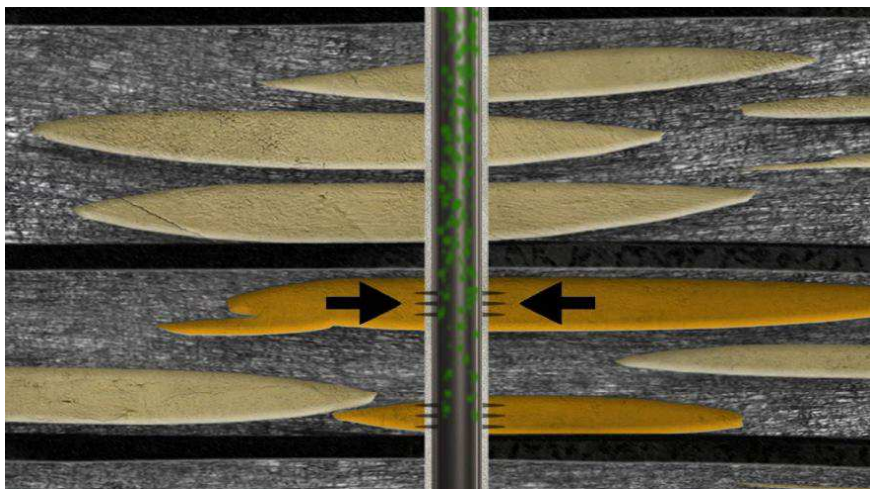


Fig. 4.9f. Wellbore and formation are clean and hydrocarbon production begins.

It should be noted that not all hydraulic fracturing fluid flows back. Fracturing fluid that does not flow out of the well is trapped in the hydrocarbon bearing formation or imbibed in the pore spaces in the rocks just like oil and gas had been trapped in the hydrocarbon bearing formation for millions of years.

Fracturing Fluid

The fracturing fluid may include a range of different fluids including water, gels, foams, nitrogen, carbon dioxide or even air in some cases. Aqueous fluids, water, and brines currently serve as the base fluid in approximately 96% of all fracturing treatments employing a propping agent.

The fracturing fluid has two major functions:

1. Create a tensile crack
2. Transport the proppant along the fracture length.

What's in Hydraulic Fracturing Fluid?

Today's fracturing fluids are primarily water and sand with a gelling agent and small percentage of different additives needed to modify reservoir conditions to improve flow, to clean the wellbore, prevent scale formation, and prevent bacterial growth in the well (Fig. 4.10). The mixture is approximately 99.5% water and sand and the rest 0.5% consists of highly diluted additives.

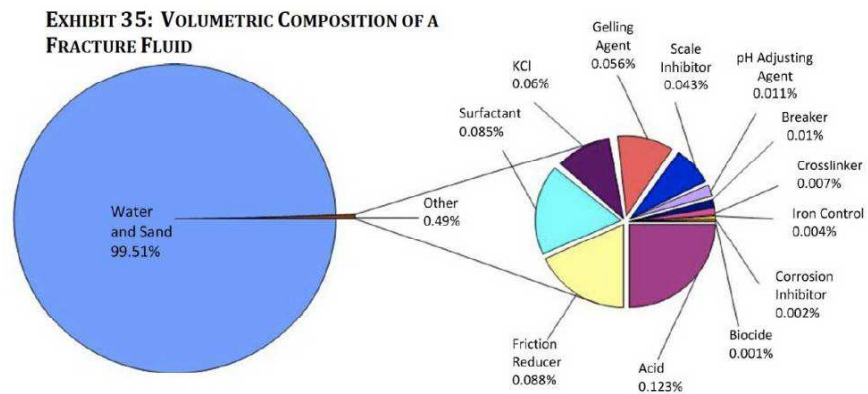


Fig. 4.10. Composition of a typical fracturing fluid (GWPC, 2009a).

These additives are common chemicals that are a part of our everyday lives. For example, the material used to make the fluid thick (viscous) is usually a natural polymer derived from guar beans—the same agent used in cosmetics, ketchup and soft ice cream. The exact formulation is variable and depends on the well conditions and reservoir characteristics. The Ground Water Protection Council (GWPC) has characterized the blend as “soap.”

The Ground Water Protection Council (GWPC) and the Interstate Oil and Gas Compact Commission (IOGCC) host a hydraulic fracturing chemical

disclosure registry called FracFocus at www.fracfocus.org. On the FracFocus website, the public can find a list and information about the additives used in hydraulic fracturing treatments. A broad range of industry participants including America's Natural Gas Alliance (ANGA), the Independent Petroleum Association of America and the American Petroleum Institute (API), support fracfocus.org.

Proppants

Proppant is solid material suspended in the fracturing fluid that holds the hydraulic fractures open. A variety of natural and manmade materials are used for proppant, including sand, resin-coated sand, and manmade ceramics. The selection of proppant is dependent on the stress conditions of the reservoir.

The concentration of sand (lbm/gal) proppant remained low until the introduction of viscous fluids, such as crosslinked water-based gel, in the mid-1960s allowed pumping higher sand concentrations. The varying sand concentrations are needed to achieve higher proppant distribution (in lbs./ft²) in the created fracture. Proppant distribution is related to conductivity in the reservoir.

Hydraulic Fracturing Treatment Steps

The placement of hydraulic fracturing treatments in the reservoir is sequenced to meet the particular needs of the formation. While hydraulic fracturing treatments are essentially the same for all wells, since every oil and gas zone is different, the steps and type of the fracturing treatment may change depending upon unique local conditions. Every fracture treatment must be tailored, i.e., specifically designed to meet local borehole and formation conditions. The "exact" hydraulic fracturing treatment blend consisting of fluid, sand and chemical additives and their proportions will vary based on the site-specific depth, thickness and other characteristics of the target formation.

The following example describes the different steps in a typical fracture treatment.

1. The hydraulic fracturing fluid pad stage (water with friction reducing additives), helps initiate the fracture and assist in the placement of proppant material.
 - a. Hydrochloric acid is used in some formations or hydraulic fracture treatments to reduce any near wellbore restriction or clear cement debris in the wellbore or to reduce fracture initiation pressures. The volume of acid used is low and it is spent (used up) within inches of the fracture entry point and yields calcium chloride, water and small amount of CO₂. No live acid is returned to the surface (George King, 2012, SPE 152596).
2. A proppant concentration stage, which may consist of several substages of water combined with proppant material. This stage may collectively use several hundred thousand gallons of water. The size of the proppant

material and the proppant concentration will vary during the treatment – starting with a lower concentration of finer particles and ramping up to higher concentrations of coarser particles.

3. A flush stage, consisting of a volume of fresh water or brine sufficient to flush the excess proppant from the wellbore.

Types of Hydraulic Fracturing Treatments

There are several different types of hydraulic fracturing treatments used in the industry that depend on the reservoir characteristics and area. The three most common types of hydraulic fracturing treatments are discussed below:

- A. **Conventional Fracture Treatments:** In this type of treatment, water is mixed with a polymer and a crosslinker to create a viscous fluid. Chemicals called breakers are pumped with the crosslinked gel and in combination with the elevated temperature in the formation, return the crosslinked gel to a viscosity approaching that of water after a predetermined time period, so that it can be recovered from the formation. Proppant is pumped along with the fluid and remains in the created fractures to hold them open. The primary advantage of gels fracs is that the higher viscosity of crosslinked gel, allows pumping of higher concentrations and larger size proppant material. Conventional gel treatments generate longer propped fracture lengths than a water frac (Rushing and Sullivan, 2003). However, gel fracs may leave some gel residue in the pore spaces of the formation. In a formation with small pores, such as low-permeability formations, the remaining gel can block the flow path of oil or natural gas to the well and reduce well production performance.
- B. **High Volume Hydraulic Fracture Treatments:** This type of fracture treatment consists of water with a very small percentage (typically less than 0.1%) of a friction-reducing chemical. Proppant is pumped along with the fluid and remains in the created fractures to hold them open. High volume hydraulic fracture treatments have limited fracture height growth. Also, since there is no gel residue, there is less risk of decreased well performance resulting from gel damage to the formation. However, the lower viscosity of the base fluid means that proppant placement in fractures is more difficult with high volume hydraulic fractures because the proppant falls out of suspension very quickly. This may affect well performance.
- C. **Hybrid Fracture Treatments:** Hybrid treatments are a type of hydraulic fracturing treatments (not high-rate gravel pack) that combine the advantages and benefits of both conventional gel and high volume hydraulic fracture treatments. They were developed in the early 2000s to improve stimulation effectiveness. In hybrid treatments, low-viscosity and hydraulic fracture treatment fluids with friction reducing additives are used initially to create the

fracture and then followed by a high-viscosity gelled fluid to place the high-concentrations of larger sized proppant.

Regulation

In 2009 the Ground Water Protection Council (GWPC) reviewed the oil and gas regulations issued by 27 states to protect groundwater. The study found that not all requirements related to casing and cementing wells are universally applied in each state studied, rather, they may only be applied on a case-specific basis (Fig. 4.11) (GWPC, 2009b).

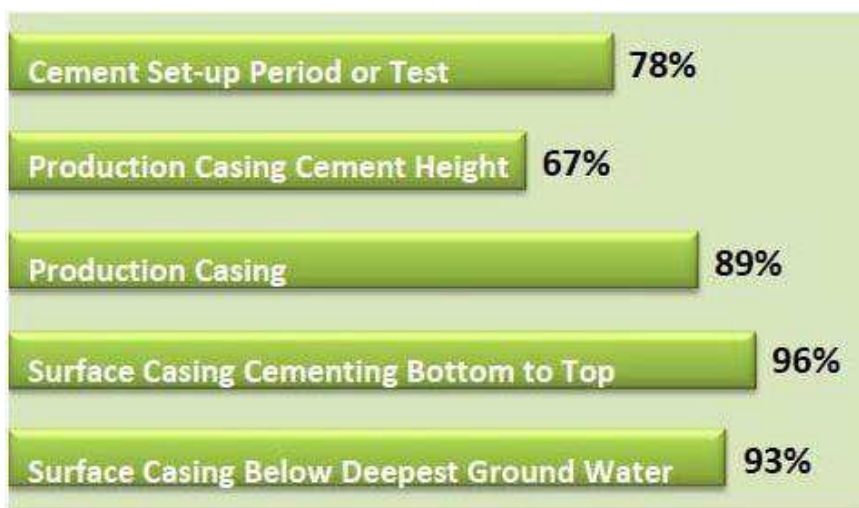


Fig. 4.11. Casing and cementing requirements by percentage of the 27 states reviewed (GWPC, 2009b)

More than 30 state and federal regulatory agencies, including the U.S. Department of Energy, the Interstate Oil and Gas Compact Commission and the Ground Water Protection Council have studied the oil and natural gas industry operations including hydraulic fracturing. The reports these agencies produced have concluded that the technology is safe and well regulated.

In California, DOGGR oversees the drilling, operation, maintenance and plugging and abandonment of oil, natural gas and geothermal wells (Source: www.conservation.ca.gov/dog/Pages/index.aspx).

DOGGR has strict guidelines on well design and well construction that operator's must comply with. DOGGR's well construction standards, consisting of the use of casing, mud, and cement, serve to prevent fluid migration and the commingling of lesser quality fluids. The hole and casing annulus space, between the top of the cement isolating the oil and gas zones and the base of the cement covering the BFW interface should have heavy mud to prevent the movement of fluids. (14 CCR §§ 1722.6 and 1723(b).) (Source: www.conservation.ca.gov).

The American Petroleum Institute (API) also provides guidance and recommended practices for well construction and well integrity for wells

that will be hydraulically fractured. The guidance provided by API helps to ensure that shallow groundwater zones will be protected.

Note: Please see Attachment 4A titled “Hydraulic Fracturing Operations – Well Construction and Integrity Guidelines” by API, First Edition, October 2009 for additional details.

Moreover, regular monitoring takes place during drilling and production operations to ensure that these operations proceed within established guidelines and in accordance with the well design, well plan, and permit requirements. Finally, the integrity of well construction is periodically tested to ensure well integrity is maintained.

Frac Packs

In the Baldwin Hills, the majority of the wells are completed using frac packs. This process is different from the hydraulic fracturing stimulation techniques used for tight sands, gas shale and coal gas recovery.

The frac pack completion technique involves two distinct injection stages performed in a single step that are discussed in Section 9.

The frac packs will be referred to as “high-rate gravel packs (HRGP)” in this report.

Note: Please refer to section 9 for additional details and discussion on “high-rate gravel pack treatments”.

References

API, 2009, Hydraulic fracturing operations—well construction and integrity guidelines: API Guidance Document HF1, 1st edition, 24 p.

API, 2010, Freeing up energy; hydraulic fracturing—unlocking America’s natural gas resources.

Clark, 1949, Hydrafrac process for well treatment, paper 826-20-A presented at the American Petroleum Institute, Production Division Spring Meeting Eastern District, Pennsylvania: Transactions AIME, v. 186, p. 1-3.

Ground Water Protection Council and ALL Consulting, 2009a, Modern shale gas development in the United States—A primer: U.S. Department of Energy, National Energy Technology Laboratory, 96 p.

Ground Water Protection Council, 2009, State oil and natural gas regulations designed to protect water resources: U.S. Department of Energy, National Energy Technology Laboratory, 63 p.

Montgomery, C.T., and Smith, M.B., 2010, Hydraulic fracturing—History of an enduring technology: Society of Petroleum Engineers, www.JPTonline.org.

Rushing, J.A., and Sullivan, R.B., 2003, Evaluation of a hybrid water-frac stimulation technology in the Bossier tight gas sand play, SPE-84394,

presented at the 2003 SPE Annual Technical Conference and Exhibition:
Society of Petroleum Engineers, 11 p

George E. King, 2012, Hydraulic Fracturing 101: What every representative, environmentalist, regulator, reporter, investor, university researcher, neighbor and engineer should know about estimating frac risk and improving frac performance in unconventional gas and oil wells, SPE-152596, presented at the 2012 SPE Hydraulic Fracturing Technology Conference held in The Woodlands, Texas, USA, 6-8 February 2012.

5. Hydraulic Fracturing and HRGP Analysis

5.1. Methodology to Perform Pressure History Matching

This section provides a detailed description of the methodology used to perform the pressure history matching that was conducted to analyze the wells for Inglewood Oil Field study. The word “history” refers to the earlier hydraulic fracturing stimulation treatments conducted at the field.

Pressure History Matching is the process of matching the actual fracturing treatment pressure curve with a simulated curve generated by a calibrated frac model. This is an iterative computational process in which the frac model is run using different values for reservoir and rock properties, while at the same time honoring the observed values obtained from logs, core, step down, Diagnostic Fracture Injection Test (DFIT) or experience, until an acceptable match is obtained.

This process helps to build a calibrated fracture model and also helps identify critical reservoir characteristics and parameters.

Data Validation and Pressure History Matching Steps

A description of the steps in the methodology used to perform history matches for the different fracturing stages in different formations in the Inglewood Oil Field follows.

- Well Log Data – Triple-combo logs (the term Triple Combo is derived from the three principle measurements collected by the tool string – resistivity, density and porosity) were available in all formations for all the wells analyzed in this report.
 - In the Vickers and Rindge formation, no dipole sonic logs were available and only limited core information was available. The *.LAS files were imported in the GOHFER model and reservoir and geologic properties were set in the model based on the available information from logs, research papers and publications, and before treatment step-down/minifrac analysis.
 - Dipole sonic information for an offset well was available from 6,000 ft. and deeper. The dipole sonic log provides information regarding the formation stresses. For the Sentous and Nodular formations, the triple combo and dipole sonic log data was processed to create an input log file for GOHFER model.
 - Core data were also available for the wells in the Nodular formation. The processed log data for the Nodular formation were also calibrated against the core data to honor the rock properties data provided by core testing.

- Grid – A grid with the following dimensions was used for all the stages of wells in all formations:
 - Grid cell size – 5 ft. X 10 ft.
 - Number of columns – 200
 - The total height of the reservoir grid varied for each stage and depended on the height of the perforation interval and relevant formation thickness. To provide enhanced visualization the length of the grid was adjusted based on the length of the fracture created.
- Real-Time Fracture Data – Real-time frac data recorded at a 1-sec interval in the field during the fracturing job were imported into the GOHFER model for each stage

Step-Down Tests were conducted for all of the stages, wherever data were available, for the analyzed wells in the Vickers and Rindge formation and for all the stages in the 2 wells analyzed in the Sentous formations. Minifrac Analysis was performed on the step-down tests, wherever available, to determine critical reservoir parameters, such as closure pressure, permeability, pressure dependent leakoff, and process zone stress. The values obtained for these parameters were taken into consideration while performing the history match.

What is Step Down Analysis?

Step-down analysis is used to calculate perforation and near wellbore friction losses and determine the number of holes open. A step-down test analysis of rate verses pressure is done to determine the number of perforations open and also near wellbore friction to enable calculation of the power-law coefficient required for calibrating injection pressures. This analysis is used to determine near-wellbore pressure loss effects (i.e., problems with anomalously high pressures that may result in a near-wellbore screenout).

This analysis is performed after fracture propagation has been established. Then during shut down the rate is decreased in a stair-step fashion for a short period of time while the pressure stabilizes. As the injection rate decreases, the pressure also decreases as a result of perforation and near-wellbore pressure losses. The relationship between the decreasing rate and pressure results in a determination of near wellbore pressure losses.

- Diagnostic Fracture Injection Tests were performed in both wells in the Nodular formation, VIC1-330 and VIC1-635. The parameter values obtained from these tests were taken into consideration while performing the history match.

Diagnostic Fracture Injection Test (DFIT)

A DFIT uses a small-volume, low-rate fluid injection followed by an extended shut-in period to evaluate individual zones. As the pressure leaks off and declines, high-resolution pressure data are recorded. These pressure data are analyzed to determine several essential reservoir parameters needed

in designing and optimizing the fracture treatment and that are also used to estimate:

- Reservoir Pressure
- Permeability
- Closure Pressure
- Pore Pressure
- Leakoff

For many low permeability reservoirs, a DFIT represents the only opportunity to determine these properties. Consistent results have been obtained from DFIT tests conducted in all types of unconventional reservoirs, such as gas shales and tight-gas sandstones.

The reservoir parameters obtained from DFIT analysis are then used in the GOHFER analysis of hydraulic fracturing stimulation treatments.

GOHFER[®]

The Grid Oriented Hydraulic Fracture Extension Replicator (GOHFER[®]) fracture simulation software was used to perform the history match. The model was run with all log and frac data imported in it until an acceptable match was obtained.

GOHFER[®] is a planar 3-D geometry fracture simulator with a fully coupled fluid/solid transport simulator that is used for the design, analysis and optimization of hydraulic fracture stimulation treatments. The software allows direct importing of digital log data and has a built-in log analysis package to create a more accurate lithological description. The GOHFER[®] simulator allows modeling of multiple fracture initiation sites simultaneously and shows diversion between perforations. Fluid composition, proppant concentration, shear, leakoff, width, pressure, viscosity and other state variables are defined at each grid block.

Note: Please refer to Attachment 5A titled “SPE Paper 107972” for the rationale for choosing GOHFER.

5.2. Well List for Hydraulic Fracturing Report

Eight wells were selected (Table 5.1) for use in the hydraulic fracturing study.

- 4 wells in the Vickers and Rindge zones
- 1 well in the Moynier zone
- 2 wells in the Nodular zone
- 2 wells in the Sentous zone

Note: The well analyzed in the Moynier zone was the same as one of the 2 wells in the Sentous zone.

High-rate gravel-pack treatments were used in the analyzed wells in the Vickers and Rindge zones and hydraulic fracture stimulation treatments were used in the other zones. A total of 21 high-rate gravel pack treatments and 8 hydraulic fracturing stimulation treatments were history matched (pressure matched) and analyzed for this Inglewood Oil Field Frac Report.

Table 5.1. Wells used in the Inglewood Oil Field Fracturing Study.

Well Name	Well #	Formation Completed	Type of Treatment	Number of Frac Stages
VRU	4243	Vickers and Rindge	High-Rate Gravel Pack	5
BC	285			6
Stocker	461			4
TVIC	274			6
TVIC	1033	Sentous	Hydraulic Fracture Stimulation	2
VIC2	1133			1
VIC2	1133	Moynier	Hydraulic Fracture Stimulation	3
VIC	330	Nodular	Hydraulic Fracture Stimulation	1
VIC	635			1

Well Selection Criteria

The wells were selected to analyze all the above listed formations.

Selection criteria included location within the field and with respect to the faults, i.e., on both sides of major faults, and the availability and accuracy of existing data, e.g., fracturing treatment, well logs, and reservoir properties.

Figure 5.1 is an aerial photo (map) view and Fig. 5.2 a side view of the Inglewood oil field showing the study well locations.

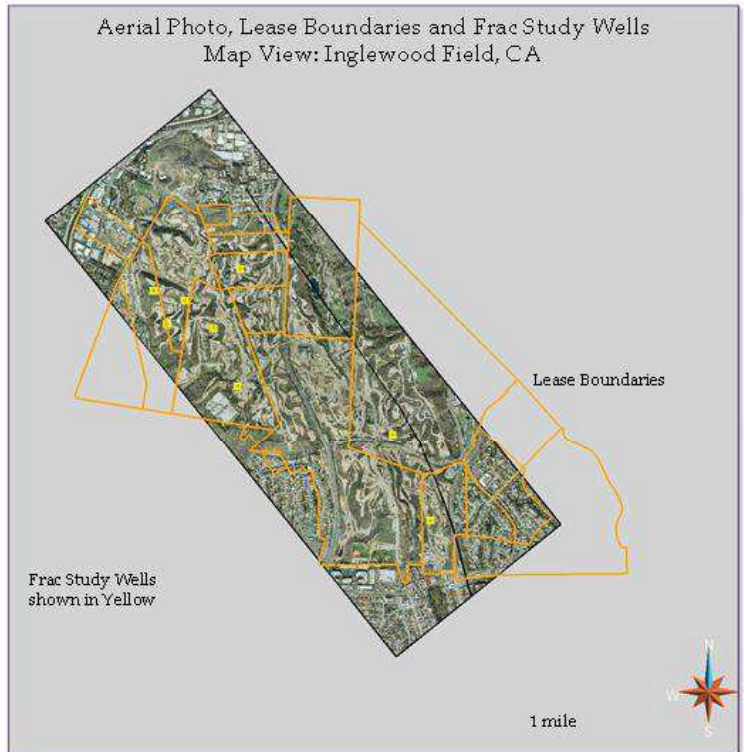


Fig. 5.1. Aerial photo of the Inglewood Oil Field showing the locations of the wells used in this fracture report.

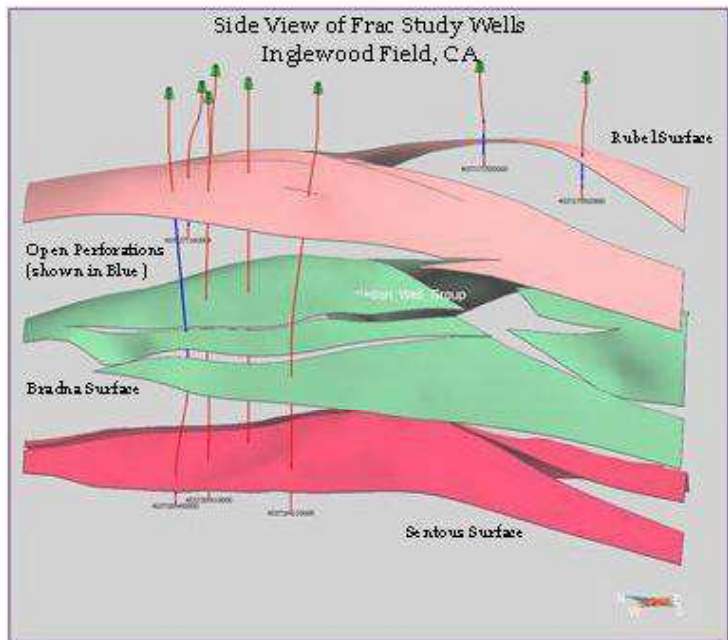


Fig. 5.2. Side view of the Inglewood Oil Field showing the locations of the fracture report wells and reservoir zone surfaces.

5.3. High-Rate Gravel Pack Analysis (HRGP)

High-rate gravel pack (HRGP) treatments were performed in the Vickers and Rindge zones of the Inglewood Oil Field. The analysis of the HRGP treatments in the Vickers and Rindge zones is discussed below.

A brief summary of the Vickers and Rindge zone is provided before the HRGP analysis.

The created HRGP geometries (as predicted by the GOHFER model) were imported into the earth model to provide visualization and a better understanding of the HRGP in relation to the formations and discontinuous groundwater bodies near the surface.

Note: Please refer to section 9 for additional details and discussion on “high-rate gravel pack treatments”.

5.3.1. Vickers and Rindge Formation

Introduction

Most of the treatments performed in the Vickers and Rindge zone are HRGP treatments. Some gravel pack treatments have also been done. The reservoir is already porous and permeable enough that it does not require conventional hydraulic fracturing.

The Inglewood Oil Field located along the Newport-Inglewood Fault trend has undergone several phases of development since its discovery in 1924. Sands within the shallow Pliocene Vickers and Rindge zones, subunits of the Pico and Repetto Formations (Fig. 5.3), are the traditional targets in this field and have accounted for more than 60% of total cumulative production at the Inglewood field (Moodie et al., 2004).

The Vickers and Rindge formations consist of a 1,200 to 1,800+ ft. sequence of friable turbidite sands that range in depth from 1,000 to 3,000 ft. The individual sands in these zones are numerous but not individually thick and represent distal turbidite deposition (Webster, 1987). Lateral continuity of the sand packages is good but vertical communication across the laminated intervals is very poor. The best permeability, 100+ md, is found at the top of the Vickers and decreases with depth to less than 50 md. Porosities range from 33% in the shallowest sands to 27% in the deeper sands (Moodie et al., 2004).

There is abundant and complicated normal faulting through the Vickers and Rindge zones. Most of these normal faults act as barriers to fluid flow due to juxtaposition of the sands. Structural dips in these zones are generally less than 20 degrees (Moodie et al., 2004).

The shallow and extensive Vickers and Rindge zones have produced more than half of all the oil historically produced at the field.

Stratigraphic Column Showing Vickers and Rindge Formations

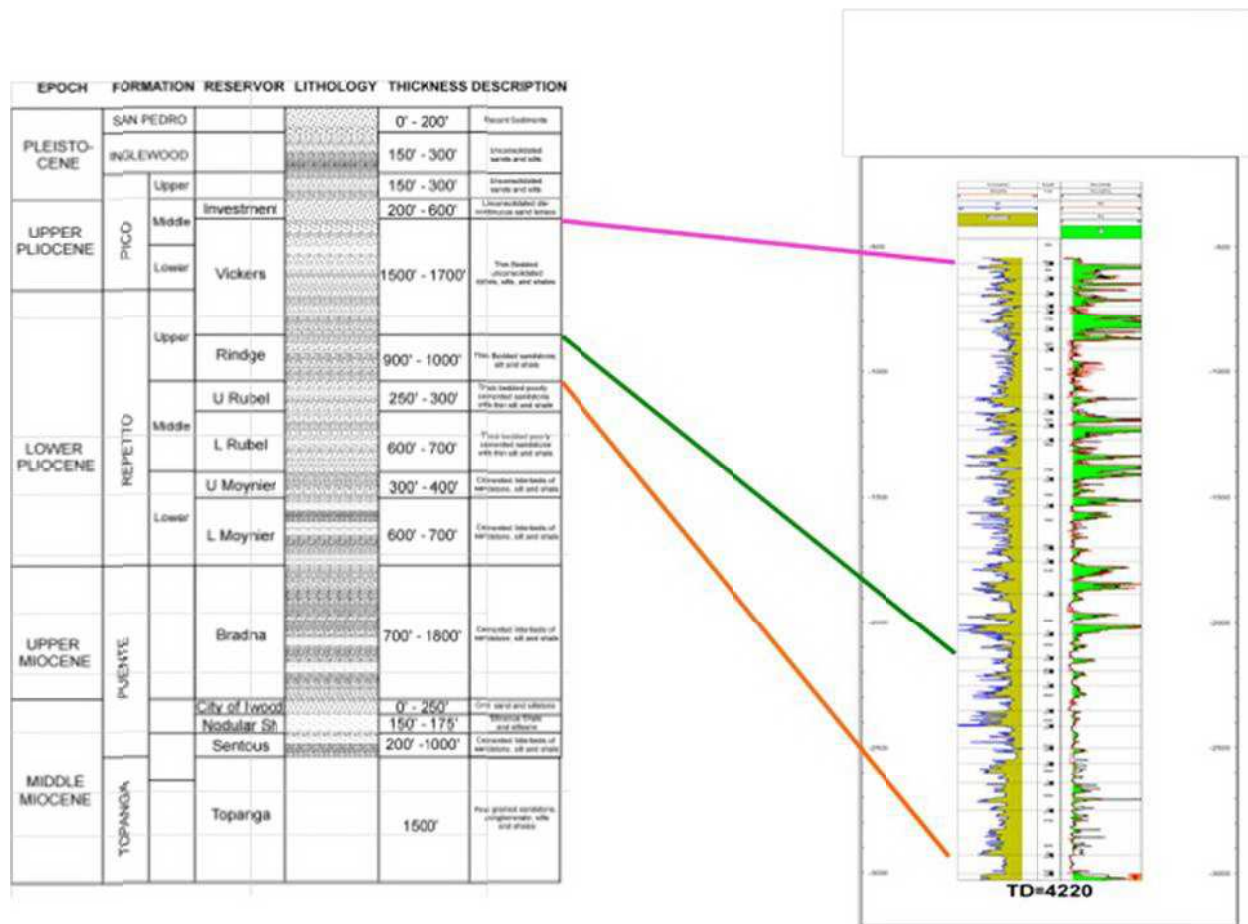


Fig. 5.3. Inglewood Oil Field stratigraphic column showing the position of the Vickers and Rindge zones (Lockman, 2005) and well log from that zone.

Well Selection List and Criterion for Analysis

Four wells that had been previously completed in the Vickers and Rindge zones using high-rate gravel pack treatments were selected for analysis: VRU-4243, TVIC-274, Stocker 461, and BC-285. The wells were selected because of their location within the field and with respect to the faults. Wells were picked on both sides of major faults. The availability and accuracy of the data (frac treatment, log data, reservoir properties etc.) also played a role in the well selection process.

Summary of Pressure History Match Analysis

Twenty-one independent high-rate gravel pack treatments from the four wells selected in the Vickers and Rindge zones were pressure history matched using the GOHFER frac model.

Note: GOHFER is a frac simulator, however the high-rate gravel pack treatments were analyzed using GOHFER to get a comparison and understanding of the gravel pack geometries. Experts in the industry have

used GOHFER to analyze similar type of high-rate gravel pack treatments and believe that it does a better job than any other model that they have applied.

The Appendices contain the final values used to obtain the history matches and the HRGP geometries for the different stages using the calibrated model after history matching.

The results of the pressure history match of the Vickers and Rindge in GOHFER model showed the following:

- The height created by the high-rate gravel packs in the Vickers and Rindge formations (as predicted by GOHFER frac model) was, on average, in the range of 100 to 170 ft. for the majority of the stage. The HRGP height in several stages was around 200 to 240 ft.
- The HRGP height is very small in relation to the depth of the fracture.
- The top of the created HRGP is at least 1,000 ft. below from the bottom of the deepest perched water zones in the area that includes the Inglewood Oil Field.

Note: Please refer to Appendix A titled “High-Rate Gravel Pack Analysis Results for Wells in Vickers and Rindge Formation” for detailed results and analysis of history matching.

HRGP Analysis Results

Figures 5.4a - f present different visualizations of the HRGP geometries predicted by the calibrated GOHFER model based on data from the high-rate gravel-pack treatments. The figures also show the relevant formation surfaces, ground surface, geologic structure including major faults, and discontinuous groundwater bodies near the surface.

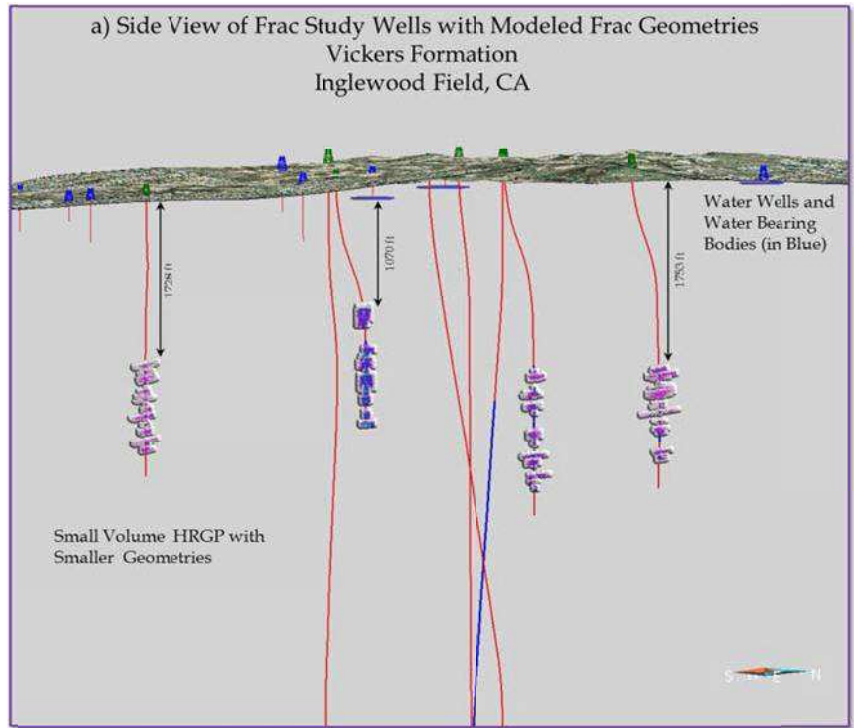


Fig.5.4a. Side view showing modeled HRGP geometries in the Vickers zone.

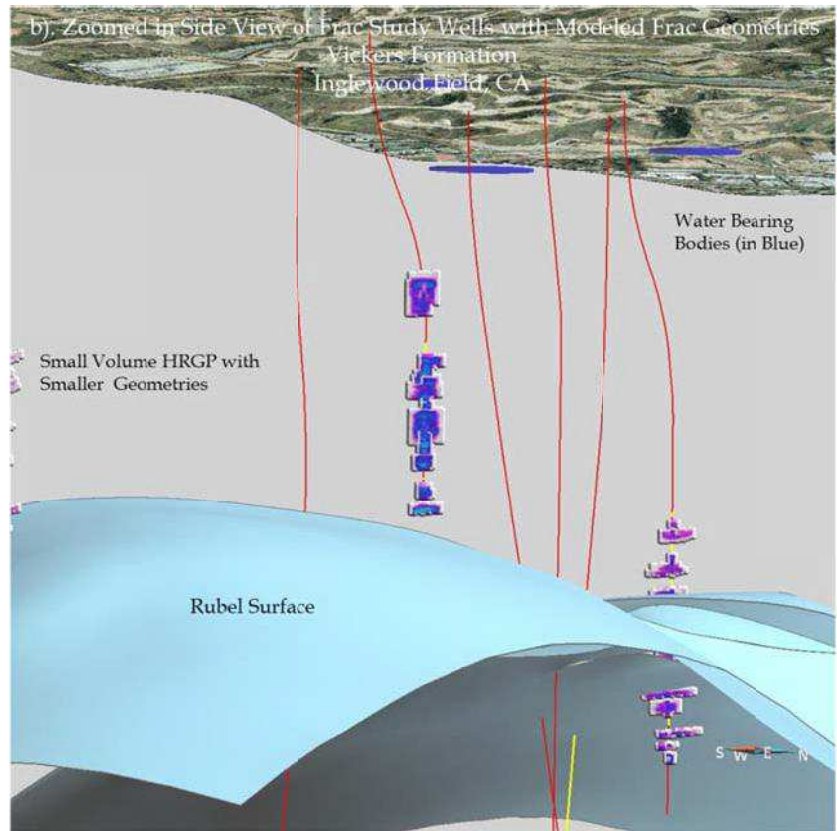


Fig. 5.4b. Zoomed in side view showing modeled HRGP geometries in the Vickers zone.

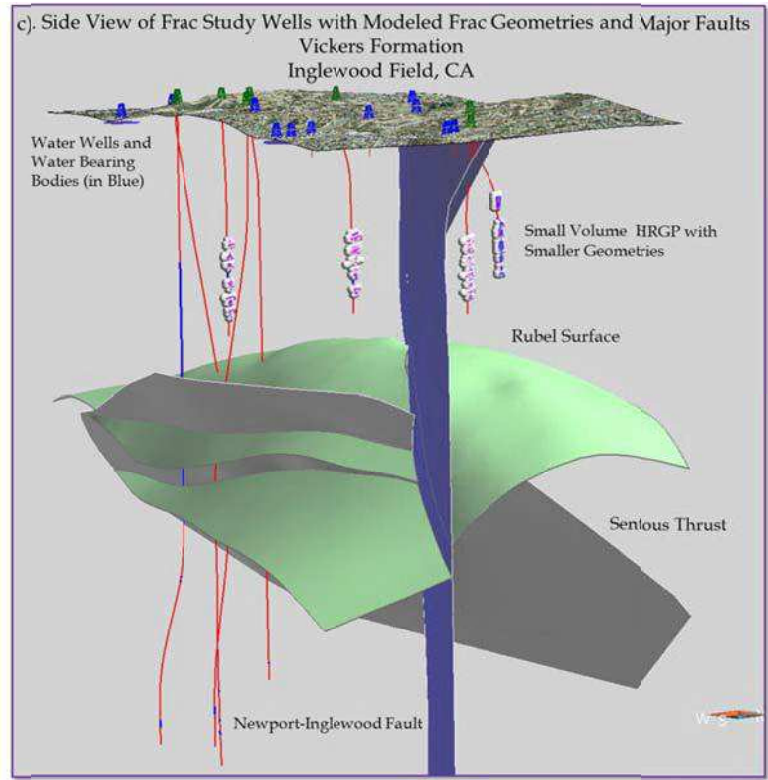


Fig. 5.4c. Side view showing modeled HRGP geometries in the Vickers zone and structure (faults).

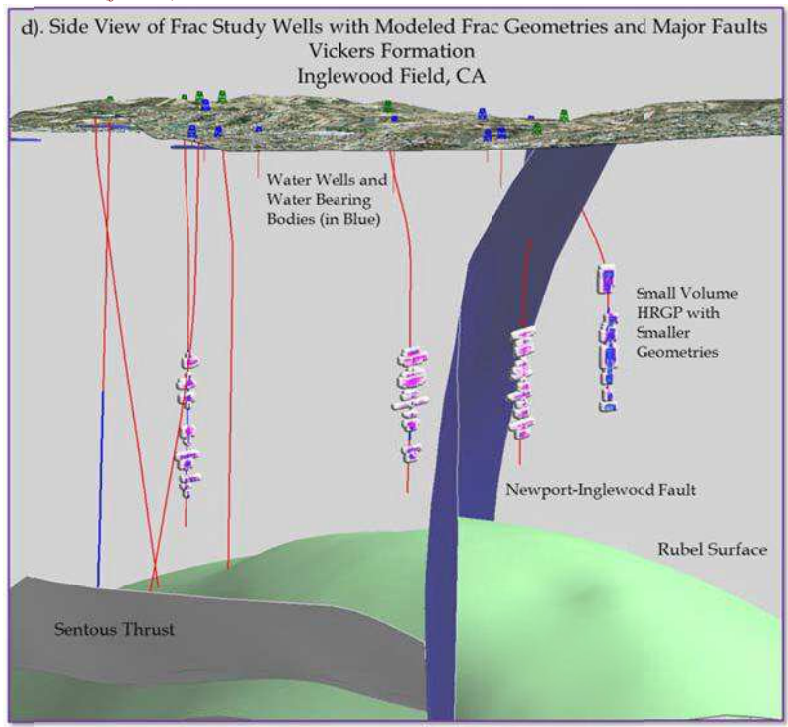


Fig. 5.4d. Side viewing showing modeled HRGP geometries in the Vickers zone and major faults.

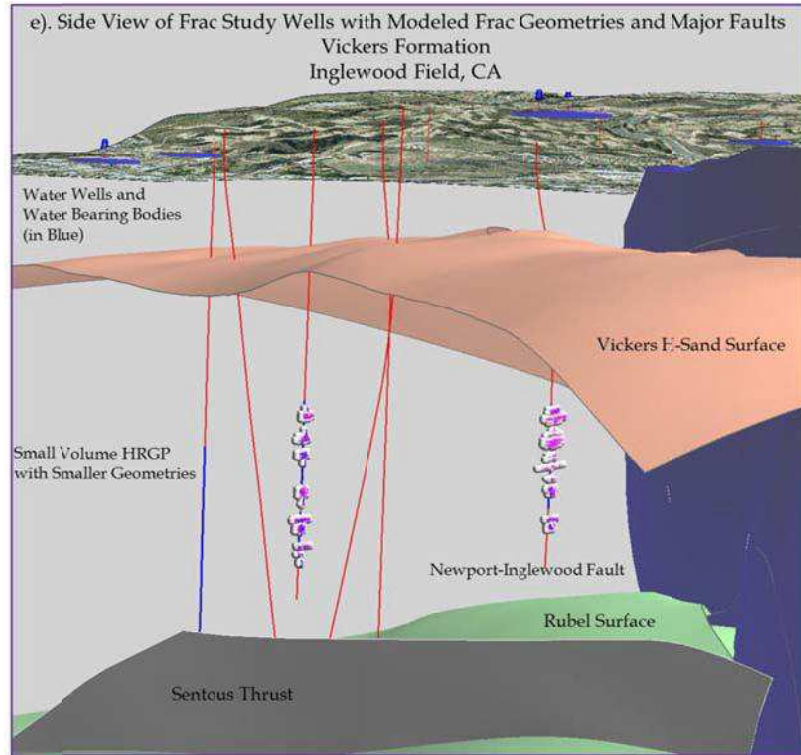


Fig. 5.4e. Side view showing modeled HRGP geometries in the Vickers zone and major faults.

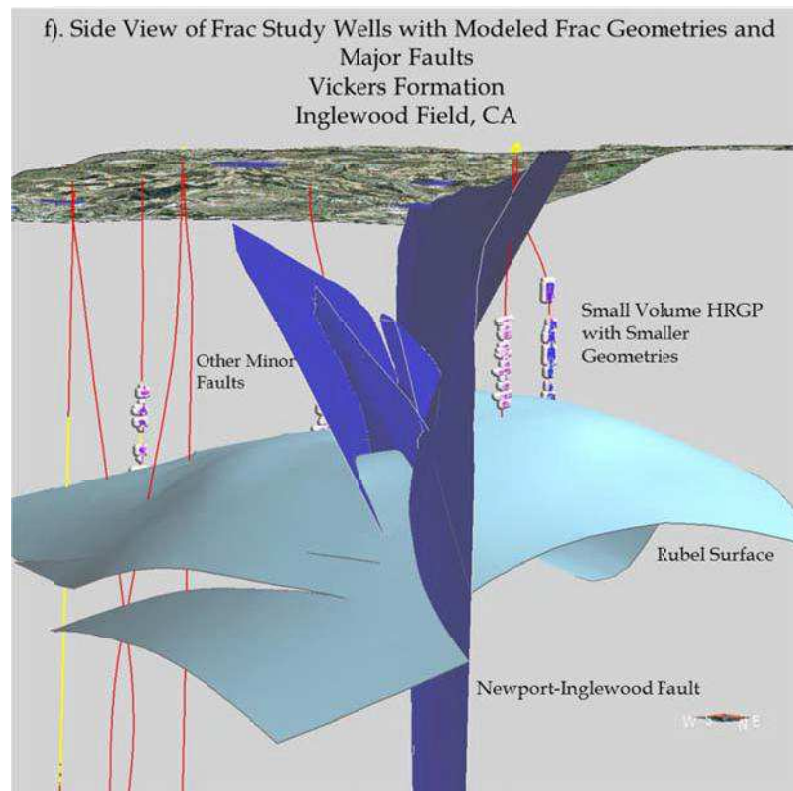


Fig. 5.4f. Side view showing modeled HRGP geometries in the Vickers zone and major faults.

5.4. Hydraulic Fracturing Analysis Results

Hydraulic fracturing treatments were performed in the other zones – Sentous, Nodular and Moynier. The analysis of the hydraulic fracturing stimulation treatments in the Sentous, Nodular and Moynier zones is discussed below.

The reservoir zones are discussed in the order of their geologic age, from oldest to youngest. A brief summary of each formation or reservoir zone is provided before the hydraulic fracturing analysis.

The created fracture geometries (as predicted by the GOHFER model) were imported into the earth model to provide visualization and a better understanding of the fractures in relation to the formations and the discontinuous groundwater bodies near the surface.

5.4.1. Sentous Formation

The Sentous zone is the oldest producing zone in the Inglewood Oil Field and also along the Newport-Inglewood fault trend. The Sentous zone is a member of the Puente Formation (Fig. 5.5). Since the early 1990s, the exploration and development focus in the Inglewood oil field has been on the Lower Pliocene and Upper and Middle Miocene, particularly the Sentous unit.

Sentous sands were deposited in approximately 1,000 ft. water depth, during the opening of the rifted basins of the Southern California continental borderland. Interbedded shales contain a microfauna of the Luisian stage, now considered early Middle Miocene—about 14 to 15 ma. Oil has accumulated in the Sentous sands down the northwest plunge of the Inglewood anticline. However, the sands become impermeable higher up on the anticlinal crest due to filling of the pore spaces with calcite cement which is believed to have been introduced by volcanic intrusives (diabase, basalt, andesite) which are localized in the vicinity of the Inglewood fault. This loss of permeability has created a stratigraphic trap for this reservoir (Wright, 1987).

Stratigraphic Column Showing Sentous Formations

The Sentous lies below the Moynier, Bradna, and Nodular Shale formations in the Inglewood Stratigraphy. Fig. 5.5 shows the Sentous formation in the stratigraphic column of the Inglewood field.

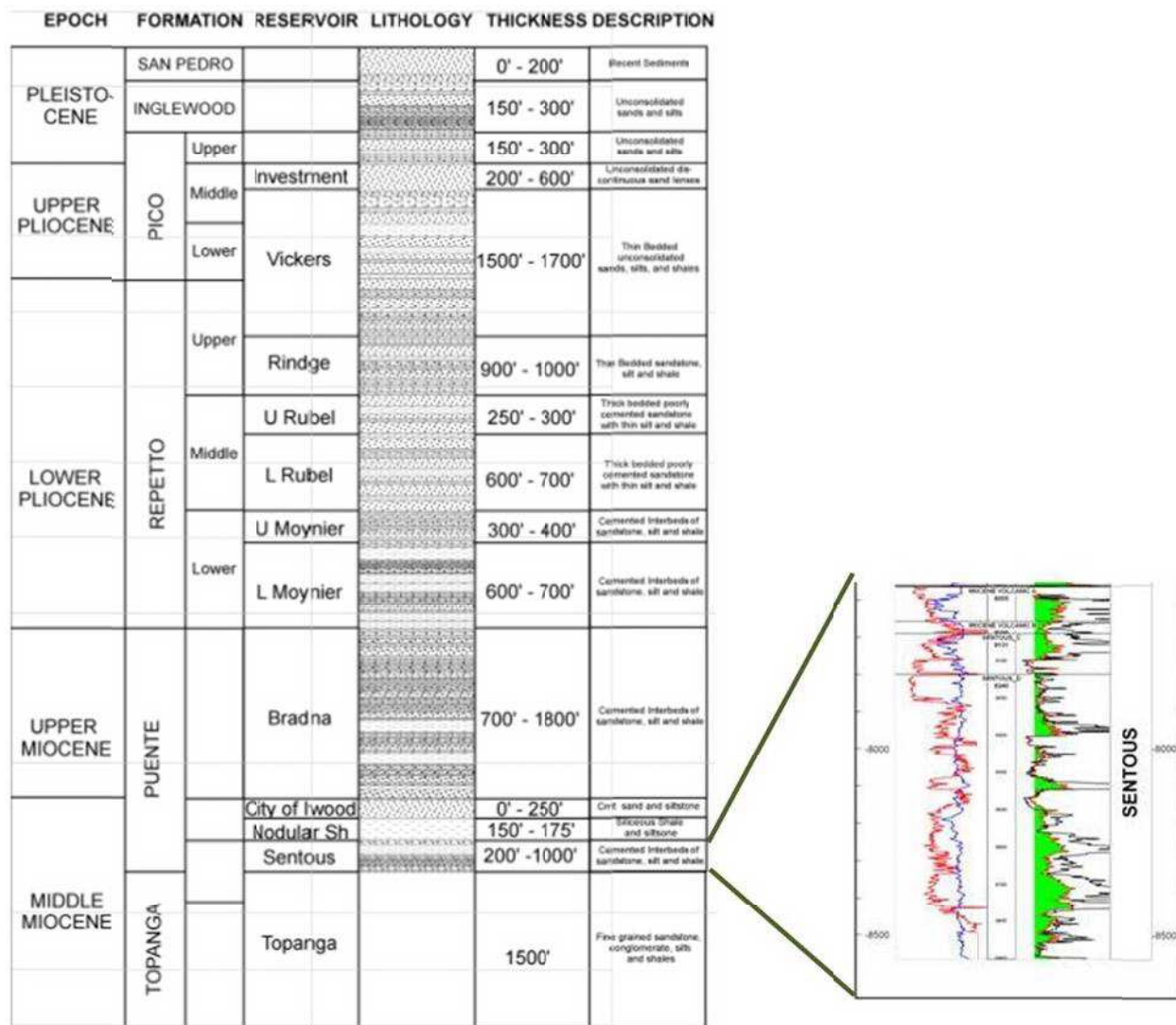


Fig. 5.5. Stratigraphic column for the Inglewood Oil Field showing the various reservoir zones (Lockman, 2005).

Well Selection List and Criterion for Analysis

Two wells, TVIC-1033 and VIC2-1133, were selected for Sentous zone analysis. The Sentous formation is located below all the faults. While fault location was not a factor in the selection of these wells, the availability and accuracy of data in the Sentous zone played a key role in the well selection process.

Summary of History Match Analysis

Three independent hydraulic fracturing stimulation treatments for the two wells were history matched using the GOHFER fracture model. The final parameters values used to obtain the history matches for each fracture stage of each well and the fracture geometries obtained for the different fracture stages using the calibrated model after history matching are provided in the Appendices.

Note: Please refer to Appendix D titled “Fracturing Analysis Results for Wells in Sentous Formation” for detailed results and analysis of the history matching

Frac Analysis Results

Figures 5.6a-e present different visualizations of the fracture geometries predicted from the hydraulic fracturing treatments by the calibrated GOHFER model. The figures include the relevant formation surfaces, ground surface, geologic structure including major faults, and discontinuous groundwater bodies near the surface.

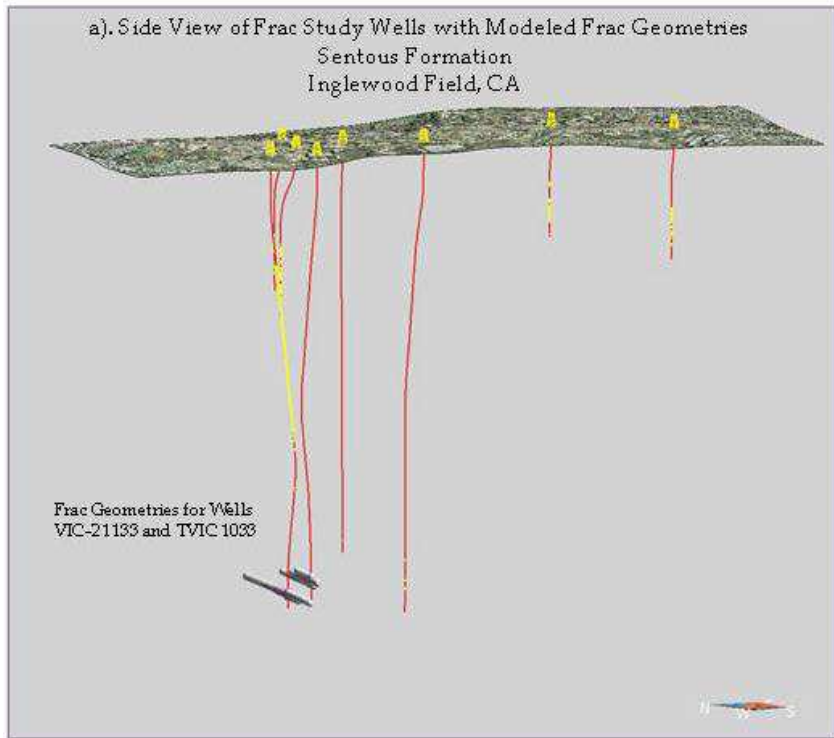


Fig. 5.6a. Side view of the Sentous zone modeled fracture geometries.

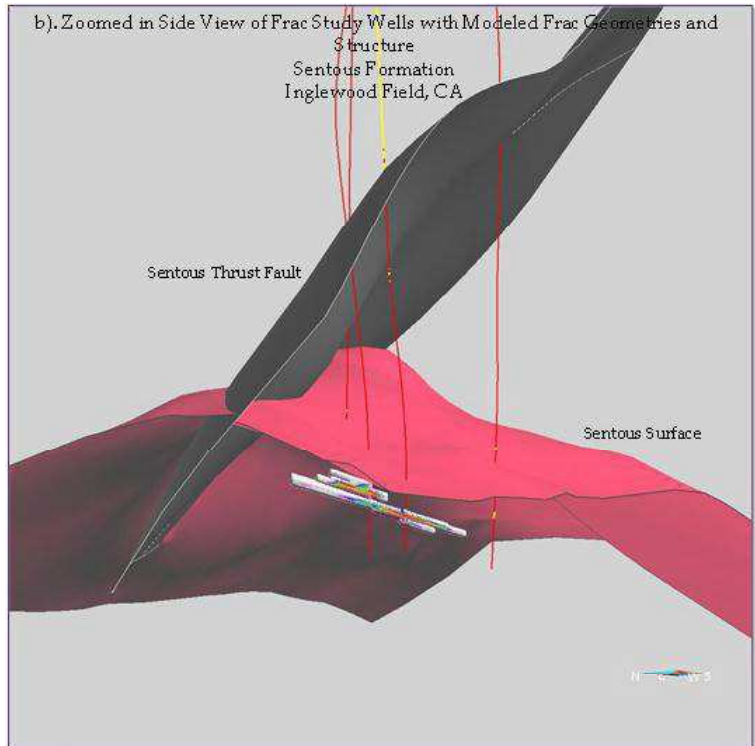


Fig. 5.6b. Zoomed in side view of Sentous zone modeled fracture geometries with structural features (faults).

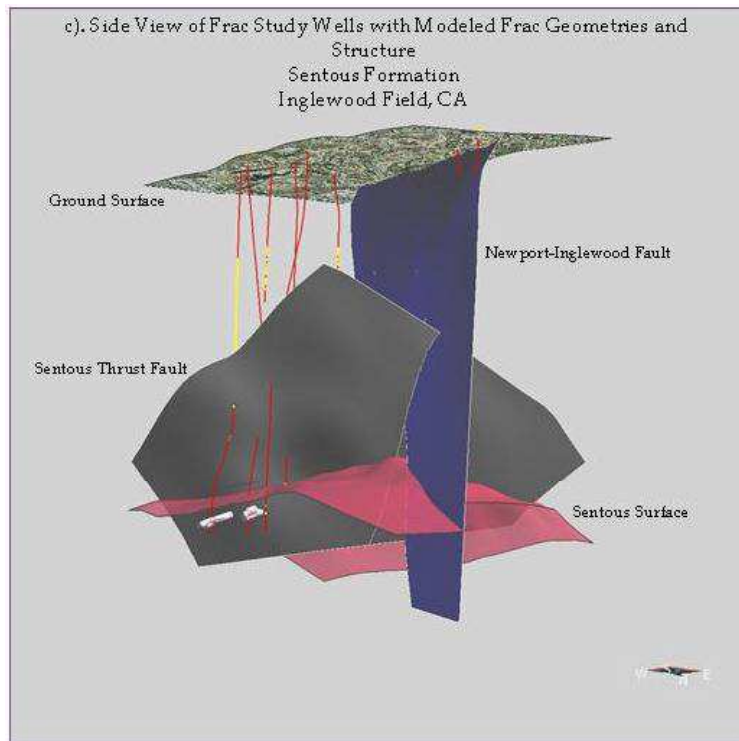


Fig. 5.6c. Side view showing modeled fracture geometries for study well in the Sentous zone together with structural features (faults).

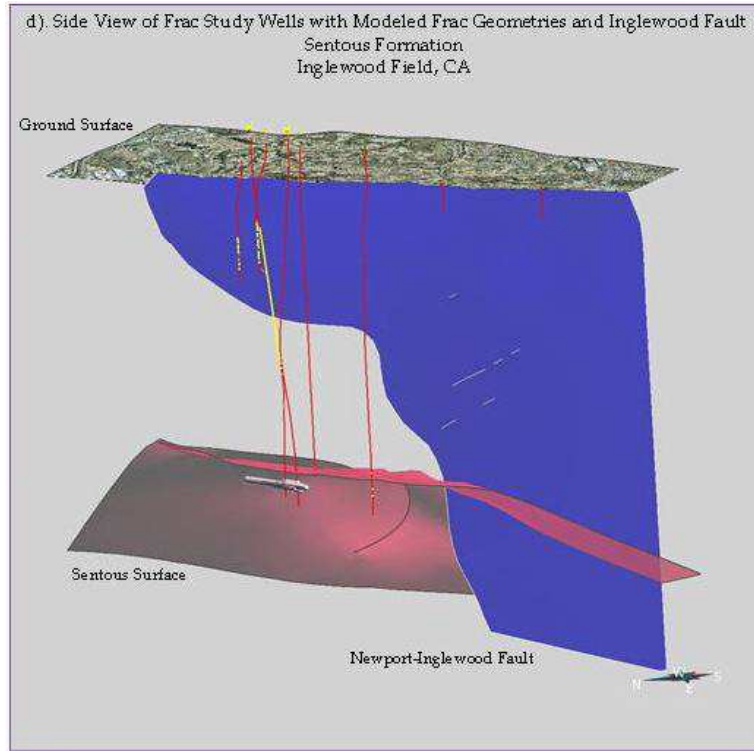


Fig. 5.6d. Side view showing the study wells with modeled fracture geometries in the Sentous zone and the Newport-Inglewood fault..

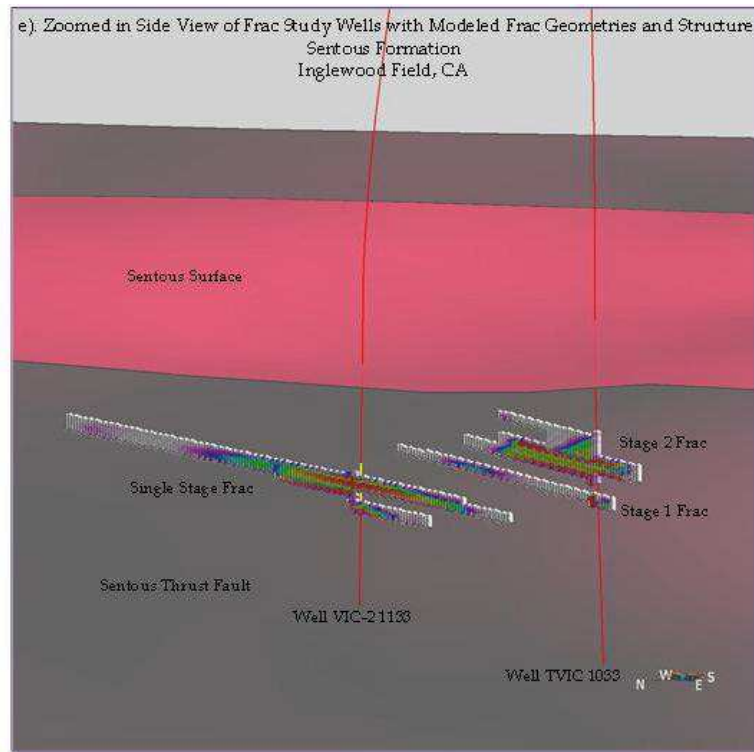


Fig. 5.6e. Detailed side view of the modeled fracture geometries in the report wells in the Sentous zone and structure.

5.4.2. Nodular Shale Zone

Introduction

The late Middle Miocene Nodular Shale zone (13 to 14 Ma) overlies Middle Miocene sands and volcanics in the Inglewood Oil Field (Fig. 5.7). The name is derived from the presence of large phosphatic nodules. The Nodular Shale is a well-compacted organic-rich shale. This rock unit and equivalents, e.g., the “black shale member” of the 237 zone in the Wilmington field, provide the source rock for much of the oil in the Los Angeles Basin (Wright, 1987). The Nodular Shale also underlies several oil fields in the western portion of the Los Angeles Basin, e.g., Playa Del Rey and El Segundo. This rock unit was deposited on deeply submerged offshore ridges and slopes through the slow accumulation of biological debris, diluted by clay particles carried in suspension by circulating ocean currents.

Younger Miocene and Pliocene sediments also contain significant organic material though diluted by mud and silts. These potential source rocks are interbedded with the main producing zones of the Inglewood Field. In the deep synclinal areas east and north of Inglewood, the younger shales were buried deeply enough to generate hydrocarbons, which then migrated into and up the extensive beds of reservoir sands to accumulate at the anticlinal crest.

Stratigraphic Column showing Nodular Formations

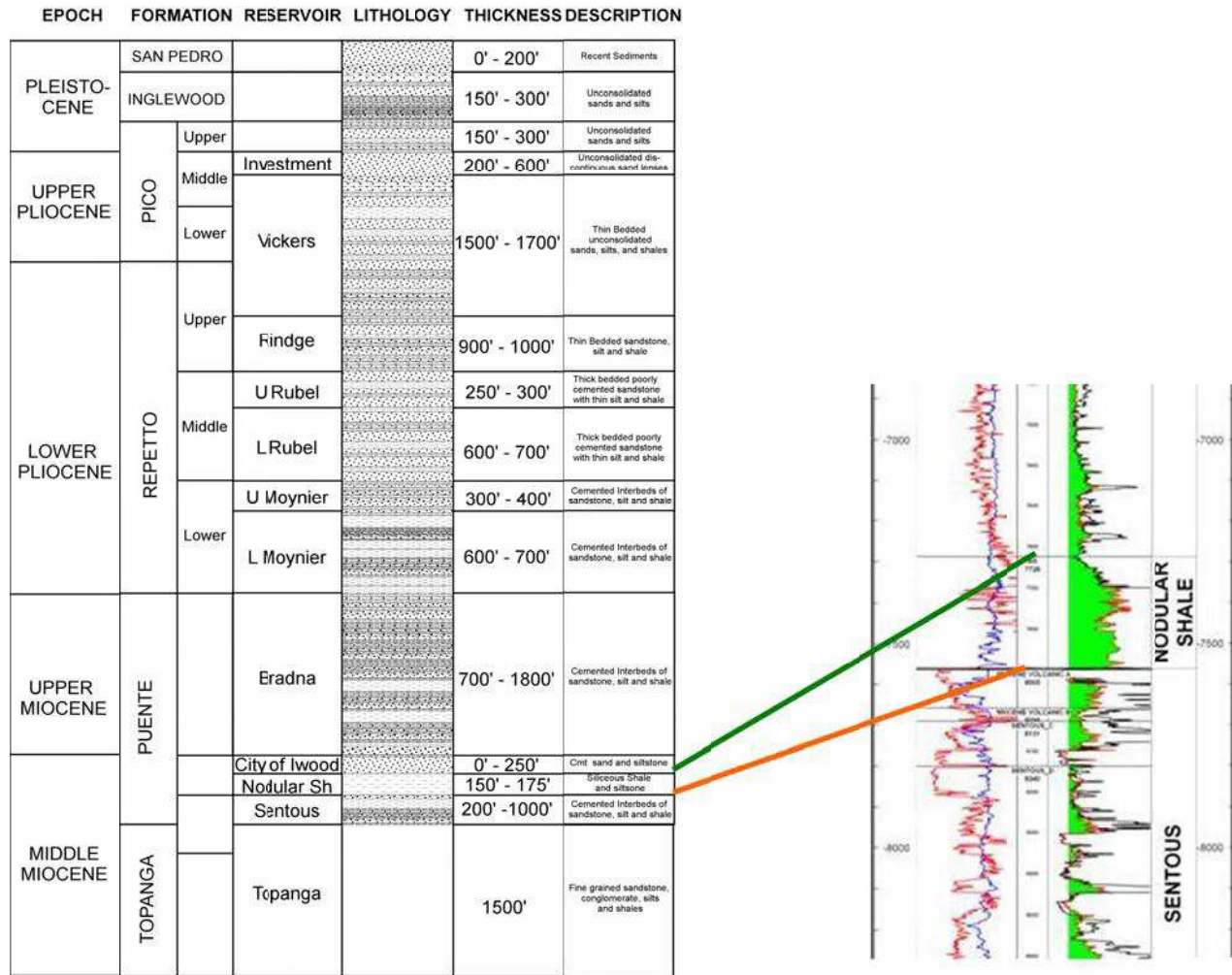


Fig. 5.7. Stratigraphic column for the Inglewood oil field showing the various reservoir zones and highlighting the Nodular zone (Lockman, 2005).

Well Selection List and Criterion for Analysis

Two wells in the Nodular shale zone, VIC1-330 and VIC1-635 were selected for the hydraulic fracturing analysis and frac study. The hydraulic fracture stimulation treatments in these two wells were conducted specifically for the purpose of this report.

Summary of History Match Analysis

Each well had only a single stage hydraulic fracturing treatment completion. The data from these independent completions were history matched using the GOHFER frac model. The Appendices list the final parameter values used to obtain the history matches and the fracture geometries using the calibrated model.

Note: Please refer to Appendix C titled “Fracturing Analysis Results for Wells in Nodular Zone” for detailed results and analysis of history matching

Frac Analysis Results

Figures 5.8a-e present different visualizations of the fracture geometries predicted by the calibrated GOHFER model based on data from the hydraulic fracturing treatments. The figures also show the relevant formation surfaces, ground surface, geologic structure including major faults, and discontinuous groundwater bodies near the surface.

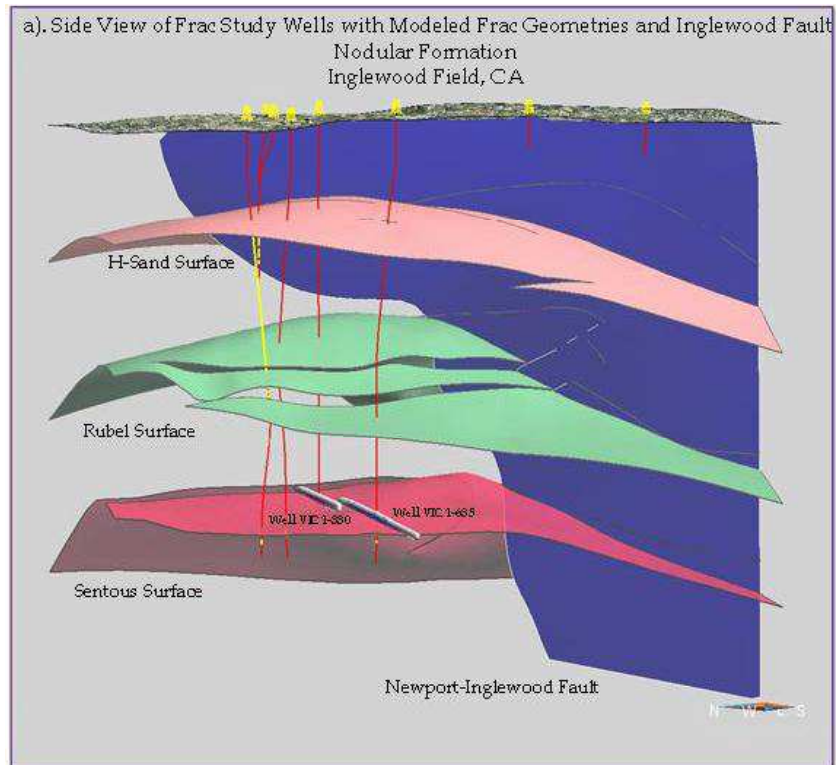


Fig. 5.8a. Side view of the Nodular shale zone modeled fracture geometries and the Newport-Inglewood fault.

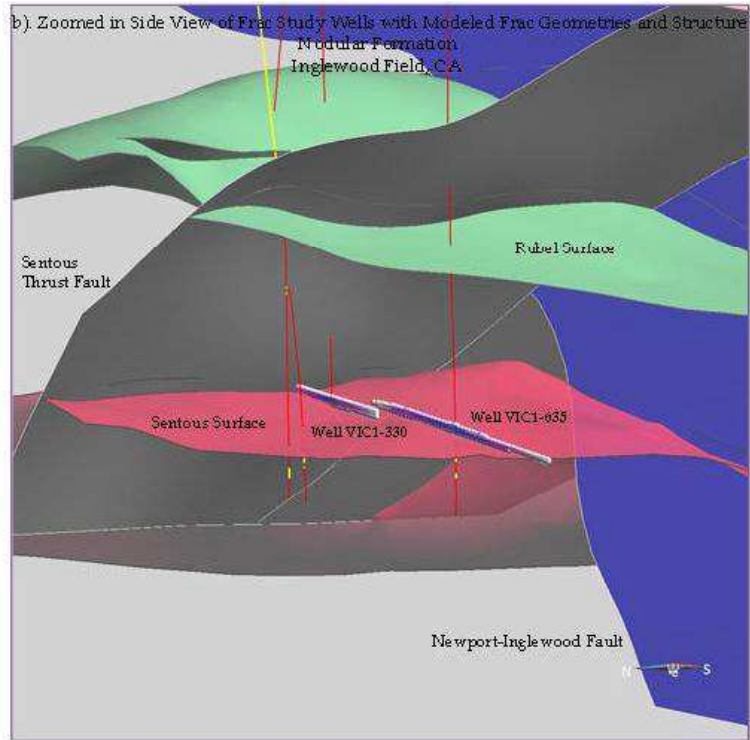


Fig. 5.8b. Zoomed in view of the Nodular shale zone modeled fracture geometries and structure (faults).

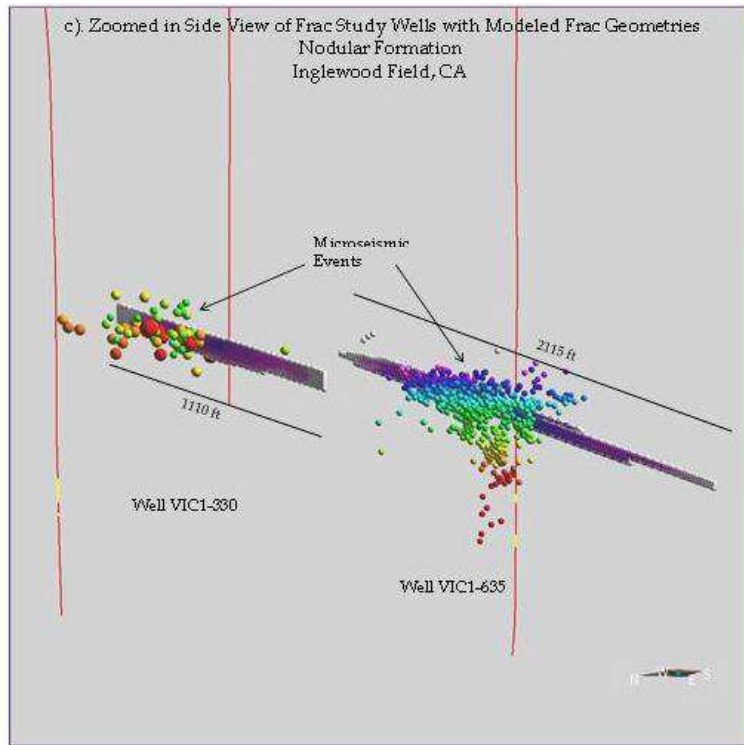


Fig. 5.8c. Zoomed in and Detailed side view of the Nodular shale zone modeled fracture geometries.

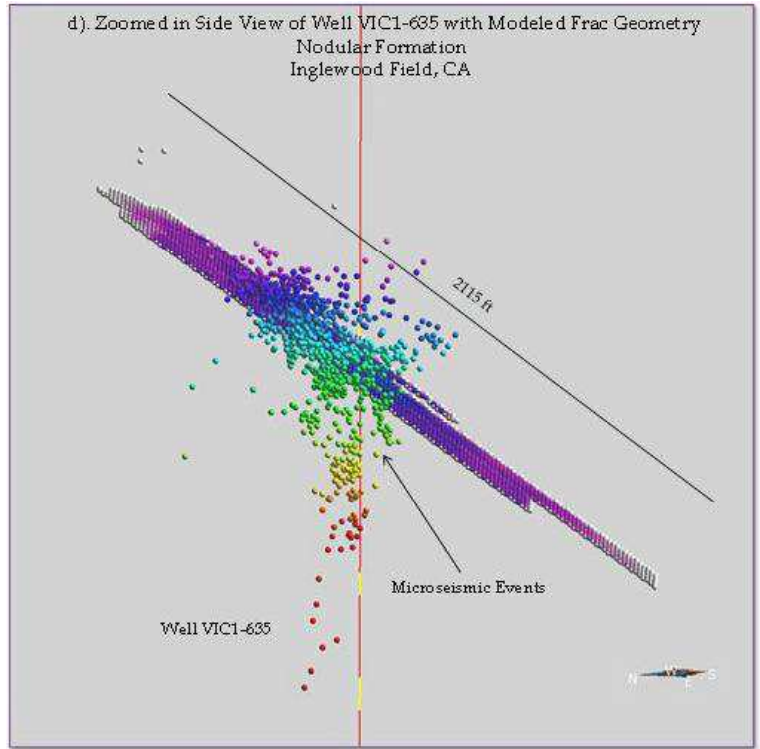


Fig. 5.8d. Zoomed in side view of Well VIC1-635 showing modeled fracture geometry in the Nodular shale zone.

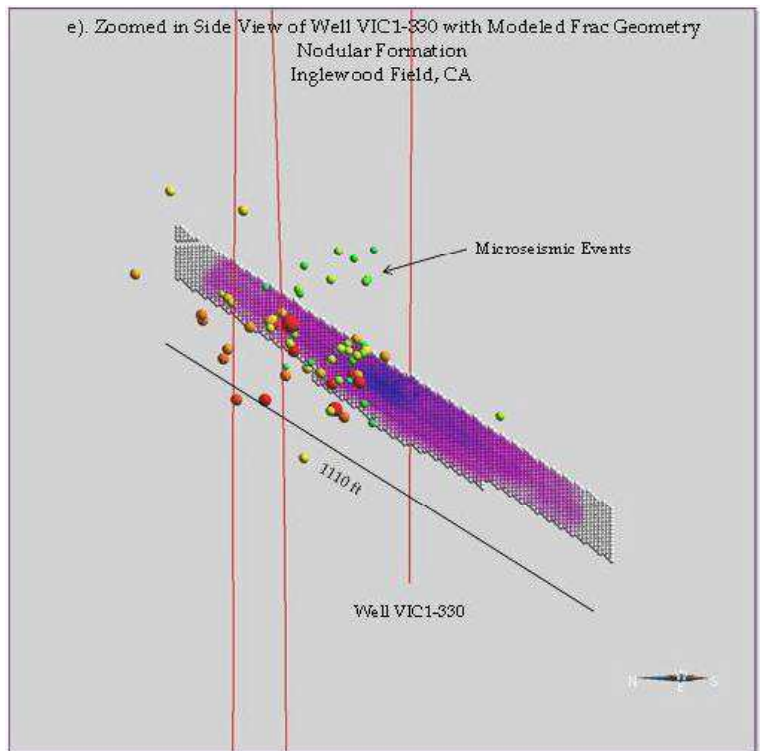


Fig. 5.8e. Zoomed in side view of Well VIC1-330 with modeled fracture geometry in the Nodular shale zone.

5.4.3. Moynier Formation

Introduction

In the Inglewood oil field the Moynier zone lies above the Bradna, Nodular Shale and Sentous zones (Fig. 5.9). The basal Pliocene Moynier sands (5 Ma) are distal deepwater fan deposits that reflect renewed source activity from uplifts to the northeast, beyond the Whittier fault, and from steeper local gradients across the rising Santa Monica Mountains to the north (Wright, 1987).

Stratigraphic Column Showing Moynier Formation

The Moynier lies above the Bradna, Nodular Shale and Sentous formations in the Inglewood Stratigraphy. Fig 5.9 shows the Moynier formation in the stratigraphic column of the Inglewood Field.

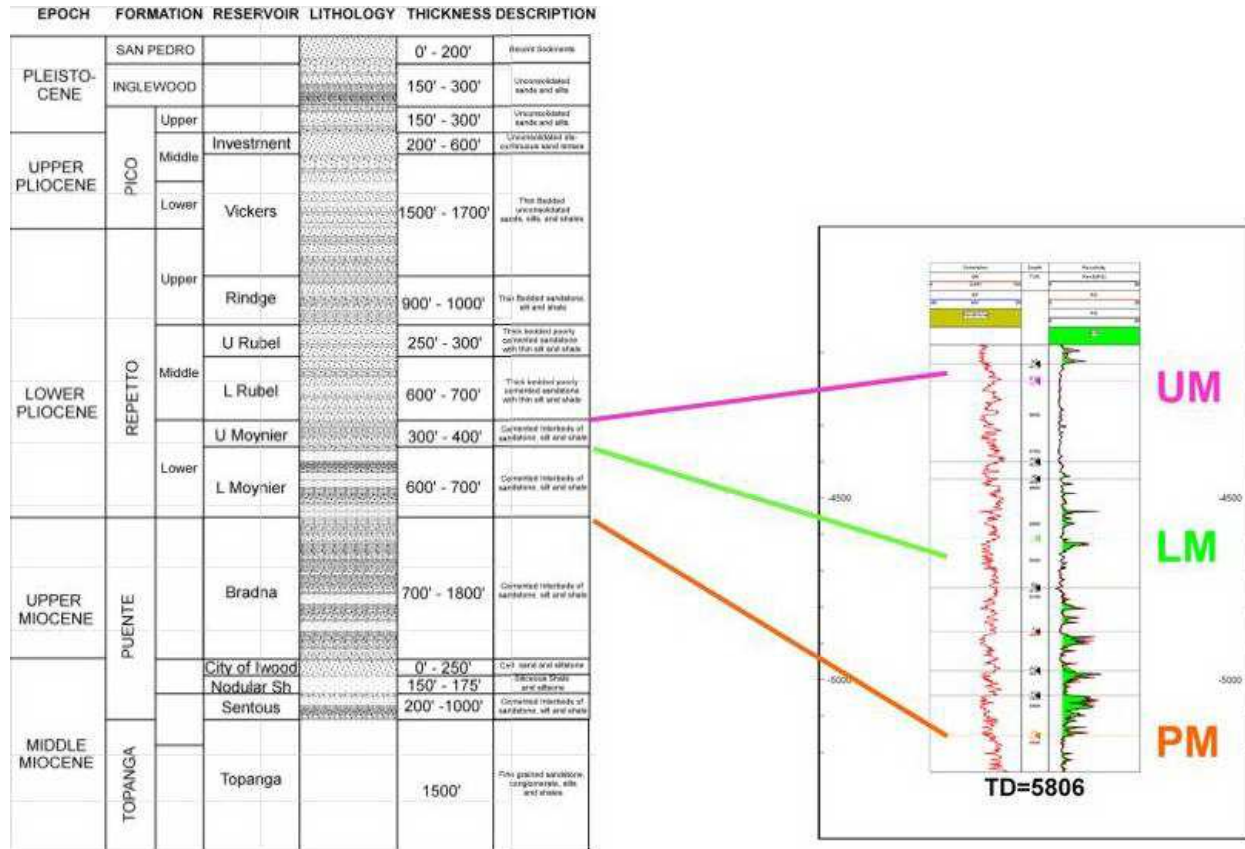


Fig. 5.9. Inglewood oil field stratigraphic column (Lockman, 2005) and a well log showing the position of the Moynier zone.

Well Selection List and Criterion for Analysis

Only one well, VIC2-1133, was selected for analysis of the Moynier zone due to the paucity of available and accurate data.

Summary of History Match Analysis

Three independent hydraulic fracturing stimulation treatments for the selected well in the Moynier formation were history matched using the GOHFER frac model. The final values of the different parameters used to obtain the history matches and the frac geometries obtained for different stages using the calibrated model after history matching are provided in the Appendices for each stage of each well.

Note: Please refer to Appendix B titled “Fracturing Analysis Results for Well in Moynier Zone” for detailed results and analysis of history matching

Frac Analysis Results

Figures 5.10a-d present different visualizations of the fracture geometries predicted from the hydraulic fracturing treatments by the calibrated GOHFER model. The figures include the relevant formation surfaces, ground surface, geologic structure including major faults, and discontinuous, groundwater bodies near the surface.

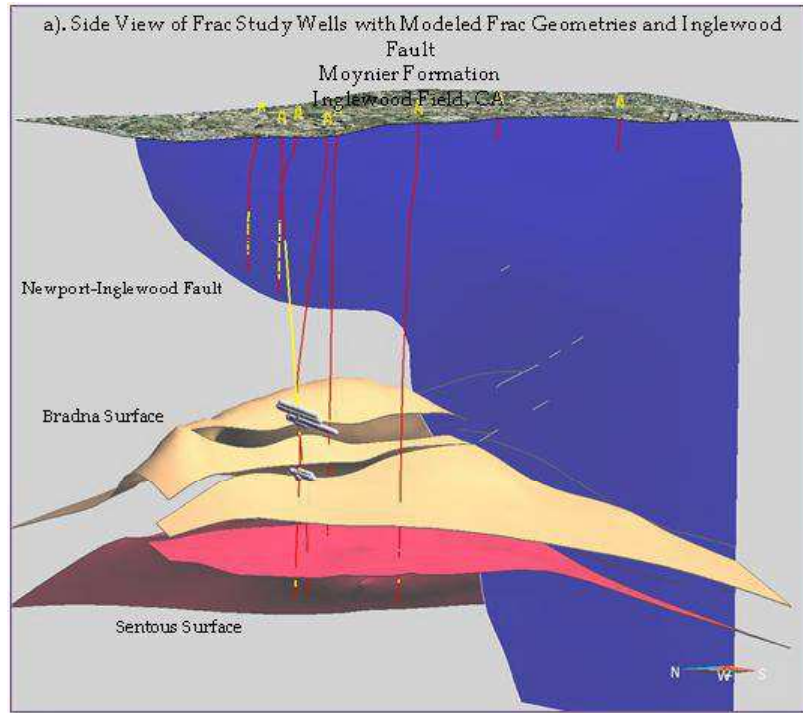


Fig. 5.10a. Side view showing the modeled fracture geometries in the Moynier zone and the Newport-Inglewood fault.

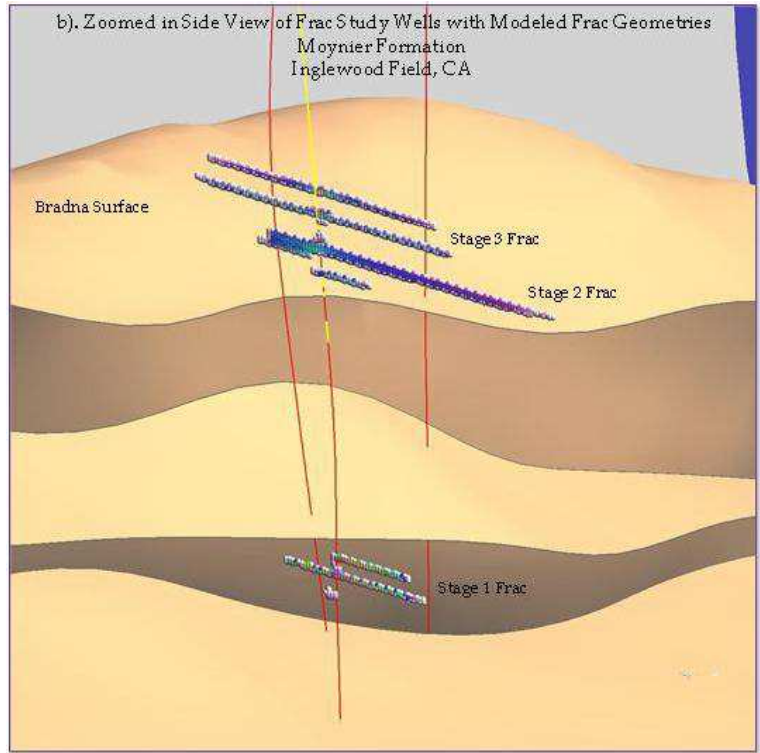


Fig. 5.10b. Detailed side view of modeled fracture geometries in the Moynier zone.

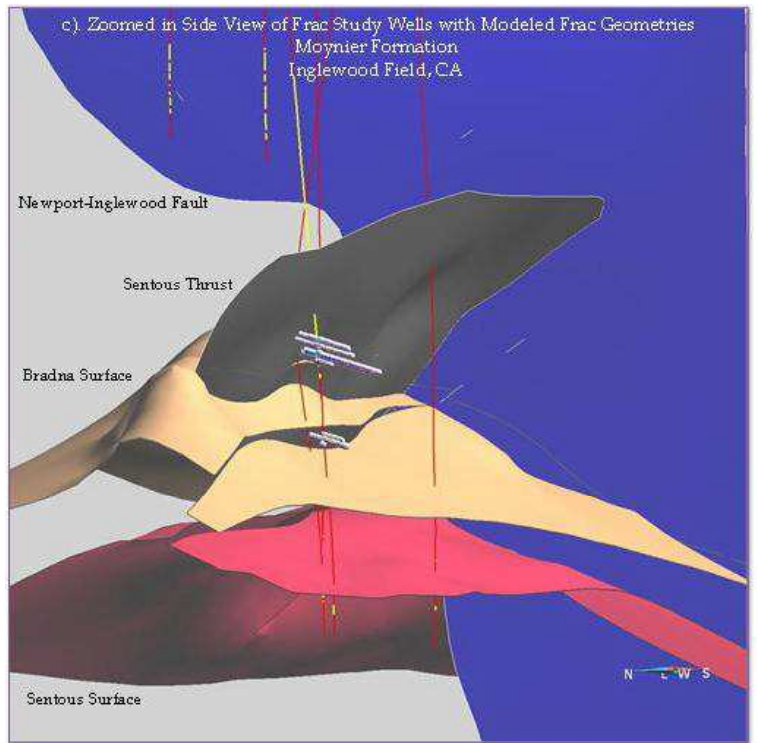


Fig. 5.10c. Detailed side view of modeled fracture geometries in the Moynier zone with structure (faults).

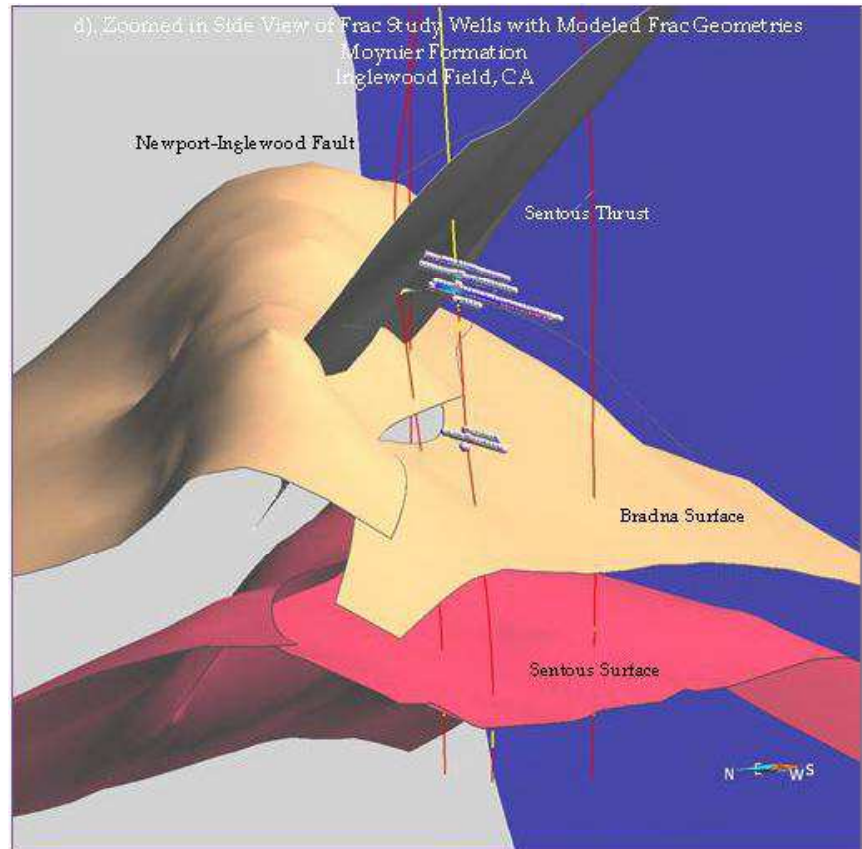


Fig. 5.10d. Detailed side view of modeled fracture geometries in the Moynier zone with structure.

References

- Lockman, D., 2005, Los Angeles 3D survey leads to deep drilling: The Leading Edge, v. 24, no. 10, p. 1008-1014.
- Moodie, W.H., Minner, W.A., Fernandez, M., Lockman, D., and Burgett, W. Jr., 2004, Multistage oil-base frac-packing in the thick Inglewood field Vickers/Rindge formation lends new life to an old producing field, paper SPE-90975, presented at the 2004 SPE Annual Technical Conference and Exhibition: Society of Petroleum Engineers, 9 p.
- Wright, T., 1987, The Inglewood oil field, in Wright, T., and Heck, R., editors, *Petroleum Geology of Coastal California*: AAPG Pacific Section Guidebook 60, p. 41-49.

6. Microseismic Monitoring

6.1. What is Microseismic Monitoring?

Microseismic monitoring is the practice of passive listening to microseismic activity caused by hydraulic fracturing, reservoir subsidence, and water, steam, or CO₂ injection or sequestration. Passive microseismic activity is recorded over time to produce images of microseismic events and source mechanisms (Fig 6.1).

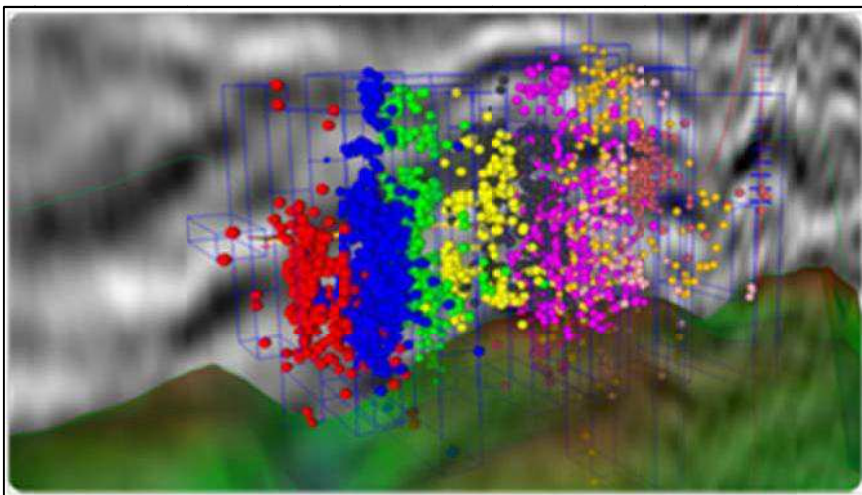


Fig. 6.1. Plot of microseismic events recorded during a fracture treatment. The colors indicate different treatment stages.

Since its development in the 1970s and its commercialization around 2000, microseismic monitoring has proved an invaluable tool for understanding and optimizing underground processes. Microseismic theory is rooted in earthquake seismology and, thus, the basic theoretical underpinnings are well understood. Microseismic monitoring has become a well-established and accepted technology for monitoring, assessing and optimizing hydraulic fractures (Warpinski, 2009).

Since 2000, thousands of fracture treatments have been monitored across the United States in formations ranging from tight sandstones and gas shales to carbonates and volcanic rocks. Monitoring has occurred at depths ranging from several hundred feet to more than 13,000 ft.

Why Microseismic Monitoring?

The most common and notable use of microseismic monitoring has been hydraulic fracture mapping. However, it is also used for reservoir monitoring of thermal processes, drill-cuttings injection, geothermal hot-dry-rock stimulations, reservoir surveillance, and many other processes in oil and gas and mining industries.

Microseismic monitoring maps the locations of induced microseismic events associated with hydraulic fracturing stimulation treatments (Fig. 6.2). It is

used to determine the vertical and lateral extent the fractures resulting from those treatments. The geometry of the event locations is used to infer fracture orientation.

Microseismic monitoring helps assure that fractures remain in the intended zone and that the entire zone is stimulated. This capability can help optimize production and minimize the number of wells and fractures required to efficiently produce the formation. Results from microseismic fracture mapping can be used to "calibrate" fracture growth models.

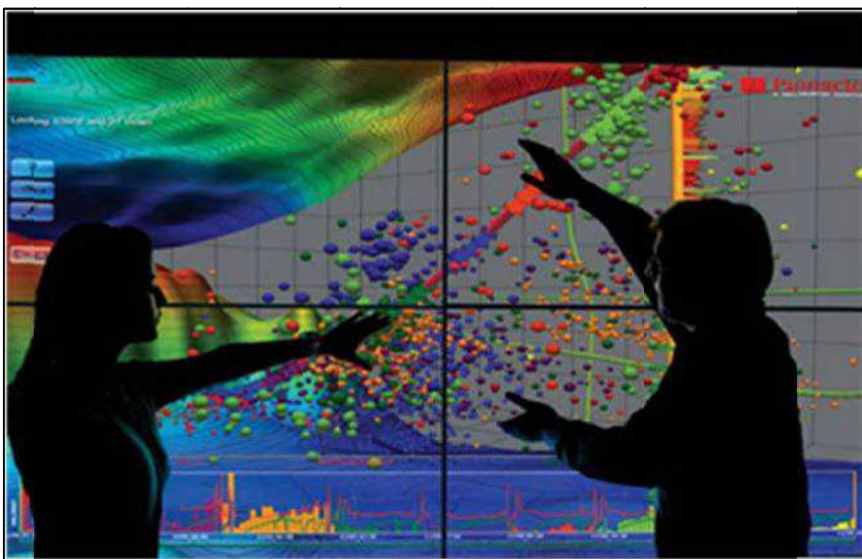


Fig. 6.2. Microseismic events imported in the structure model being analyzed to identify the extent of hydraulic fracturing treatment.

Specifically, microseismic monitoring provides the following important information

- Fracture height and length;
- Fracture azimuth and asymmetry;
- Fracture growth vs. time;
- Understanding staging effectiveness;
- Stimulated volume;
- Complexity and network growth;
- Natural fractures;
- Fault interactions; and,
- Reservoir behavior as a result of hydraulic fracture treatment.

This information, in turn, is used to answer questions related to

- Horizontal well direction and length;
- Zone coverage;
- Out-of-zone growth/risk of growth into water;
- Staging strategies;
- Well placement and spacing;
- Optimal completion and fracture design.

Microseismic mapping data can be integrated with production modeling, staging strategies and well interference data to improve completion processes, well spacing and placement strategies and can be used to optimize the fracture design and field development.

How is Microseismic Monitoring Done?

A hydraulic fracture induces an increase in the formation stress proportional to the net fracturing pressure as well as an increase in pore pressure due to fracturing fluid leakoff. As a result of these geomechanical changes, small slippages are induced in natural fractures, bedding planes, faults, and other weak features in the reservoir. These slippages are called microseisms and they help track the fracture location and any interaction with existing natural fractures and other geologic features. Monitoring and locating of these microseismic events is achieved using a downhole array of passive seismic receivers or geophones that can detect low energy changes resulting from changes in stress or pressure induced by the fracturing treatment. These geophones are located at or near the reservoir level and deployed by a wireline in one or more nearby observation wells (Fig 6.3). The array detects the seismic energy generated by the microseisms by use of three-component geophones or accelerometers. The algorithms are then processed to locate the “event” using an assortment of information obtained from compressional (P-wave) and shear (S-wave) arrivals detected by the array.

Geophones in monitor wells identify and map the precise location of these events. The distance between the well receiving the hydraulic fracture stimulation treatment and the offset monitoring wells range anywhere from 500 to 3,500 feet depending on formation type and treatment rate and volume. The events are transmitted to the frac van and/or customer location for real time viewing and analysis so that the decisions can then be made as to whether modifications in the process are required or if the operation should be shut down if problems are encountered.

Once the microseisms are located, the actual fracture is interpreted within the envelope of microseisms mapped.

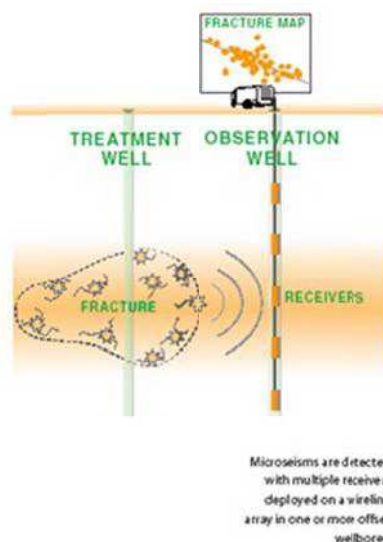


Fig 6.3. Typical layout of Treatment and Observation Wells used in a microseismic monitoring

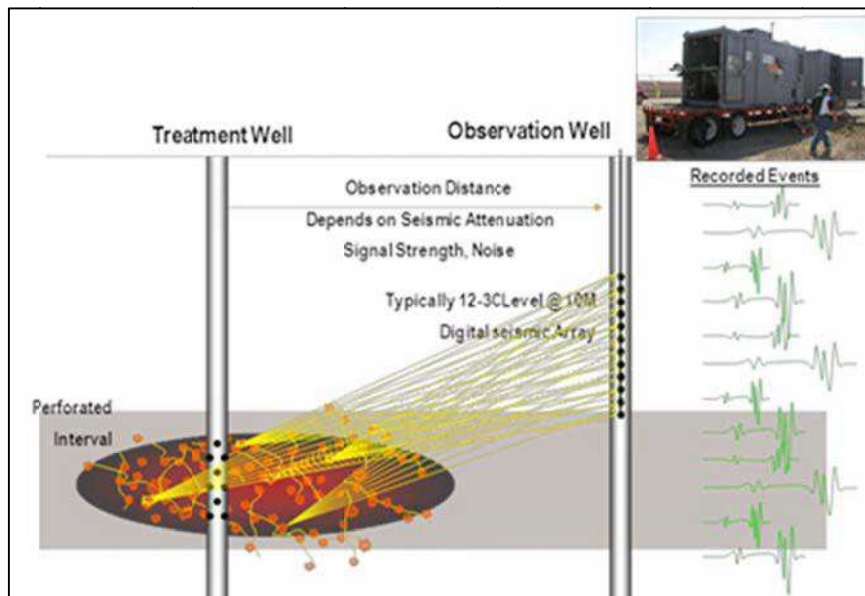


Fig 6.4. Typical layout used in a microseismic monitoring test.

The acoustic-receiver array in the monitor well is positioned near the depth of the fracture treatment.

Geophones in monitor wells identify and map the precise locations of these events. The distance between the treated well and the offset monitoring (observation) well can range from 500 to 3,500 ft., depending on formation type and treatment rate and volume. The events are transmitted to the fracture van and/or customer location for viewing and analysis in real time to allow decisions to be made as to whether modifications in the process are required, or if problems are encountered, whether the operation should be shut down.

Once the microseisms are located, the actual fracture is interpreted within the envelope of the mapped microseisms.

Because acoustic energy decays with distance there is a maximum monitoring distance that can be used in any test with respect to both horizontal and vertical positioning. When a test is properly designed and ambient noise is relatively low, microseisms can be detected several thousand feet from the monitoring array. Because the microseisms are located relatively close to the hydraulic fractures (stress effects decay rapidly), this technology can be used to monitor fracture geometry and growth behavior.

What are Microseisms and how big are they?

There are two scales used to measure the intensity and effects of seismic energy the magnitude scale (logarithmic) and the Modified Mercalli Intensity scale. Magnitude reflects the energy released during any seismic motion and intensity is a measure of the effects of this energy release on people, human structures, and the natural environment (USGS website).

Microseisms are very low-energy events, typically ranging in magnitude from -4 to +2. Microseisms generated by hydraulic fracturing stimulation treatments are generally < -2 (magnitude uses a logarithmic scale). For comparison, a magnitude of 3 is generally the minimum that is felt at the surface. These events are caused by (1) changes in stress and pressure resulting from fluid leakoff during the treatment, and (2) movement (shear slippage) along existing fracture planes in the rock.

Note: The different magnitudes and their intensities observed are discussed on the USGS site.

Because these events are so small (low energy) monitoring companies generally use downhole monitoring arrays rather than surface arrays to record them. The detection and locations of these microseisms depends not only on the pumping rate and volume of the hydraulic fracture stimulation treatment, but also on the formation properties—the harder the rock, the farther the signal will travel.

For perspective, any movement that can be felt at the surface will have a magnitude of roughly +3, which translates into a moment of 3×10^{13} ft-lbf and energy of 1.5×10^9 ft-lbf. A typical large microseism, with a magnitude of -2, has a moment of $\sim 1.0 \times 10^6$ ft-lbf and an energy of ~ 50 ft-lbf, equivalent to the total work in lifting a 10-lbm weight 5 ft. off the ground. It is also important to note that, because of the $2/3$ factor in the magnitude equation, the energy increases a factor of 32 for every increase of one magnitude unit (Warpinski et al. 2012, SPE 151597).

Hydraulic Fracturing and Induced Seismicity

Recently, concerns have been expressed regarding potential hazards associated with induced seismicity generated during multistage fracturing of horizontal wells in gas shales and tight sandstone reservoirs.

Figure 6.5 shows the moment magnitude of microseismic events recorded during hydraulic fracturing treatments in different gas shale reservoirs. The figure shows that most of the microseismic events related to hydraulic fracturing are less than magnitude -0.5.

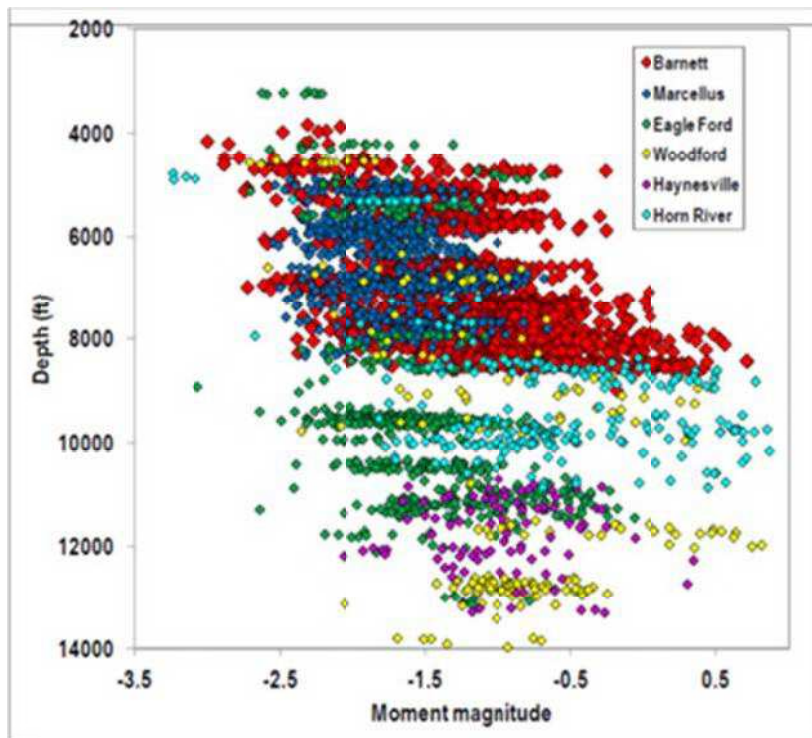


Fig. 6.5 Summary of the magnitude of microseismic events in different gas-shale basins (data in this figure taken from SPE 151597).

Energy and Volume: Microseisms vs. Fracture

A review of thousands of microseismically monitored fracturing treatments shows that induced seismicity associated with hydraulic fracturing is very small and not a problem under any normal circumstances (Warpinski et al., 2012).

Table 6.1 Energy & Volume: Microseisms Versus Fracture				
Magnitude	Energy		Volume	
	1 microseism	500 microseisms in a typical fracture treatment	1 microseism	500 microseisms in a typical fracture treatment
-2	~>50J	~25KJ	0.000084m ³	0.0335m ³
-1	~1,600J	~800KJ	0.042m ³	1.33m ³

Table 6.1. Comparison of the seismic energy released and rock volume affected different magnitude events generated by a hydraulic fracture treatment (Warpinski).

The event moment magnitude recorded in the microseismic monitoring of VICI-635 well ranged from -3.8 to -2.2 Mw, with an average of -3.4 for the VIC1-735 array and ranged from -4.0 to -2.4 with an average of -3.4 for the VIC-925 array.

The event moment magnitude recorded in the microseismic monitoring of VICI-330 well ranged from -3.2 to -1.3

These events recorded in both the wells in the Nodular zone were extremely smaller than the moment magnitude of +3 which can be felt on surface.

Note: Please refer to Attachment 6A titled “SPE 151597 – Measurements of Hydraulic Fractured Induced Seismicity in Gas Shales” by Warpinski et al. 2012 for additional information. Results are presented for six major shale basins in North America.

6.2. Microseismic Fracture Mapping Analysis and Results

Microseismic monitoring was conducted in both study wells completed in the Nodular Shale zone, VIC1-330 and VIC1-635, in the Inglewood Oil Field. For well VIC1-330 microseismic monitoring services were provided by Schlumberger, and for well VIC1-635 these services were provided by Pinnacle (a Halliburton company).

Figure 6.6 presents a detailed earth model side view visualization showing the locations of microseismic events detected during the mainstage fracture treatment

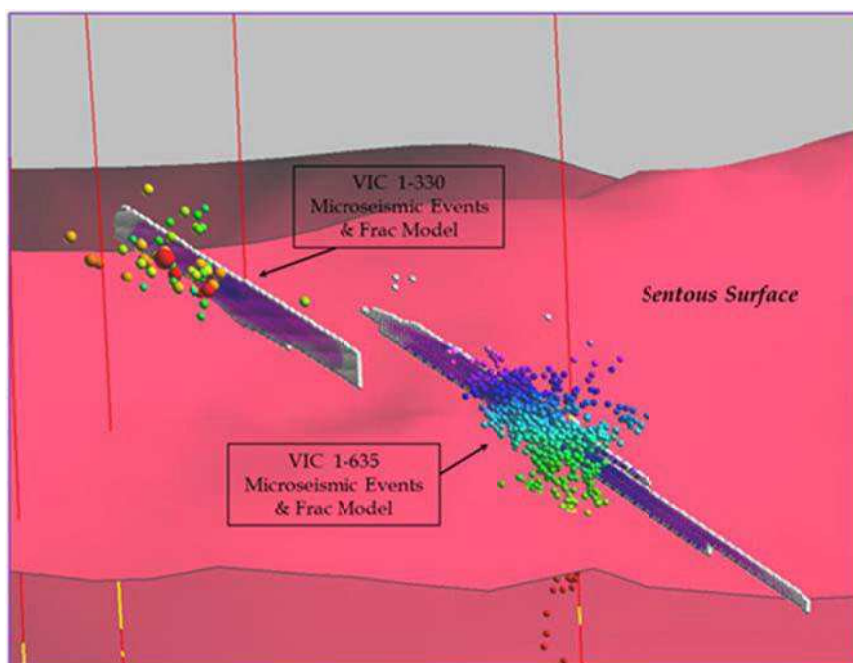


Fig. 6.6. Zoomed in and Detailed side view of the microseismic events detected during the hydraulic treatments in the Sentous zone in Wells VIC1-330 and VIC1-635.

Fig. 6.7 presents an earth model visualization of the microseismic events recorded during hydraulic fracture treatments in the Nodular Shale zone in wells VIC1-330 and VIC1-635. The distance between the top of the created fracture and the near-surface water bodies is approximately 7,700 ft. Total number of microseismic events observed during Well VIC1-635 treatment were 939. Out of these, only 5 events were observed out of zone above the Nodular Shale. All these events were within 20 ft. of the top of Nodular Shale.

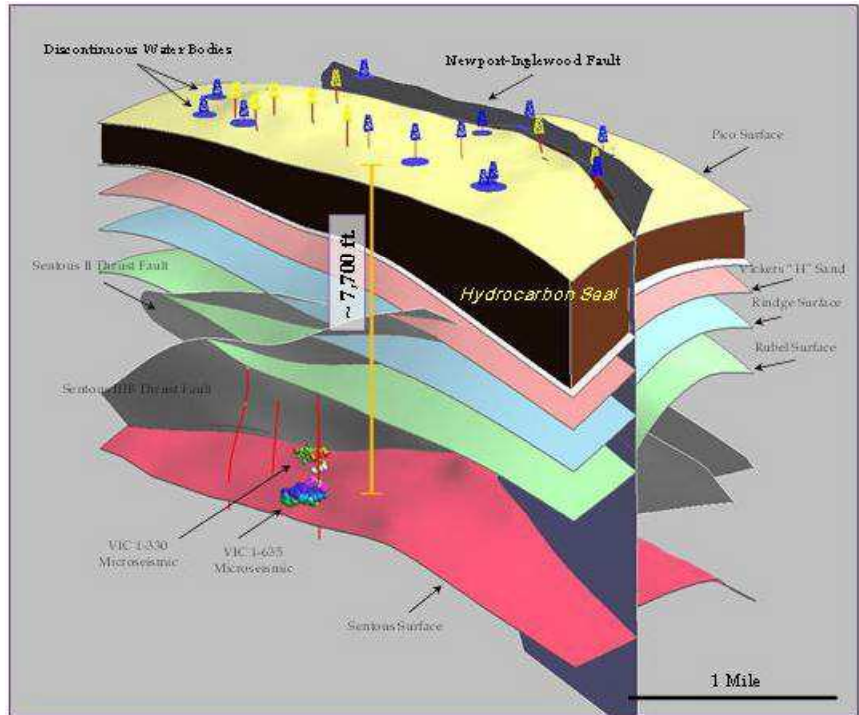


Fig 6.7. Earth model visualization showing the microseismic events recorded during hydraulic fracture treatment in the Nodular Shale zone in wells VIC1-330 and VIC1-635.

6.2.1. Well VIC1-330 Analysis and Results

Well VIC1-330 the Nodular Shale zone was stimulated through 5-1/2 in. casing and a single jet of perforations from 8,030 to 8,050 ft. (MD). Halliburton provided the fracturing services on this well. One stimulation treatment was conducted, monitored and evaluated.

Well VIC1-934, located 700 ft. away, was used as the monitoring well during this fracture treatment. The downhole receiver array consisted of 12VSI* geophones spaced 100-ft apart. Fig. 7.7 shows the geophone locations relative to the treatment perforations. The distance from the center of the geophone array to the perforations in the VIC1-330 treated well is approximately 700 ft.

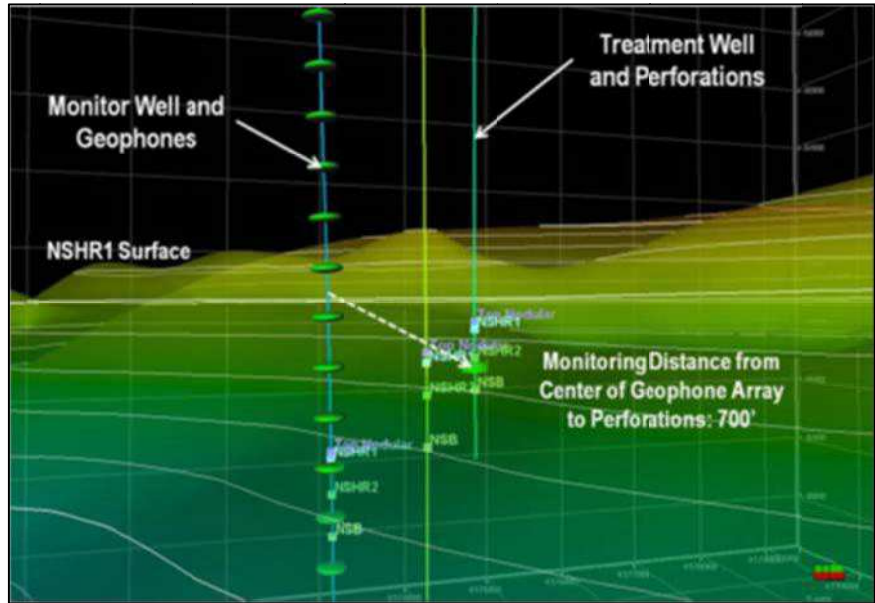


Fig 6.8. Earth model visualization showing the location of the treated well perforations and geophones in the monitor well. Distances measured from the midpoint of the geophone array to the mid-perforation location of the stages shown.

Microseismic activity occurred throughout the treatment and a total of 47 microseismic events were located during the stimulation treatment. Fig. 6.9 is a detailed earth model side view visualization showing the locations of the microseismic events detected during the mainstage fracture treatment.

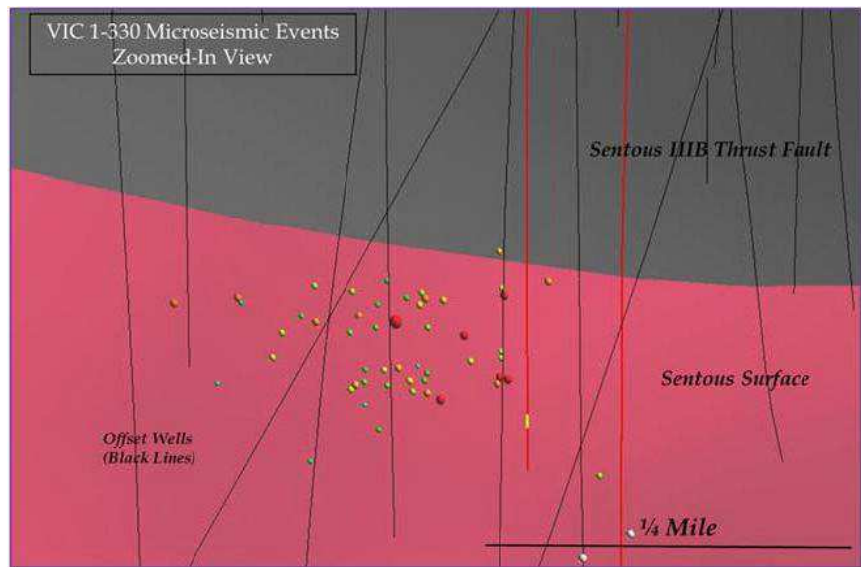


Fig 7.8. Detailed Zoomed in side view visualization of the microseismic events recorded during fracture treatment in the Sentous zone in Well VIC1-330

In Fig. 6.10 is a map (plan) view of the located microseismic events, which is color coded to the time of day as indicated in the plot legend. Fig 6.11 shows the events in depth view, as viewed from the south. The arrow on the

images points north, with green indicating a viewpoint above the events, and red indicating that the view is from below. The reference grid has been reduced to cover only the volume of rock where microseismic events were located.

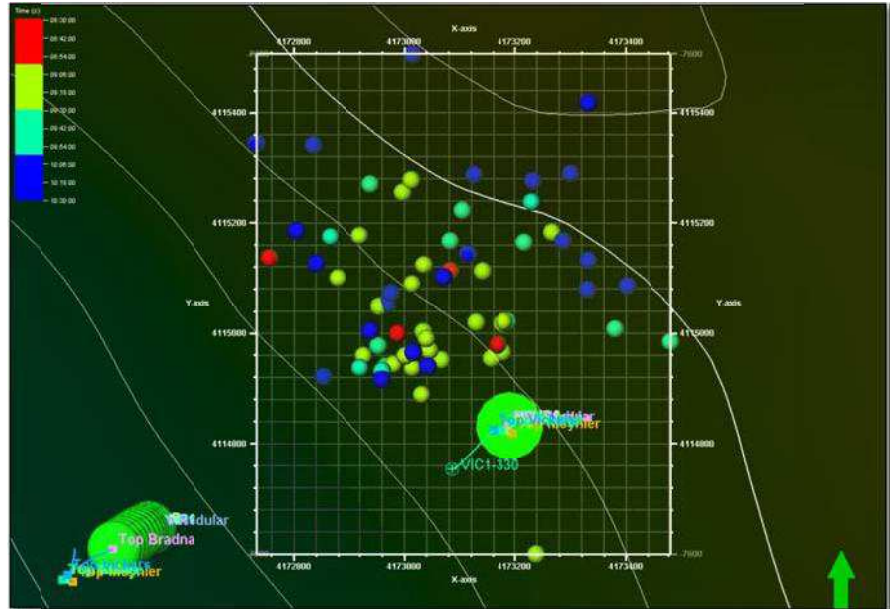


Fig 6.10. Map view showing the microseismic event locations color coded by time.

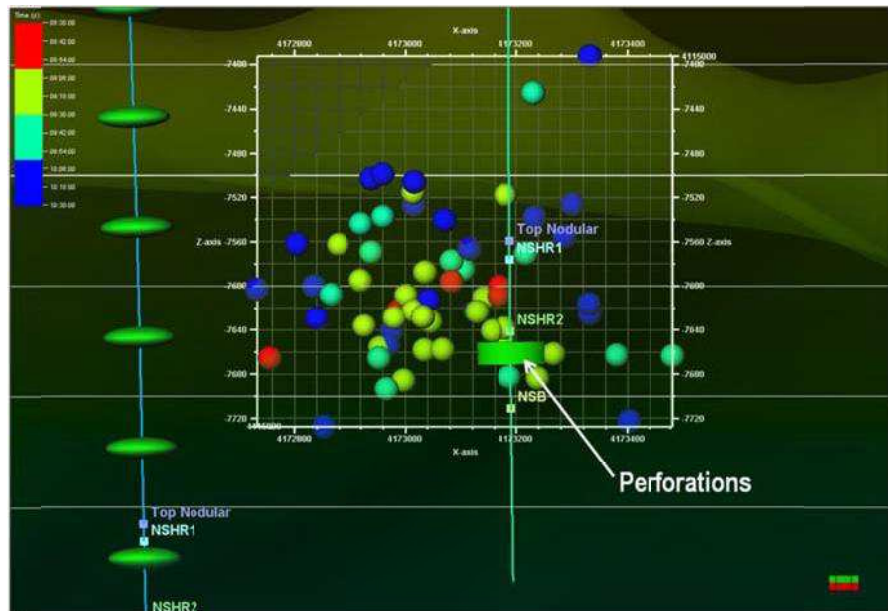


Fig 6.11. Depth view visualization towards north of showing microseismic events color coded by time.

Conclusions

The results of the microseismic mapping (Schlumberger, 2011) indicate that the geometry of the Nodular Shale zone in the Inglewood Oil Field is complex. Fracture extension took place in three directions and paralleled the reservoir structure. First, length extension occurred along formation strike, which was followed later in the fracture treatment by upward growth and lateral extension paralleling formation dip (*source: Schlumberger's Microseismic Report, 2011*).

Note: Please refer to Attachment 6B, 6C and Attachment 6D entitled "StimMAP Evaluation Report" by Schlumberger for additional details on the Microseismic Analysis for VIC1 – 330 well in the Nodular Shale.

6.2.2. Well VIC1-635 Analysis and Results

Pinnacle provided microseismic monitoring services for the hydraulic fracture stimulation of the VIC1-635 well on January 5th, 2012 and January 6th, 2012. The well was completed with 4.5-in. 11.6-lb P-110 cemented casing in the Nodular Shale formation using a single-stage hydraulic fracture treatment.

The VIC1 635 well was drilled to a measured depth of 9,500ft to target the Nodular formation. The well was perforated between 8,430 to 8,450 ft. with a single 3 shot-per-foot (spf) perforating gun over a 20-ft interval. Two monitor wells were used, VIC1-735, located 660 ft. northeast of the treated well, and VIC1-935, located 330 ft. west of the treated well. A dual microseismic array across the Nodular formation was used.

Fig. 6.12 is an aerial (map) view showing the locations of the treated well (VIC1-635) and the two observation wells (VIC1- 735 and VIC1-935).

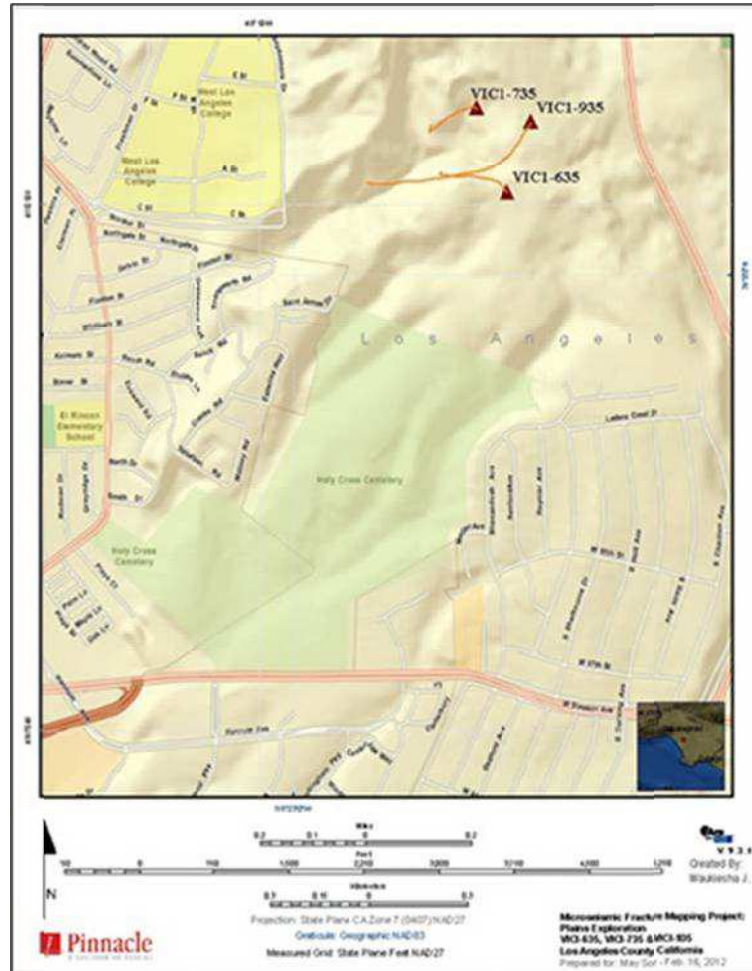


Fig 6.12: Map view showing the surface location of the treated well, VIC1-635, and the two monitor wells, VIC1-735 and VIC1-935.

The placement of the two arrays provided a good zonal coverage across the Nodular Shale zone with receivers above and below the target zone.

The second area of quality assurance is the location of perforation-string shot events with respect to the wellbore. Fig. 6.13 shows the perforation-string shot aligned with the wellbore from above.

Fig. 6.13 shows the top and side views of the three wells along with the location of the geophone arrays in the two observation wells (left) and the zone tops (right).

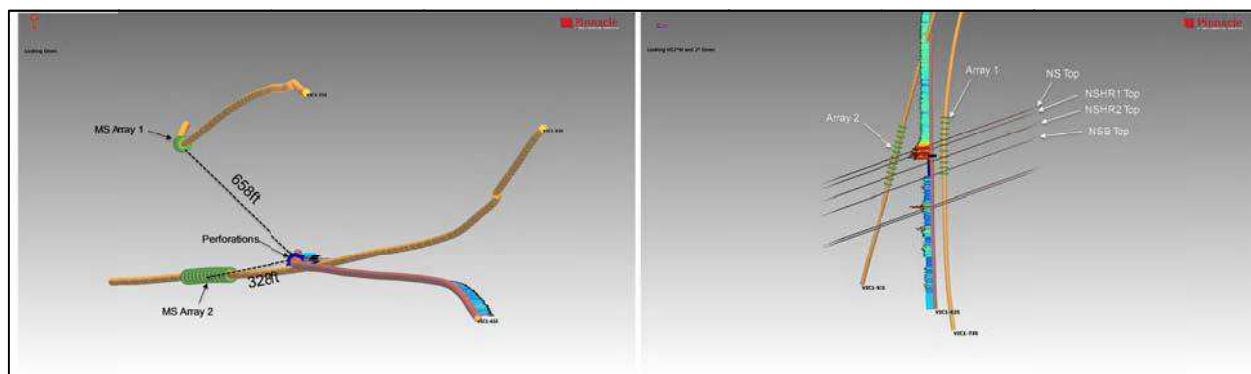


Fig 6.13. Top (map) (left) and side (cross section) (right) views of the perforation string shot and their alignment with the wellbore.

Fig. 6.14 shows a detailed earth model side view visualization of the locations of microseismic-event detected during the mainstage fracture treatment.

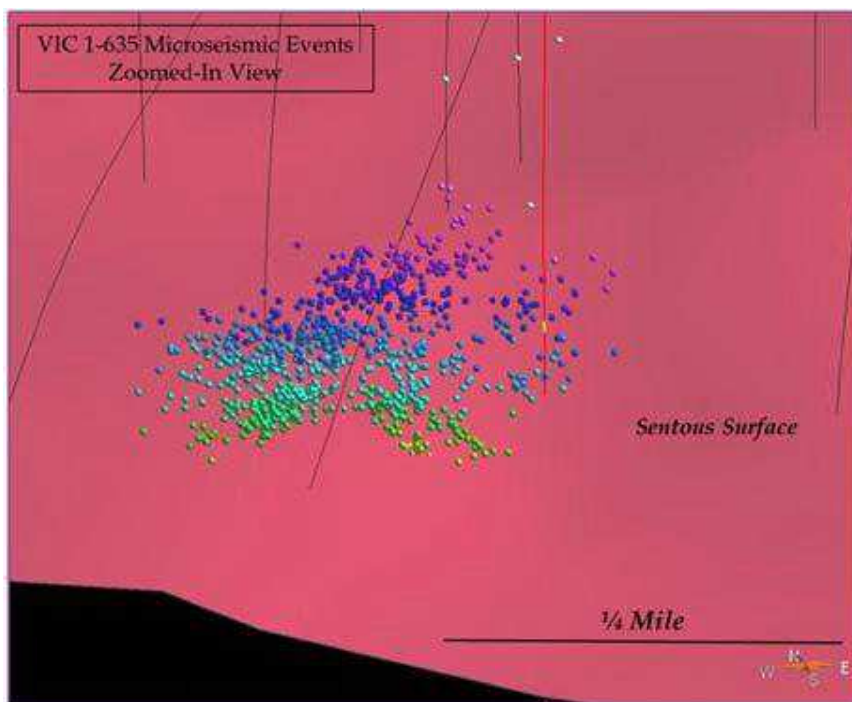


Fig 6.14 Detailed side view visualization showing the microseismic events recorded in Well VIC1-635.

The objectives of the fracture mapping service were to:

- Determine fracture pay zone coverage along the vertical wellbore;
- Measure fracture geometry (height and length) and azimuth;
- Determine the extent of hydraulic fracture treatment;
- Determine the relative degree of induced fracture complexity;
- Provide information that could be used for future lateral well placement and infill drilling strategies for lateral wells; and,
- Estimate stimulated reservoir volume (SRV) for the stage completed;

Microseismic Events Monitored

Fig. 6.15 shows the plan (map) view of the mapped microseismic events.

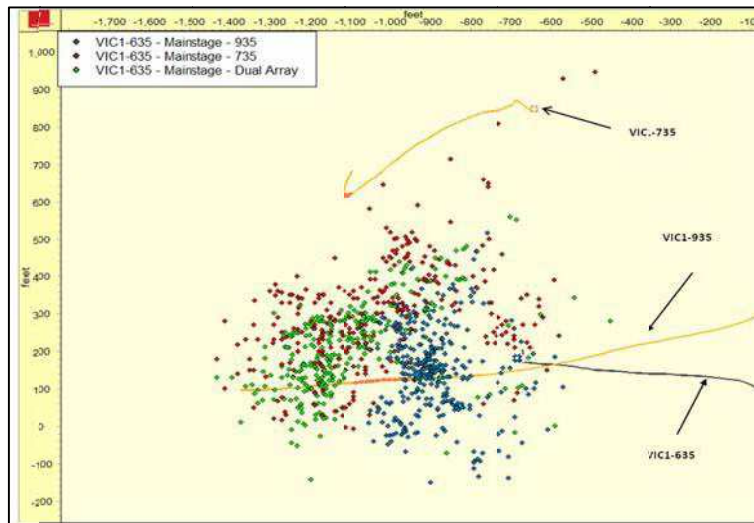


Fig. 6.15. Map view of the microseismic events recorded during the VIC1-635 stage 1 fracture treatment.

Fig. 6.16 shows the mapped microseismic events for the VIC1-635 mainstage fracture treatment in map view (left) and cross section (right).

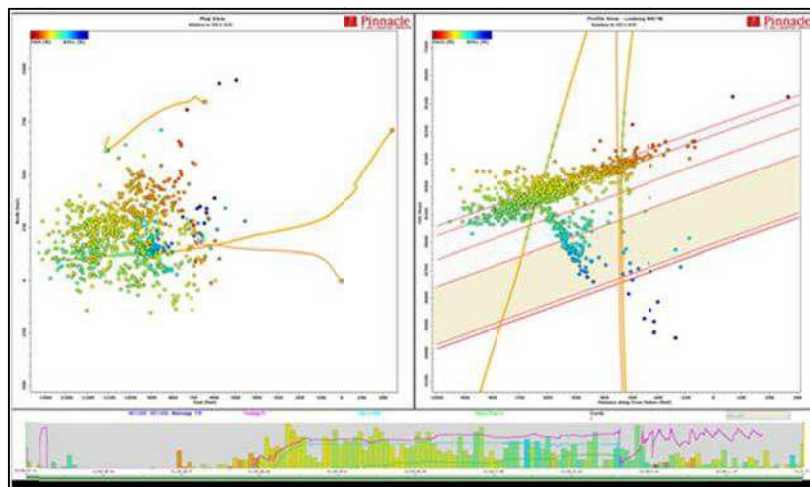


Fig.6.16 Microseismic events mapped for the VIC1-635 mainstage fracture treatment are shown in plan (map) view (left) and in cross section (right).

Summary and Conclusions

The results from microseismic mapping indicated that the target zone was effectively simulated and that fracture growth occurred along formation dip. Monitoring of activity was continued after the treatment termination, and microseismic response was recorded for about 40 minutes post shut down.

Overall, the relative degree of fracture complexity was considered to be high for this treatment, and it is probable that multiple sets of parallel and conjugate fractures were present.

Total number of microseismic events observed were 939. Out of these, only 5 events were observed out of zone above the Nodular Shale. All these events were within 20 ft. of the top of Nodular Shale.

Note: *Please refer to Attachment 6E entitled “Fracturing Mapping Results for the VIC1-635” by Pinnacle for additional details on the Microseismic Analysis for VIC1–635 well in the Nodular Shale*

References

Schlumberger, 2011, Well VIC1-330 StimMAP Evaluation Report.

Warpinski, N.R., 2009, Microseismic monitoring—inside and out, paper SPE 118537: *Journal of Petroleum Technology*, 61(11), 81-85.

Warpinski, N.R., Du, J., and Zimmer, U., 2012, Measurements of hydraulic-fracture-induced seismicity in gas shales, paper SPE 151597, presented at the 2012 SPE Hydraulic Fracturing Technology Conference: Society of Petroleum Engineers, 19 p.

7. Hydraulic Fracturing Fluids Disclosure

Sand and water typically comprise more than 99.5 percent of the fluid system used in hydraulic fracturing. However, to get that fluid to formations thousands of feet underground requires advanced chemistry and engineering to:

- Deter the growth and buildup of bacteria in the fluid and the wellbore;
- Ensure the sand (or proppant) is properly suspended, enabling it to be delivered into the fracture; and,
- Reduce the surface tension of the water in contact with the reservoir to improve production

The information given in the Frac Focus reports provided by Halliburton name the additives in the fracturing solutions, list the constituents, and explain some of their other, more common household and industrial uses. Halliburton typically tailors the fracturing fluids used to different geologic formation /zones; therefore, the composition varies by location.

Please see the link below for more information on Halliburton's corporate fluids disclosure policies.

http://www.halliburton.com/public/projects/pubsdata/Hydraulic_Fracturing/fluids_disclosure.html

Frac Focus Reports

The Frac Focus reports for VIC1-330 and VIC1-635 provide the following Hydraulic Fracturing Fluid Product Component Information:

- Supplier, purpose, ingredients chemical abstract service # (CAS #) and maximum ingredient concentrations in additives and hydraulic fracturing fluid (% by mass);
- List of typical fracturing fluid additives used in the Nodular formation; and
- Composition of fracturing fluid for the Nodular formation

7.1. Frac Focus Report for VIC1-330 in the Nodular Formation

The details of the “Frac Focus Report for VIC1-330” are provided in the following tables.

List of Typical Fracturing Fluid Additives at Inglewood Nodular Formation			
Additive Type	Typical Main Compound	Purpose	Common use of Main Compound
Biocide	Propionamide	Prevents or limits growth of bacteria	Agricultural - Antimicrobial Agent
Breaker	Sodium Persulfate	Agent used to degrade viscosity	Hair Dye, Industrial Circuit Boards, Industrial Metal Cleaner
Breaker	Ammonium Persulfate	Agent used to degrade viscosity	Hair Dye, Industrial Circuit Boards, Industrial Metal Cleaner
Crosslinker	Borate	Developing viscosity	Cocoa and Chocolate Products, Infant and Young Children Foods, Cottage Cheese
Gel	Polysaccharide	Gelling agent for developing viscosity	Herbal Supplements, Fruit Jelly, Beer and Malt Beverages, Mustard
	Naphtha hydrotreated heavy		Industrial Cleaning Solution, Tire Repair, Agricultural Insecticide
KCL	Potassium Chloride	Clay Control	Agricultural - fertilizer
pH Adjusting Agent	Acetic Acid	Adjusts pH to proper range for fluid	Vinegar, Cleaning Products
pH Adjusting Agent	Potassium Carbonate	Adjusts pH to proper range for fluid	Soap, Glass Production
pH Adjusting Agent	Sodium Hydroxide	Adjusts pH to proper range for fluid	Laundry Detergent, Toothpaste, Cocoa, Milk Products, Chocolate
Proppant	Silica	Holds open fracture to allow oil and gas to flow to well	Hand Cleaner, Laundry Cleaner, Cat Litter
Surfactant	Ethanol	Aids in recovery of water used during frac	Ginseng, Deodorizer, Dish Soap, Cologne, Makeup (Mascara), Mouthwash
Water	Water	Base fluid creates fractures and carries proppant, also can be present in some additives	

Table 7.1. List of typical fracturing fluid additives at VIC1-330 well in the Inglewood Nodular formation

**Plains Exploration & Production Company
Inglewood Oil Field Hydraulic Fracturing Report**

Composition of Fracturing Additive for Inglewood Nodular Formation												
Common Name	Supplier Chemical Name	Common Description	Component listed on MSDS	Common Chemical Name	Purpose	Component Weight % of Chemical	Component loading gal/1000 gal	Gallons of Component / stage	Weight of Component / stage	Concentration Component of Total Stage Fluid		
Water		Water						168,210	1,401,189	by % Vol	by % Weight	ppm
Biocide	BE-3S	Biocide			Eliminate Bacteria		0.15 ppt		30.00			
			2-Monobromo-3-nitriropropionamide			1-5%					0.0001%	0.9
			2,2 Dibromo-3-nitriropropionamide			60-100%					0.0018%	17.5
Liquid Gel Concentrate	LGC-36 UC	Gelling Agent			Adds Viscosity		6.0 gpt		515			
			Guar Gum	Polyscharide or Long chain made of sugars		30-60%			2317.50		0.135%	1353.1
			Naphtha, hydrotreated heavy			30-60%				0.183%		1826.5
Breaker	SP Breaker	Gel Breaker			Reduces Viscosity		0 - 1.0 ppt					
			Sodium Persulfate			60-100%			40		0.002%	23.4
Breaker	OptiFlo III	Gel Breaker			Reduces Viscosity		1.0 - 2.0 ppt					
			Ammonium Persulfate			60-100%			150		0.009%	87.6
			Crystalline Silica	Beach Sand		10-30%					0.003%	26.3
Friction Reducer	FR-66	Friction Reducer			Reduces pipe friction		1.0 gpt		85			
			Hydrotreated Light Petroleum Distillate			10-30%				0.015%		150.7
Crosslinker	K-38	Crosslinker			Increases Viscosity		0.6 ppt					
			Disodium Octoborate Tetrahydrate			60-100%			32		0.002%	18.7
Crosslinker	CL-28M	Crosslinker			Increases Viscosity		1.2 gpt		80			
			Borate Salts			30-60%					0.003%	28.0
			Crystalline Silica	Beach Sand		5%					0.000%	2.3
Acid	Fe-1A	Acid			Lowers pH		0.25 gpt		8			
			Acetic Anhydrite			60-100%					0.000%	4.7
			Acetic Acid			30-60%					0.000%	2.8
Buffer	BA-40L	Buffer			pH Buffer		1.0 gpt		90			
			Potassium Carbonate			30-60%				0.032%		319.2
Buffer	MO-67	Caustic			pH Buffer		0.2 gpt		15			
			Sodium Hydroxide	Caustic soda or lye		10-30%				0.003%		26.6
Surfactant	Losurf-300M	Surfactant			Aids in fluid recovery		1.0 gpt		175			
			Ethanol	Grain alcohol or Drinking alcohol (spirits)		30-60%				0.062%		620.6
			Poly(oxy-1,2-ethanediy), alpha-(4-nonylphenyl)-omega-hydroxy-, branched			5-10%				0.010%		103.4
			Naphthalene	Mothball Crystals		0 - 1%				0.001%		10.3
			1,2,4 Trimethylbenzene	Aromatic or Cyclic Hydrocarbon		0 - 1%				0.001%		10.3
			Heavy aromatic petroleum naphtha	Petroleum Distillate		10 - 30%				0.031%		310.3
KCL	KCL	Potassium Chloride	7%	Muriate of potash (fertilizer)	Clay control		585 ppt		98000		5.72%	57217.6
PRC Sand	Proppant	Quartz		Beach sand	Holds open fracture		2.0 - 6.0 ppg		145000		8.5%	84658.8
100 mesh Sand	Proppant	Quartz		Beach sand	Holds open fracture		0.5 ppg		6000		0.4%	3503.1
Sand	Proppant	Quartz		Beach sand	Holds open fracture		0.5 - 2.0 ppg		60000		3.5%	35031.2
							Total	169,178	1,712,759			

Table 7.2. Composition of fracturing fluid additives in VICI-330 well in the Inglewood Nodular formation

**Plains Exploration & Production Company
Inglewood Oil Field Hydraulic Fracturing Report**

Hydraulic Fracturing Fluid Product Component Information Disclosure

Fracture Date:	9/15/2011
State:	California
County:	Los Angeles
API Number:	0403726720
Operator Name:	P WESTERN BUSINESS UNIT
Well Name and Number:	VIC 1-330
Longitude:	
Latitude:	
Long/Lat Projection:	
Production Type:	
True Vertical Depth (TVD):	8,030
Total Water Volume (gal)*:	168,210

Hydraulic Fracturing Fluid Composition

Trade Name	Supplier	Purpose	Ingredients	Chemical Abstract Service Number (CAS #)	Maximum Ingredient Concentration in Additive (% by mass)**	Maximum Ingredient Concentration in HF Fluid (% by mass)**	Comments
7% KCL Water	Operator				100.00%	86.77644%	Density = 8.700
SAND - PREMIUM WHITE	Halliburton	Proppant	Crystalline silica, quartz	14808-60-7	100.00%	3.70605%	
PRC SAND	Halliburton	Proppant	Crystalline silica, quartz	14808-60-7	100.00%	8.59803%	
			Hexamethylenetetramine	1009-7-0	2.00%	0.17196%	
			Phenol / formaldehyde resin	900303-35-4	5.00%	0.42990%	
SSA-2	Halliburton	Sand	Crystalline silica, quartz	14808-60-7	100.00%	0.35578%	
FR-66	Halliburton	Friction Reducer	Hydrotreated light petroleum distillate	64742-47-8	30.00%	0.01335%	
LOSURF-300M™	Halliburton	Surfactant	1,2,4 Trimethylbenzene	95-63-6	1.00%	0.00079%	
			Ethanol	64-17-5	60.00%	0.04763%	
			Heavy aromatic petroleum naphtha	64742-94-5	30.00%	0.02382%	
			Naphthalene	91-20-3	1.00%	0.00079%	
			Poly(oxy-1,2-ethanediy), alpha-(4-nonylpheny	127087-87-0	10.00%	0.00794%	
CL-28M CROSSLINKER	Halliburton	Crosslinker	Crystalline silica, quartz	14808-60-7	5.00%	0.00249%	
			Borate salts	Confidential Business In	60.00%	0.02989%	
MO-67	Halliburton	Buffer	Sodium hydroxide	1310-73-2	30.00%	0.00283%	
BA-40L BUFFERING AGENT	Halliburton	Buffer	Potassium carbonate	584-08-7	60.00%	0.03990%	
FE-1A ACIDIZING COMPOSITION	Halliburton	Misc Additive	Acetic acid	64-19-7	60.00%	0.00255%	
			Acetic anhydride	108-24-7	100.00%	0.00425%	
K-38	Halliburton	Crosslinker	Disodium octaborate tetrahydrate	12008-41-2	100.00%	0.02099%	
LGC-36 UC	Halliburton	Gelling Agent	Guar gum	9000-30-0	60.00%	0.16582%	
			Naphtha, hydrotreated heavy	64742-48-9	60.00%	0.16582%	
BE-3S BACTERICIDE	Halliburton	Biocide	2,2 Dibromo-3-nitripropionamide	10222-01-2	100.00%	0.00119%	
			2-Monobromo-3-nitripropionamide	1113-55-9	5.00%	0.00006%	
OPTIFLO-III DELAYED RELEASE BREAKER	Halliburton	Breaker	Ammonium persulfate	7727-54-0	100.00%	0.00889%	
			Crystalline silica, quartz	14808-60-7	30.00%	0.00267%	
SP BREAKER	Halliburton	Breaker	Sodium persulfate	7775-27-1	100.00%	0.00237%	

* Total Water Volume sources may include fresh water, produced water, and/or recycled water

** Information is based on the maximum potential for concentration and thus the total may be over 100%

All component information listed was obtained from the supplier's Material Safety Data Sheets (MSDS). As such, the Operator is not responsible for inaccurate and/or incomplete information. Any questions regarding the content of the MSDS should be directed to the supplier who provided it. The Occupational Safety and Health Administration's (OSHA) regulations govern the criteria for the disclosure of this information. Please note that Federal Law protects 'proprietary', 'trade secret', and 'confidential business information' and the criteria for how this information is reported on an MSDS is subject to 29 CFR 1910.1200(i) and Appendix D.

HALLIBURTON

The information in this document is provided for general information purposes only. While Halliburton strives to provide timely, accurate and complete information, this document may contain inadvertent typographical, technical, factual, or other errors or omissions in the information provided. UNDER THESE CIRCUMSTANCES HALLIBURTON MAKES NO GUARANTEES, WARRANTIES OR REPRESENTATIONS, EXPRESS OR IMPLIED, CONCERNING THE SECURITY, TIMELINESS, RELEVANCY, SUFFICIENCY, ACCURACY, RELIABILITY, MERCHANTABILITY, FITNESS FOR ANY PARTICULAR PURPOSE, TITLE OR OTHER PROPRIETARY RIGHTS, NON-INFRINGEMENT OR COMPLETENESS OF ANY DATA, INFORMATION, OR SERVICES FURNISHED TO YOU IN OR THROUGH THIS DOCUMENT, OR CONCERNING THE INFORMATION YOU PROVIDE TO US. HALLIBURTON IS PROVIDING THE INFORMATION AND OTHER CONTENT CONTAINED HEREIN ON AN "AS IS, WHERE IS, AS AVAILABLE" BASIS, AND ALL WARRANTIES (EXPRESS OR IMPLIED) ARE DISCLAIMED.

Table 7.3. Composition of fracturing fluid in VICI-330 well in the Inglewood Nodular formation

7.2. Frac Focus Report for VIC1-635 in the Nodular Formation

The details of the “Frac Focus Report for VIC1-635” provided in the following tables:

List of Typical Fracturing Fluid Additives at Inglewood Nodular Formation			
Additive Type	Typical Main Compound	Purpose	Common use of Main Compound
Activator	EDTA / Copper Chelate	Agent used to degrade viscosity	Fertilizer for Agricultural Use and Farm Animal Hoof Infection Treatment
Biocide	Propionamide	Prevents or limits growth of bacteria	Agricultural - Antimicrobial Agent
Breaker	Sodium Persulfate	Agent used to degrade viscosity	Hair Dye, Industrial Circuit Boards, Industrial Metal Cleaner
Crosslinker	Borate	Agent used for developing viscosity	Cocoa and Chocolate Products, Infant and Young Children Foods, Cottage Cheese
Clay Control	alkylated quaternary Chloride	Clay-stabilization additive which helps prevent clay particles from migrating in water-sensitive formations.	Laundry Detergent, Floor Cleaner, Industrial Grinding Fluid
Gel	Polysaccharide	Gelling agent for developing viscosity	Herbal Supplements, Fruit Jelly, Beer and Malt Beverages, Mustard
	Naphtha hydrotreated heavy		Industrial Cleaning Solution, Tire Repair, Agricultural Insecticide
KCL	Potassium Chloride	Clay Control	Agricultural - fertilizer
pH Adjusting Agent	Sodium Hydroxide	Adjusts pH to proper range for fluid	Laundry Detergent, Toothpaste, Cocoa, Milk Products, Chocolate
Proppant	Silica	Holds open fracture to allow oil and gas to flow to well	Hand Cleaner, Laundry Cleaner, Cat Litter
Surfactant	Ethanol	Aids in recovery of water used during frac	Ginseng, Deodorizer, Dish Soap, Cologne, Makeup (Mascara), Mouthwash
Water	Water	Base fluid creates fractures and carries proppant, also can be present in some additives	

Table 7.4. List of typical fracturing fluid additives at VIC1-635 well in the Inglewood Nodular formation

Plains Exploration & Production Company Inglewood Oil Field Hydraulic Fracturing Report

Composition of Fracturing Additive for Inglewood Nodular Formation													
Common Name	Supplier Chemical Name	Common Description	Component listed on MSDS	Common Chemical Name	Purpose	Component Weight % of Chemical	Component loading gal/1000 gal	Gallons of Component / stage	Weight of Component / stage	Concentration Component of Total Stage Fluid			
										by % Vol	by % Weight	ppm	
Water		Water						125,248	1,043,316	99.3%	82.43%	990000	
Biocide	BE-3S	Biocide	2-Monobromo-3-nitropropionamide		Eliminate Bacteria	1-5%	0.15 ppt		6.00		0.0000%	1	
			2,2-Dibromo-3-nitropropionamide			60-100%					0.0005%	15	
Liquid Gel Concentrate	LGC-36 UC	Gelling Agent	Guar Gum	Polysaccharide or Long chain made of sugars	Adds Viscosity	30-60%	4.0 - 5.0 gpt	466		2097.00	0.166%	2200	
			Naphtha, hydrotreated heavy			30-60%				0.222%		2970	
Breaker	SP Breaker	Gel Breaker	Sodium Persulfate		Reduces Viscosity	60-100%	2gpt		82		0.006%	200	
Buffer	MO-67		Sodium Hydroxide	Caustic soda or lye	pH Buffer	10-30%	1 gpt	75			0.018%	300	
Surfactant	Losurf-300M	Surfactant	Ethanol	Grain alcohol or Drinking alcohol (spirits)	Aids in fluid recovery	30-60%	1.0 gpt	130			0.062%	590	
			Poly(oxy-1,2-ethanediyl), alpha-(4-nonylphenyl)-omega-hydroxy-, branched			5-10%					0.010%	10	
			Naphthalene	Mothball Crystals		0 - 1%					0.001%	10	
			1,2,4 Trimethylbenzene	Aromatic or Cyclic Hydrocarbon		0 - 1%					0.001%	10	
			Heavy aromatic petroleum naphtha	Petroleum Distillate		10 - 30%					0.031%	300	
Friction Reducer	FR-66	Friction Reducer	Hydrotreated light petroleum		Reduce Friction	0-30%	1gpt	60			0.03%	300	
Conductivity Enhancer	SandWedge		Isopropanol	Petroleum Distillate	Increases Viscosity	30-60%	2.0 -2.5 gpt	130			0.06%		
			Heavy aromatic petroleum Naphtha	Petroleum Distillate		5-10%					0.01%	2200	
			Methanol	Grain alcohol or Drinking alcohol (spirits)		1-5%					0.005%	2970	
Buffering Agent	BA-40L		Potassium carbonate	Baking Soda		3- 60%	1gpt	50			0.02%	600	
Crosslinker	CL-28		Borate salts	Table Salt	Increase Viscosity	3- 60%	0.7gpt	10			0.005%	600	
			Crystalline silica, quartz	Sand		1-5%					0.0004%	1100	
Acidizing Composition	FE-1A		Acetic anhydride			60-100%	X	5				200	
			Acetic acid	Vinegar		30-60%					0.0024%	600	
Crosslinker	K-38		Disodium octaborate tetrahydrate		Increase Viscosity	60 -100%	0.5gpt	5			0.00040%	0.00000%	600
KCL	KCL	Potassium Chloride	3%	Muriate of potash (fertilizer)	Clay control	60 -100%	250 ppt		31312	0.024739	2.47%	24500	
Sand 2/40 premium white	Proppant	Quartz	Crystalline silica, quartz	sand	Holds open fracture				36800	2.907%	2.9%	29074.53	
Sand CRC 16/30	Proppant	Quartz	Crystalline silica, quartz	sand	Holds open fracture				147100	11.622%	11.6%	116219.1	
Sand common 100 mesh	Proppant	Quartz	Crystalline silica, quartz	sand	Holds open fracture				5000	0.395%	0.4%	3950.343	
							Total		126,179	1,265,713			

Table 7.5. Composition of fracturing fluid additives in VICI-635 well in the Inglewood Nodular formation

**Plains Exploration & Production Company
Inglewood Oil Field Hydraulic Fracturing Report**

Hydraulic Fracturing Fluid Product Component Information Disclosure

Fracture Date:	1/5/2012
State:	California
County:	Los Angeles
API Number:	0403726421
Operator Name:	P WESTERN BUSINESS UNIT
Well Name and Number:	Vic1 635
Longitude:	
Latitude:	
Long/Lat Projection:	
Production Type:	Gas
True Vertical Depth (TVD):	8,430
Total Water Volume (gal):	125,248

Hydraulic Fracturing Fluid Composition

Trade Name	Supplier	Purpose	Ingredients	Chemical Abstract Service Number (CAS #)	Maximum Ingredient Concentration in Additive (% by mass)**	Maximum Ingredient Concentration in HF Fluid (% by mass)**	Comments
SAND - COMMON WHITE	Halliburton	Proppant	Crystalline silica, quartz	14808-60-7	100.00%	1.42615%	
SAND - PREMIUM WHITE	Halliburton	Proppant	Crystalline silica, quartz	14808-60-7	100.00%	24.30405%	
CRC SAND	Halliburton	Proppant	Crystalline silica, quartz	14808-60-7	100.00%	69.98805%	
			Hexamethylenetetramine	1009-7-0	2.00%	1.39976%	
			Phenol / formaldehyde resin	900303-35-4	5.00%	3.49940%	
LOSURF-300M™	Halliburton	Surfactant	1,2,4 Trimethylbenzene	95-63-6	1.00%	0.00473%	
			Ethanol	64-17-5	60.00%	0.28366%	
			Heavy aromatic petroleum naphtha	64742-94-5	30.00%	0.14183%	
			Naphthalene	91-20-3	1.00%	0.00473%	
			Poly(oxy-1,2-ethanediyl), alpha-(4-nonylphenyl)-omega-hydroxy-, branched	127087-87-0	10.00%	0.04728%	
K-38	Halliburton	Crosslinker	Sodium octaborate tetrahydrate	12008-41-2	100.00%	0.26926%	
FR-66	Halliburton	Friction Reducer	Hydrotreated light petroleum distillate	64742-47-8	30.00%	0.07556%	
SandWedge® NT	Halliburton	Conductivity Enhancer	Dipropylene glycol monomethyl ether	34590-94-8	60.00%	0.29738%	
			Heavy aromatic petroleum naphtha	64742-94-5	10.00%	0.04956%	
BA-40L BUFFERING AGENT	Halliburton	Buffer	Potassium carbonate	584-08-7	60.00%	0.17770%	
CL-28M CROSSLINKER	Halliburton	Crosslinker	Crystalline silica, quartz	14808-60-7	5.00%	0.00250%	
			Borate salts	Confidential Business Information	60.00%	0.02995%	
FE-1A ACIDIZING COMPOSITION	Halliburton	Misc Additive	Acetic acid	64-19-7	60.00%	0.01278%	
			Acetic anhydride	108-24-7	100.00%	0.02130%	
LGC-36 UC	Halliburton	Gelling Agent	Guar gum	9000-30-0	60.00%	1.20290%	
			Naphtha, hydrotreated heavy	64742-48-9	60.00%	1.20290%	
MO-67	Halliburton	Buffer	Sodium hydroxide	1310-73-2	30.00%	0.11359%	
BE-3S BACTERICIDE	Halliburton	Biocide	2,2 Dibromo-3-nitropropionamide	10222-01-2	100.00%	0.00285%	
			2-Monobromo-3-nitropropionamide	1113-55-9	5.00%	0.00014%	
K-38	Halliburton	Crosslinker	Sodium octaborate tetrahydrate	12008-41-2	100.00%	0.01902%	
SP BREAKER	Halliburton	Breaker	Sodium persulfate	7775-27-1	100.00%	0.01949%	

* Total Water Volume sources may include fresh water, produced water, and/or recycled water
 ** Information is based on the maximum potential for concentration and thus the total may be over 100%

All component information listed was obtained from the supplier's Material Safety Data Sheets (MSDS). As such, the Operator is not responsible for inaccurate and/or incomplete information. Any questions regarding the content of the MSDS should be directed to the supplier who provided it. The Occupational Safety and Health Administration's (OSHA) regulations govern the criteria for the disclosure of this information. Please note that Federal Law protects 'proprietary', 'trade secret', and 'confidential business information' and the criteria for how this information is reported on an MSDS is subject to 29 CFR 1910.1200(i) and Appendix D.

HALLIBURTON

The information in this document is provided for general information purposes only. While Halliburton strives to provide timely, accurate and complete information, this document may contain inadvertent typographical, technical, factual, or other errors or omissions in the information provided. UNDER THESE CIRCUMSTANCES HALLIBURTON MAKES NO GUARANTEES, WARRANTIES OR REPRESENTATIONS, EXPRESS OR IMPLIED, CONCERNING THE SECURITY, TIMELINESS, RELEVANCY, SUFFICIENCY, ACCURACY, RELIABILITY, MERCHANTABILITY, FITNESS FOR ANY PARTICULAR PURPOSE, TITLE OR OTHER PROPRIETARY RIGHTS, NON-INFRINGEMENT OR COMPLETENESS OF ANY DATA, INFORMATION, OR SERVICES FURNISHED TO YOU IN OR THROUGH THIS DOCUMENT, OR CONCERNING THE INFORMATION YOU PROVIDE TO US. HALLIBURTON IS PROVIDING THE INFORMATION AND OTHER CONTENT CONTAINED HEREIN ON AN "AS IS, WHERE IS, AS AVAILABLE" BASIS, AND ALL WARRANTIES (EXPRESS OR IMPLIED) ARE DISCLAIMED.

Table 7.6. Composition of fracturing fluid in VICI-635 well in the Inglewood Nodular formation

8. Fracture Height Growth and Containment of Hydraulic Fractures

A significant amount of discussion has taken place about the vertical growth of hydraulic fractures, particularly in gas shales, tight sands, and shallow reservoirs in regards to whether these hydraulic fractures can create pathways for the fracturing fluids or hydrocarbons to migrate upward and contaminate groundwater supplies.

The vertical extent that a created fracture can propagate is controlled by the upper confining zone or formation, and the volume, rate, and pressure of the fluid that is pumped. The confining zone will limit the vertical growth of a fracture because it either possesses sufficient strength or elasticity to contain the pressure of the injected fluids or an insufficient volume of fluid has been pumped. This is important to note because the greater the distance between the fractured formation and the groundwater or water-bearing zones, the more likely it is that multiple formations will possess the qualities necessary to impede the growth of hydraulic fractures.

Fracture lengths can sometimes exceed 1,000 ft. when contained within a relatively homogenous layer, but due to the layered geological environment and other physical parameters fracture lengths are typically much smaller, and are usually measured in tens or hundreds of feet (Fisher and Warpinski, 2011).

Micrseismic monitoring can detect the small slippages or microseisms induced in natural fractures, bedding planes, faults, and other weak features in the reservoir and they help track the fracture location and any interaction with existing natural fractures and other geologic features.

Note: Please refer to Section 6, titled, "Microseismic Monitoring", for additional details

Fracture Height in Inglewood Field

Fig. 8.1 shows the HRGP geometries (including the height) for all the different stages of the wells analyzed in the Vickers and Rindge zones. The discontinuous groundwater bodies (perched zones) in the Inglewood Oil Field are also shown.

The model calculated vertical distances between the top of the created HRGPs in the study wells and the discontinuous groundwater bodies (perched zones) near the surface are also indicated in Fig. 8.1. The shortest vertical distance was 1,070 ft. and the distances in the other study wells ranged from 1,728 to 1,758 ft. It is clear from the model results shown in Fig. 8.1 that in the study wells in the Vickers and Rindge zones, the created HRGPs did not come close to the discontinuous groundwater bodies (perched zones) on the surface.

The Vickers and Rindge zones are the shallowest reservoirs, the other zones in the Inglewood Oil Field are much deeper. Consequently, the distances between the modeled fractures created in the other zones and the discontinuous groundwater bodies are even greater, for eg., about 7,700 ft in the case of Nodular shale zone. As stated earlier, the physical properties of the multiple layered formations in the Inglewood Oil Field confined the height growth of the the high-rate gravel packs in the Vickers Rindge and the fractures in the other zones.

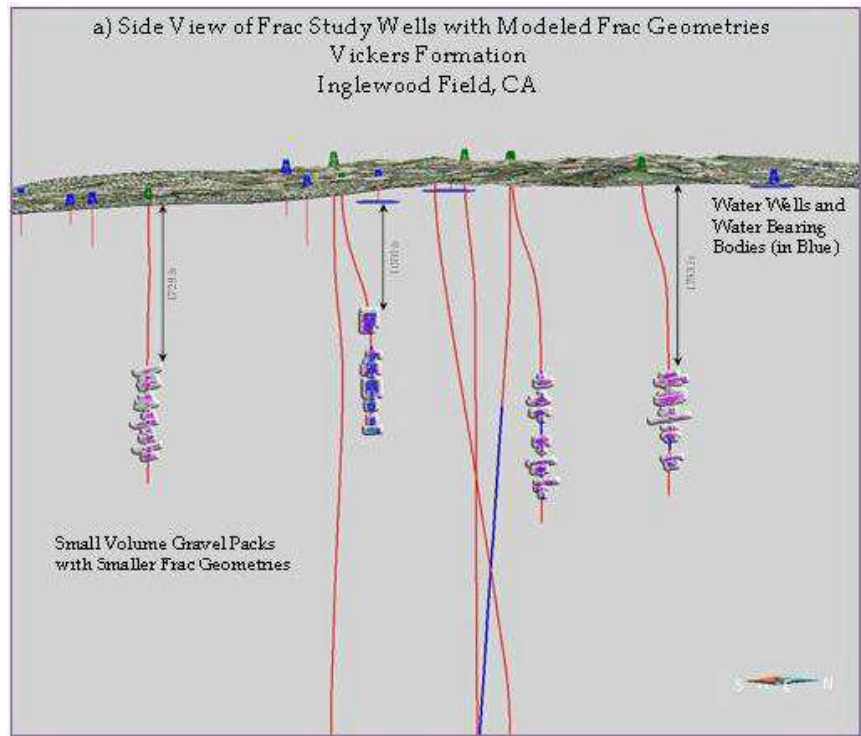


Fig. 8.1. Side view visualization showing the modeled HRGP geometries in the Vickers zone.

Fracture Growth in other Shale Reservoirs in North America

A recent study that analyzed actual fracture growth data mapped during thousands of fracturing treatments in gas shales and tight-sand reservoirs found similar results (Fisher and Warpinski, 2011). This paper includes an in-depth discussion of fracture-growth limiting mechanisms augmented by other studies that examined hydraulic fracture growth.

Figures 8.2a-c present data collected during thousands of hydraulic-fracturing stimulation treatments in some of the most active gas-shale plays in North America: the Barnett shale in Texas, the Woodford shale in Oklahoma, and the Marcellus shale in the Northeastern United States (Fisher and Warpinski, 2011). More fracture treatments have been mapped in the Barnett shale than in any other reservoir.

Each graph plots the fracture top and bottom for all mapped fracture treatments performed in each reservoir from early 2001 through the end of 2010. All depths are true vertical depth (TVD). Perforation depths are indicated by the red band for each stage. The colored curves show the mapped fracture top and bottom corresponding to the counties in which the well is located. The dark blue bars at the top of each graph show the depth of deepest reported drinking water bearing zones in each of the counties where the fractures were mapped. The depth scale in the vertical axis varies from reservoir to reservoir because of large differences in the depths of the reservoir zones. The plots show that the largest directly measured upward growth of all of these mapped fractures still places the fracture tops several thousand feet below the deepest known aquifer level in each of the reservoirs presented (Fisher and Warpinski, 2011), removing any potential of the hydraulic fracturing operation to impact the aquifer (if present).

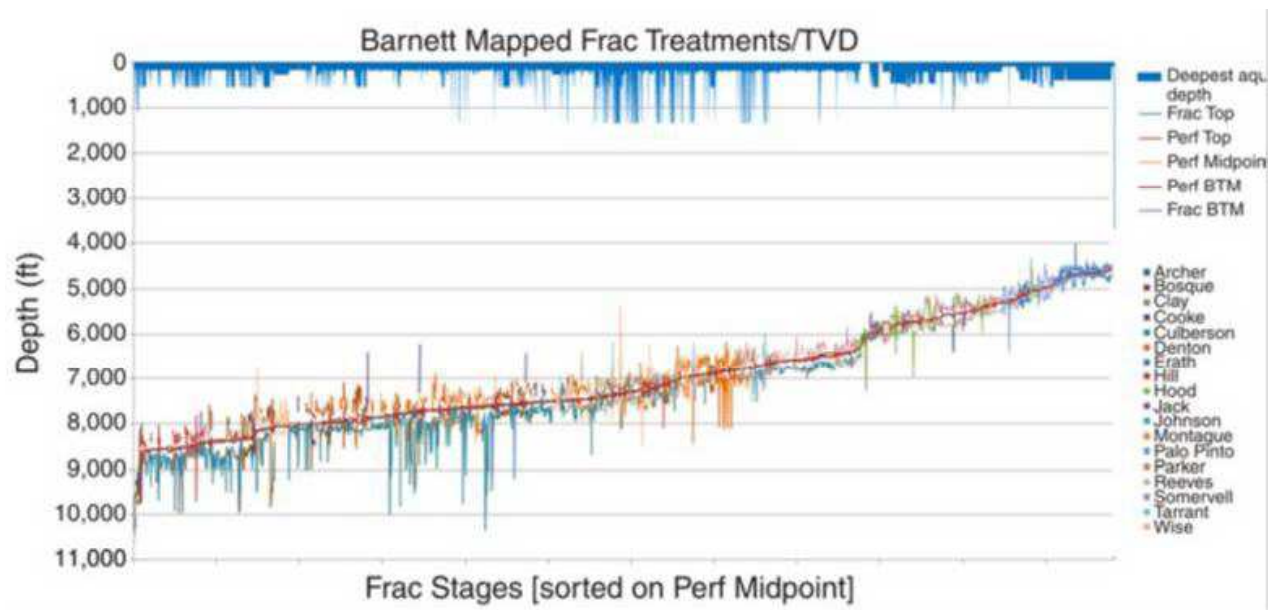


Fig. 8.2a. Barnett shale measured fracture heights sorted by depth and compared to aquifers (Fisher and Warpinski, 2011)

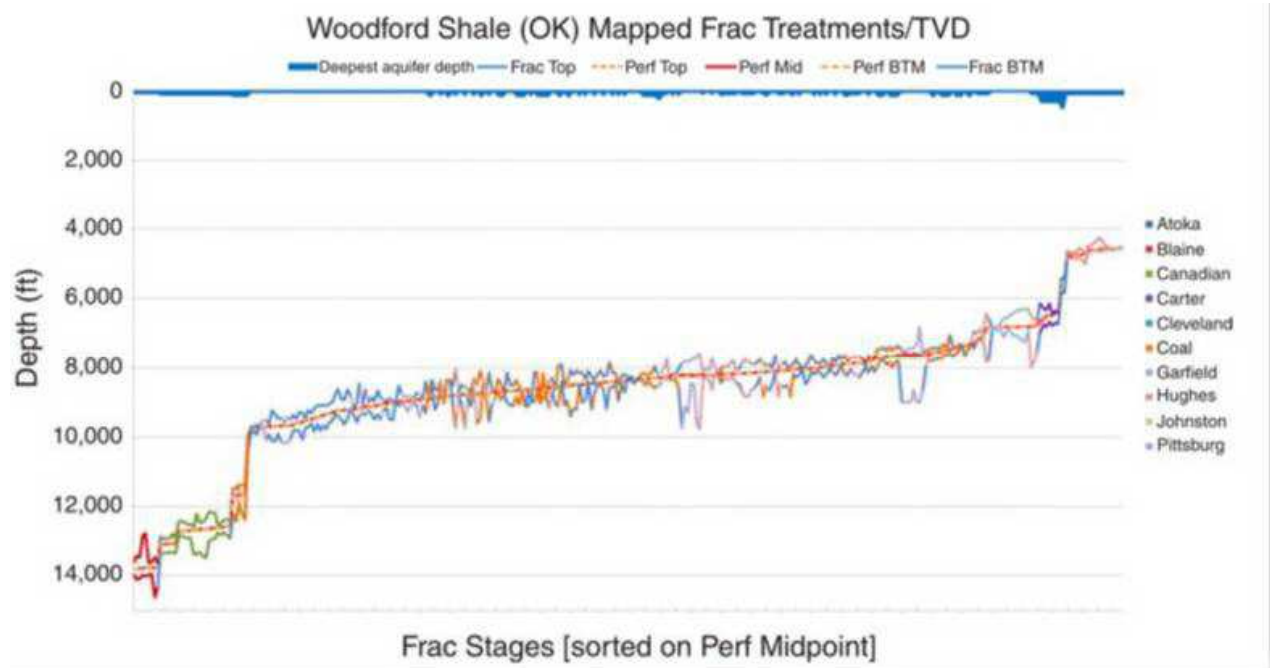


Fig. 8.2b. Woodford shale measured fracture heights sorted by depth and compared to aquifer depths (Fisher and Warpinski, 2011).

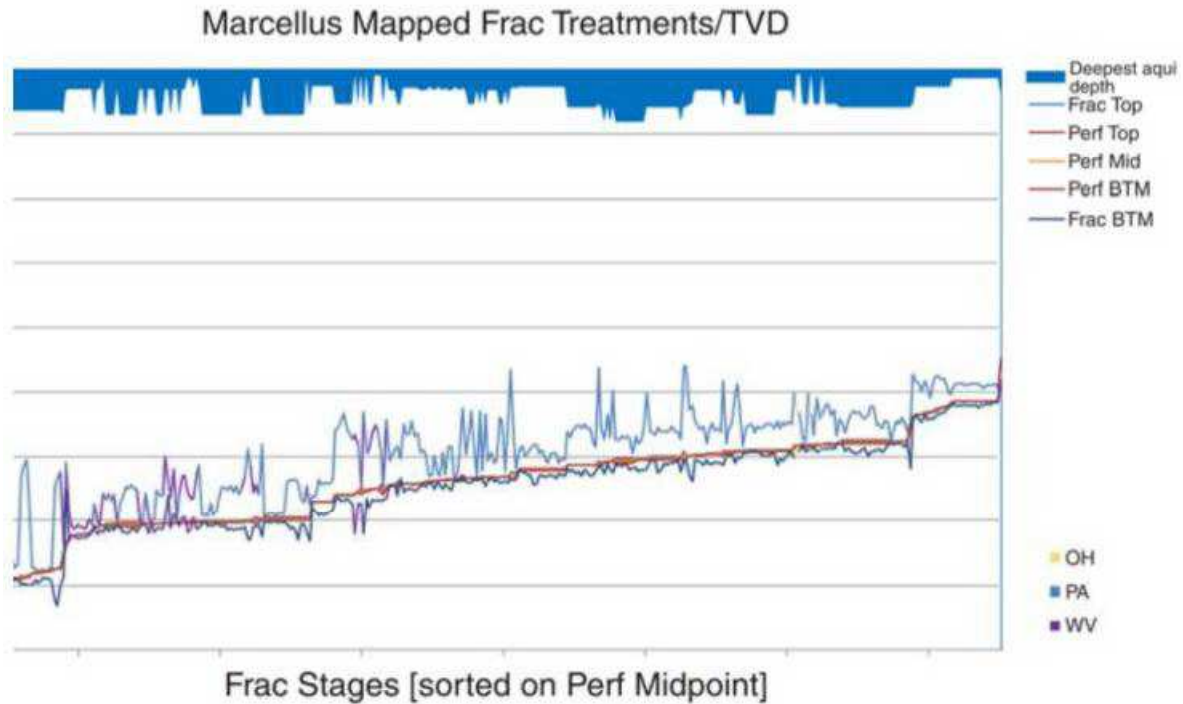


Fig. 8.2c. Marcellus shale measured fracture heights sorted by depth and compared to aquifer depths (Fisher and Warpinski, 2011).

8.1. Factors Contributing to Fracture Height Containment

The paper by Fisher and Warpinski (2011) discusses several additional factors and means for containing fracture height.

- Fractures in common geologic environments show varying degree of complexity (non-planar). As a result of this complexity fractures tend to grow shorter than they would if they were planar fractures;
- The layering of sedimentary rocks creates large variations in rock stresses. The combination of variability in rock stress with varying interface properties creates an environment that hinders the vertical growth of fractures. The large variations in stress across rock strata act to trap the fractures in low stress zones. These conditions favor lateral fracture because it is the path of least resistance. Therefore it is highly unlikely that the fractures will propagate very far vertically;
- Fracture growth occurs perpendicular to the direction of least principal stress, i.e., in the direction of maximum stress. In all the sedimentary basins where measurements have been made, the vertical stress generated by the weight of the rock overburden is the minimum stress at depths less than approximately 2,000 ft. At these relatively shallow depths, fracture growth will be primarily in the horizontal direction and not vertically. It is possible some shallow individual rock layers may have a horizontal in-situ stress that is the minimum stress, which would result in vertical fracture growth within these layers. However, the majority of near-surface rock layers would have horizontal fractures that do not propagate vertically. In addition, mixed fracture growth, in both horizontal and vertical directions would significantly limit vertical growth;
- In cases where a fracture might cross over a boundary between adjacent rock layers where the principal stress direction changes, the fracture would attempt to reorient itself perpendicular to the direction of least stress. Therefore, if a fracture propagated from a deeper to a shallower formation it would reorient itself from a vertical to a horizontal pathway and grow sideways along the bedding planes of the rock strata; and,
- Under normal circumstances, where hydraulic fracturing is conducted at deep depths, there is no physical mechanism by which a fracture can propagate through the various rock layers and reach the surface. This fact was observed in all of the fracture mapping data in different gas-shale plays and is expected based on the application of basic rock-mechanics principles deduced from mineback, core, lab, and modeling studies.

The actual data collected using microseismic and microdeformation or tiltmeter fracture-mapping technologies on many thousands of hydraulic fracturing jobs indicate that hydraulic-fracture heights are relatively well-contained (Fisher and Warpinski, 2011).

Note: Please refer Attachment 8A, Technical paper SPE 145949 entitled “Hydraulic Fracture-Height Growth: Real data” for additional details and information

8.2. Hydraulic Fracturing and Water Contamination

Hydraulic fracturing has been in use for over 60 years and both state and federal regulatory agencies, including the EPA, have repeatedly stated that that they are not aware of any instances of hydraulic fracturing resulting in contamination of drinking water aquifers (IOGCC, 2009)).

- *Note: Please refer to Attachment 8B entitled “Regulatory Statements on Hydraulic Fracturing” submitted by the States in June 2009 for additional details.*
- *Note: Please refer to Attachment 8C entitled “Data Confirm Safety of Well Fracturing” an article by Kevin Fisher from American Oil & Gas Reporter, July 2010. The article presents a first look at the actual field data based on direct measurements acquired while fracture mapping more than 15,000 frac jobs during the past decade. The article also addresses the concerns surrounding the possibility of groundwater contamination.*

Well operators are currently applying hydraulic fracturing treatments in approximately 35,000 wells per year in the U.S. with no evidence of resulting groundwater contamination (Tippee, 2008).

Similar results were observed during the hydraulic fracturing stimulation treatments of the two wells in the Nodular Shale zone. The distances of the created fractures from the discontinuous groundwater bodies near the surface were too significant (about 7,700 ft.) to have any effect on the discontinuous groundwater bodies near the surface. This is clear from the Fig. 8.3 that shows a side view of the Inglewood Oil Field Structure along with the location and depth of the microseismic events that were recorded during the hydraulic fracturing stimulation treatments in Wells VICI-330 and VICI-635 in the Nodular Shale zone.

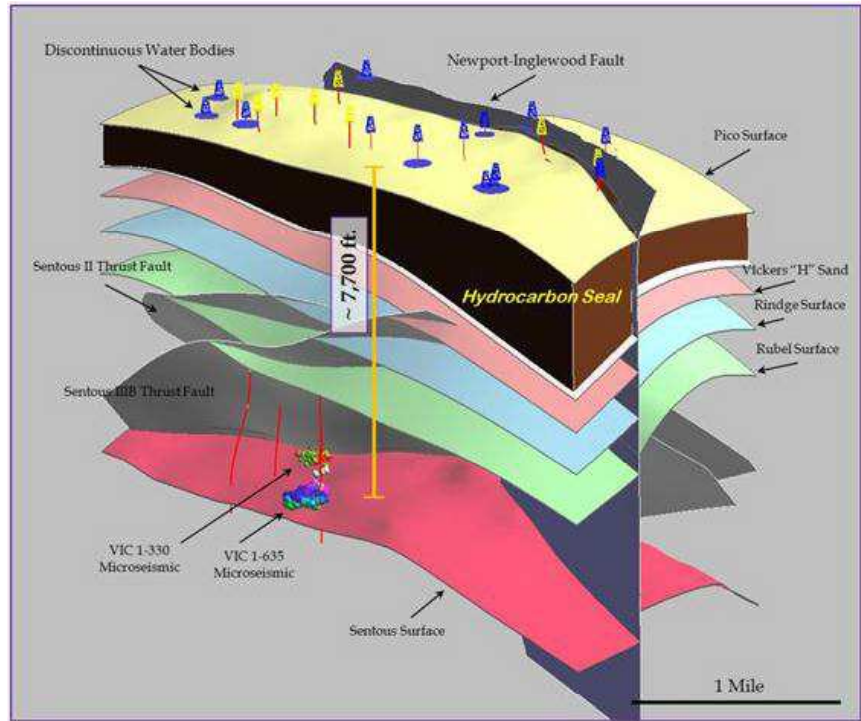


Fig. 8.3. Side View of the Inglewood Oil Field structure with the microseismic events recorded in the two wells completed in the Nodular Shale zone

References

- Fisher, K., and Warpinski, N., 2011, Hydraulic fracture-height growth—real data, paper SPE-145949, presented at the 2011 SPE Annual Technical Conference and Exhibition: Society of Petroleum Engineers, 18 p.
- IOGCC, 2009, Regulatory statements on hydraulic fracturing submitted by the states: Interstate Oil and Gas Compact Commission.
- Tippee, B., 2008, Political fracturing: Oil & Gas Journal, November 17, 2008, p. 20.

9. High-Rate Gravel Packs

In the Baldwin Hills, the majority of the wells are completed using high-rate gravel pack (HRGP) treatments. This process is different from the hydraulic fracturing stimulation techniques used for tight sands, gas shale and coal gas recovery.

The HRGP completion technique involves two distinct injection stages performed in a single step.

The first stage creates a hydraulic crack and terminates its growth by tip screenout. The second stage involves continuous injection of high concentration slurry after the screenout, resulting in inflation and packing of the gravel pack through the near wellbore area to the production zone (Fan and Llave, 1996). These treatments are pumped down the tubing/casing annulus and have a wire wrapped screen installed in the well.

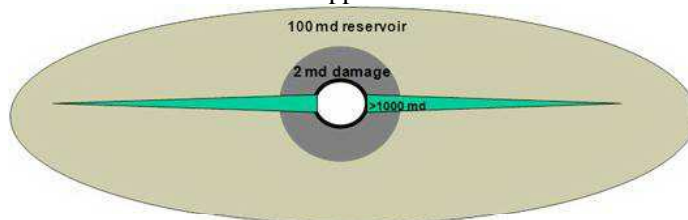


Fig. 9.1. Illustration of the high-rate gravel pack process.

The high-rate gravel pack is an established method for increasing production by creating a high-conductivity gravel pack that bypasses the reduced permeability zone in the near-wellbore region that was created during either drilling, cementing, perforating or fluid loss management processes. The HRGP creates a conduit for the flow of reservoir fluids at lower pressures.

Details of the High-Rate Gravel-Pack Process

In the high-rate gravel pack process, the rate is stepped down at the end of a typical propped treatment. With only a few barrels of the treatment left and a high sand concentration in the annulus, the choke is opened at the surface. This action drops the pressure in the tubing and diverts a part of the fluid away from the sand/water mixture. The sand slurry is dehydrated as it attempts to flow through the screen and up the tubing resulting in a screen packoff. After the treatment is shut down, the sand pack surrounding the screen is allowed to dehydrate for a few minutes further before the tubing is shut in (Moddie, Fernandez et al., 2004, SPE 90975)

Comparison of Sand and Fluid Volumes between High Rate Gravel Pack and Hydraulic Fracturing Treatments

In comparison with the average hydraulic fracturing stimulation treatment, the volumes of sand and fluid used in high-rate gravel pack treatments are usually small in terms of volume, pump time and hydraulic horsepower required. Table 9.2 is an actual example from the Inglewood Oil Field comparing the different parameters.

Treatment Summary Comparison		
Parameters	High Rate Gravel Packs Well VRU-4243 Stage 2	Hydraulic Fracturing Well VIC1-635
Pump Time (mins)	27.68	141.87
Clean Volume (bbls)	418.45	2992.18
Slurry Volume (bbls)	458.89	3210.35
Average Treating Pressure (psi)	768	6914
Max. Treating Pressure (psi)	1343	8818
Proppant Mass (100*lb)	373.79	2013.48

Table 9.2. Comparison between high-rate gravel pack and hydraulic fracture treatment

Comparison of Fracture Geometry

Table 9.3 shows that the length created by the high-rate gravel-pack treatment in the Vickers and Rindge zones is significantly less than the fracture length created by the hydraulic fracturing treatments performed in the Nodular Shale zone.

Well Name and #	Stage #	Formation	Type of Treatment	Fracture Length Tip to Tip (ft)	Fracture Height (ft)
VRU-4243	2	Vickers	High Rate Gravel Packs	140	110
VIC1-635	1	Nodular	Hydraulic Fracturing	2115	84

Table 9.3. Comparison of the geometry created in the Vickers zone by a high-rate gravel-pack treatment with that created in the Nodular Shale zone by a hydraulic fracturing treatment.

Reference

Fan, Y., and Lave, F.M., 1996, Tip screenout fracturing of gas wells, paper SPE35636: SPE Journal, v. 1, no. 4, p. 463-472.

Moodie, W. H.; Minner, W. A.; Fernandez, M.; Lockman, D., and Burgett, W. Jr., 2004, Multistage Oil-Base Frac-Packing in the Thick Inglewood Field Vickers/Rindge Formation Lends New Life to an Id Producing Field, Paper SPE 90975.

10. Summary and Conclusions

- The Los Angeles Basin is a stratigraphic and structural basin in Southern California, USA and is a major oil and gas province.
 - Major northwest-trending strike-slip faults, such as the Whittier, Newport–Inglewood, and Palos Verdes faults, dominate the present-day basin and provide trapping mechanisms for the oil; and
 - More than 65 fields have been discovered in the Los Angeles Basin since oil production began in 1880.
- The Inglewood Oil Field, located in the northwestern portion of Los Angeles Basin, 10 miles southwest of downtown Los Angeles, is located along the Newport-Inglewood fault trend.
 - The field is the largest urban oil field in the United States—covering an area of over 1,000 acres;
 - Since the discovery of the Inglewood Oil Field in 1924, about 1,829 wells have been drilled within the historical boundaries of the field; and,
 - All of the oil and natural gas produced from the Inglewood Oil Field are consumed within California.
- The geologic structure of Inglewood Oil Field is very complex.
- A 3D structural earth model was constructed for Inglewood Oil Field to improve our knowledge of complex earth structure and our abilities to characterize the effect of hydraulic fracturing on near-surface groundwater and seismic ground motion.
 - The 3D earth model helped in gaining a clear and much better understanding and visualization of the fault network in the Inglewood Field and how it relates to the different formations
 - A 3D model can capture the full physics of hydraulic fracture propagation, thus leading to a more complete understanding of the impact of hydraulic fracturing at the surface;
 - The 3D structural earth model was built with data from well logs identifying faults and horizons (formation tops and faults picks);
 - The number of geologic formation tops, available from well control, used to construct the individual horizons in the 3D Earth Model were higher in the shallower zones of the model such as Pico, Vickers, Vickers "H" Sand and Rindge (~550 well tops) and lower in the deeper zones of the model such as the Bradna, Nodular and Sentous zones (~120 well tops). This is primarily due to the fact that there

- are more well penetrations in the shallower zones of Inglewood Field as compared to the deeper zones;
 - Data management procedures and quality control measures were applied to ensure consistency between the geologic horizons and fault networks in the model;
 - Special emphasis and efforts was placed on determining how the complex fault network within the field and the geologic horizons was interrelated; and,
 - 3D visualization techniques were extensively used and were an important role step in validating the final input data into the 3D model.
- Eight wells were selected for analysis in this hydraulic fracturing report of the Inglewood Oil Field. The wells analyzed had either multiple independent hydraulic fracturing stimulation treatments or high-rate gravel pack treatments.
 - Selection criteria included location within the field and with respect to the faults, i.e., on both sides of major faults, and the availability and accuracy of existing data, e.g., fracturing treatment, well logs, and reservoir properties.
 - Data Validation and Processing
 - Triple Combo and Dipole Sonic log (where available) data was processed to create an input file for GOHFER model;
 - Core data was available only for the wells in the Nodular zone. The processed logs were calibrated against the core data;
 - Minifrac Analysis was performed on the step-down tests, wherever available, to determine critical reservoir parameters, such as closure pressure, permeability, pressure dependent leakoff, and process zone stress;
 - The Grid Oriented Hydraulic Fracture Extension Replicator (GOHFER[®]) fracture simulation software was used to perform the pressure history match. The model was calibrated using all available log and fracturing treatment data and was run until an acceptable match was obtained.
Note: GOHFER is a frac simulator, however the HRGP treatments were analyzed using GOHFER to get a comparison and understanding of the geometries created. Experts in the industry have used GOHFER to analyze similar type of HRGP treatments and believe that it does a better job than any other model that they have applied.
 - The modeled fracture geometries were imported into the 3D earth model to provide visualization and a better understanding of the fractures in relation to the formations and discontinuous groundwater bodies on surface.

- A total of 21 high-rate gravel pack treatments were pressure history matched in the Vickers and Rindge zones
 - For the majority of the stages, the modeled gravel pack height created by the high-rate gravel packs in the Vickers and Rindge zones ranged from 100 to 170 ft. The path height in few stages ranged from 200 to 240 ft.;
 - Modeled height is relatively small compared to the modeled depth;
 - The shortest vertical distance between the top of the modeled gravel pack in the shallowest reservoirs, the Vickers and Rindge zones, and the discontinuous groundwater bodies in the study wells is 1,070 ft.;
 - In other study wells in the Vickers and Rindge zone, the vertical distance ranged from 1,728 to 1,758 ft.;
 - The gravel packs created in the Vickers and Rindge zones in the study wells were found to be nowhere near the discontinuous groundwater bearing bodies near the surface;
 - The volume of sand and fluid typically used in the high-rate gravel pack treatments was small in comparison to the volume used in typical hydraulic fracturing stimulation treatments; and,
 - The modeled gravel pack length created by the high-rate gravel-pack treatments in the Vickers and Rindge zones is significantly less than that created by the hydraulic fracturing treatments performed in the Nodular Shale zone.

- A total of 8 hydraulic fracturing stimulation treatments were pressure history matched and analyzed in the wells analyzed in this report in the Moynier, Sentous and Nodular zones.
 - The vertical distances from the top of the modeled fractures in the deeper zones to the discontinuous groundwater bodies are in the range of several thousand feet.
 - In the case of study wells in the Nodular Shale zone, the actual distances from the tops of the created hydraulic fractures, after completing the well treatments, to the discontinuous groundwater bodies was approximately 7,700 ft.
 - This depth is sufficiently large for the hydraulic fracture treatments to have no effect on the discontinuous groundwater bodies.

- Microseismic monitoring was conducted for the VIC1-330 and VIC1-635 hydraulic fracturing treatments, completed in the Nodular Shale zone.
 - The event moment magnitude recorded in the microseismic monitoring of VIC1-635 well ranged from -3.8 to -2.2 Mw,

with an average of -3.4 for the VIC1-735 array and ranged from -4.0 to -2.4 with an average of -3.4 for the VIC-925 array;

- The event moment magnitude recorded in the microseismic monitoring of VIC1-330 well ranged from -3.2 to -1.3;
 - These events recorded in both the wells in the Nodular zone were extremely smaller than the moment magnitude of +3 which can be felt on surface; and,
 - Similar results were found in another study. An extensive review of microseismic monitoring of fracturing treatments conducted in the US (Warpinski et al., 2012) demonstrates that the very small induced seismicity associated with hydraulic fracturing is not a problem under normal circumstances.
- Hydraulic fracturing is *NOT* a “drilling process.” Hydraulic fracturing is a well completion method that is performed after the well has been drilled and the drilling rig has moved off.
 - Sand and water typically comprise more than 99.5% of the fluid system used in hydraulic fracturing.
 - The fracturing fluids pass down the well inside of the steel casing until they reach the zone to be fractured.
 - The GWPC and IOGCC host a hydraulic fracturing chemical disclosure registry called FracFocus at www.fracfocus.org where public can find a list and information about the additives used in hydraulic fracturing stimulation treatments.
 - Groundwater and discontinuous groundwater bodies are protected from the fluid contents of the well during drilling and production operations by a combination of steel casing, cement sheaths, and other mechanical isolation devices installed as a part of the well construction process.
 - Casing and cementing help isolate freshwater bearing zones and groundwater, where present, from the contents of the wellbore, including drilling fluids, completion fluids and flowback, or produced oil and natural gas and also help prevent fluids from moving between the formation layers. Proper sealing of annular spaces with cement creates a barrier to both vertical and horizontal fluid migration.
 - DOGGR has strict guidelines on well design and well construction that well operators must comply with. Adhering to DOGGR’s well construction standards regarding the use of casing, mud, and cement, serve to

prevent fluid migration and the commingling of lesser quality fluids.

- Regular monitoring takes place during drilling and production operations to ensure that these operations proceed within established guidelines and in accordance with the well design, well plan, and permit requirements.
 - In California, DOGGR oversees the drilling, operation, maintenance and plugging and abandonment of oil, natural gas and geothermal wells (Source: www.conservation.ca.gov/dog/Pages/index.aspx).
 - Hydraulic fracturing has been in use for over 60 years and both state and federal regulatory agencies, including the EPA, have repeatedly stated that they are not aware of any instances of hydraulic fracturing resulting in contamination of drinking water aquifers (IOGCC, 2009).
 - More than 30 state and federal regulatory agencies, including the U.S. Department of Energy, the Interstate Oil and Gas Compact Commission and the Ground Water Protection Council have studied oil and natural gas industry operations, including hydraulic fracturing. The reports produced by these agencies all reach the conclusion that that hydraulic fracturing technology is safe and well regulated.
- The layering of sedimentary rocks creates large variations in rock stresses. The combination of variation in rock stress and changes in rock properties at the interface between different layers creates an environment that hinders the vertical growth of fractures.
- The fracture-height growth in the Inglewood field is limited by the physical properties of the multiple layered formations. For eg., in the Nodular shale zone, the total number of microseismic events observed during fracturing treatment were 939. Out of these, only 5 events were observed out of zone above the Nodular Shale. All these events were within 20 ft. of the top of Nodular Shale.